MRI and CT in Traumatic Brain Injury

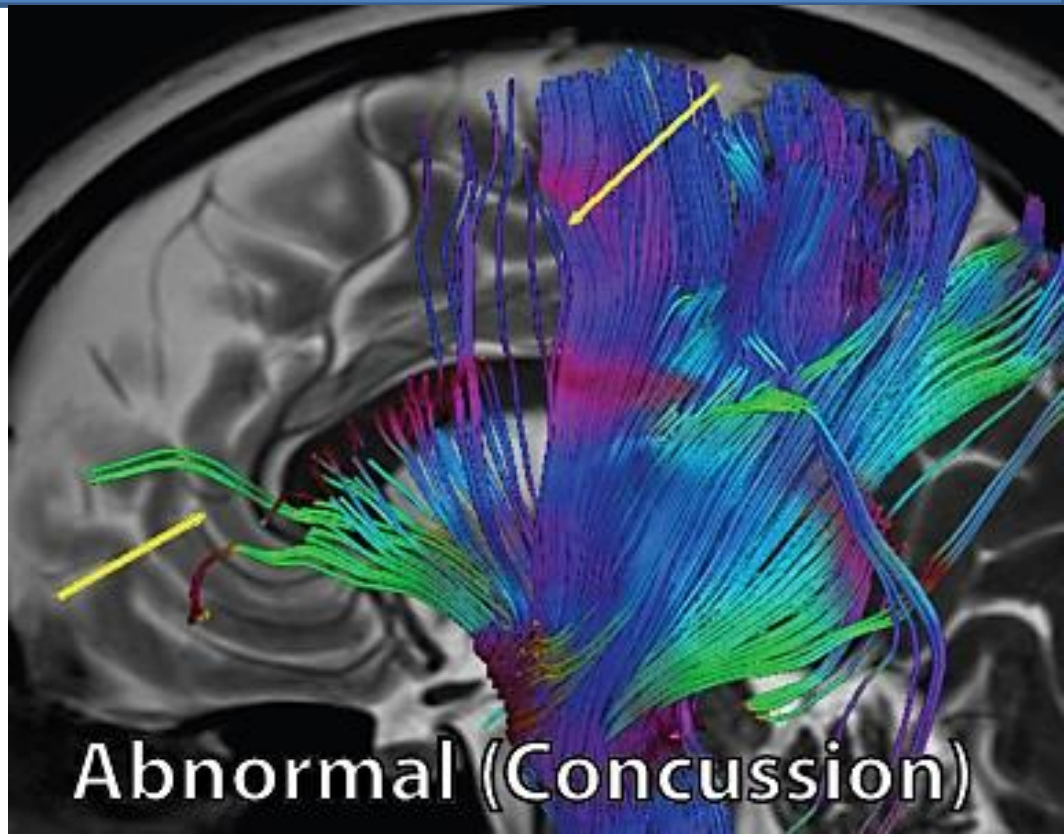

3T
TOMORROW'S
TECHNOLOGY TODAY
FROM LOS GATOS MRI

Murray A. Solomon, M.D.
InSight - Los Gatos MRI

Los Gatos MRI


BAD NEWS, HUMPTY.
DiagnosticImaging.com • cartertoons.com

MRI and CT in Traumatic Brain Injury

Is There Still a Roll for Plain X-Rays in the Evaluation of TBI Patients?

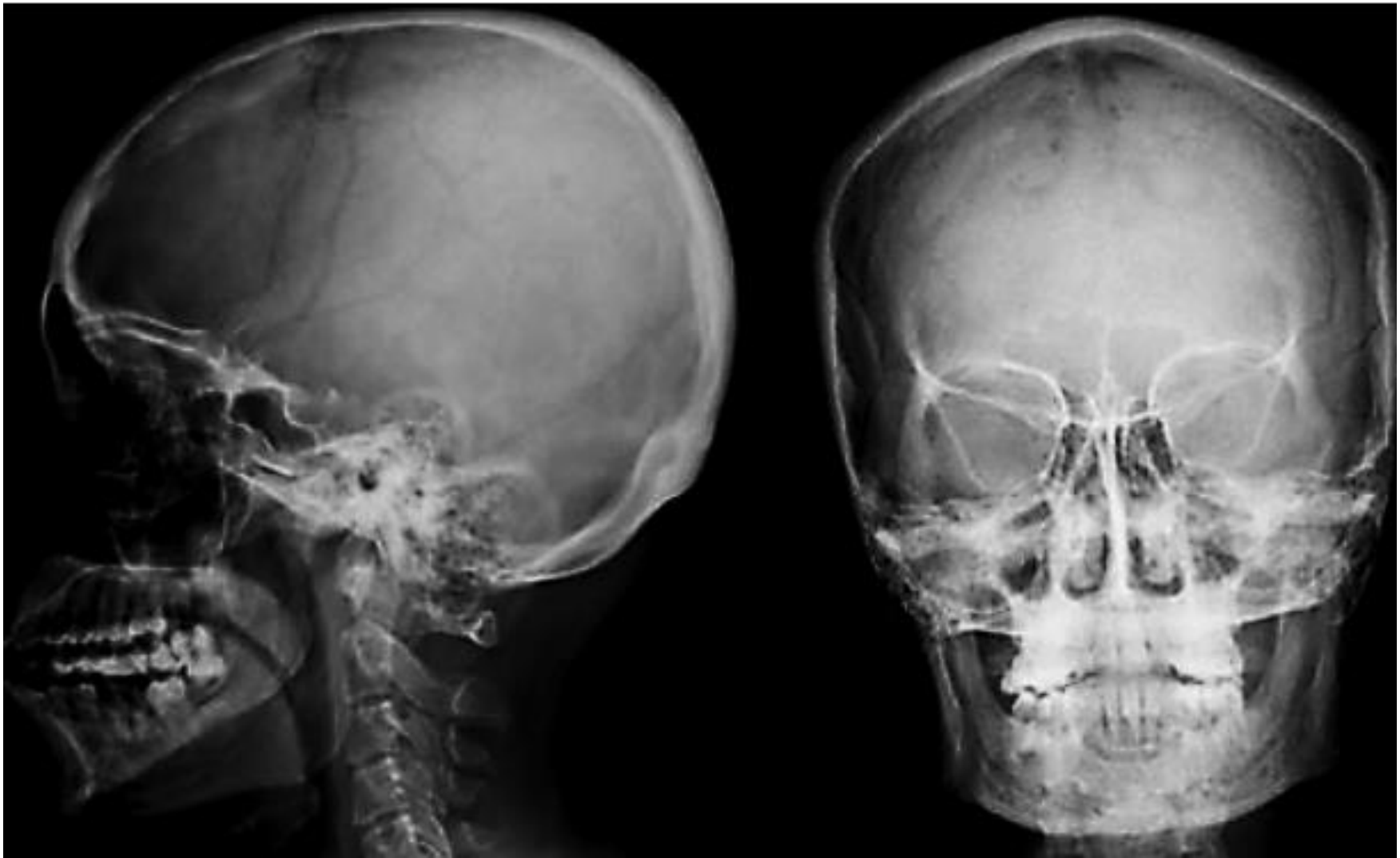

Table 2 The Royal College of Surgeons of England indications for skull X-ray

Where CT is available
Suspected non-accidental injury
Presence of a boggy swelling particularly in the parietotemporal region
Suspected penetrating injury
Suspected compound fracture

References

1. The Royal College of Surgeons of England. *Report of the Working Party on the Management of Patients with Head Injury*. London: RCSE, 1999.

MRI and CT in Traumatic Brain Injury

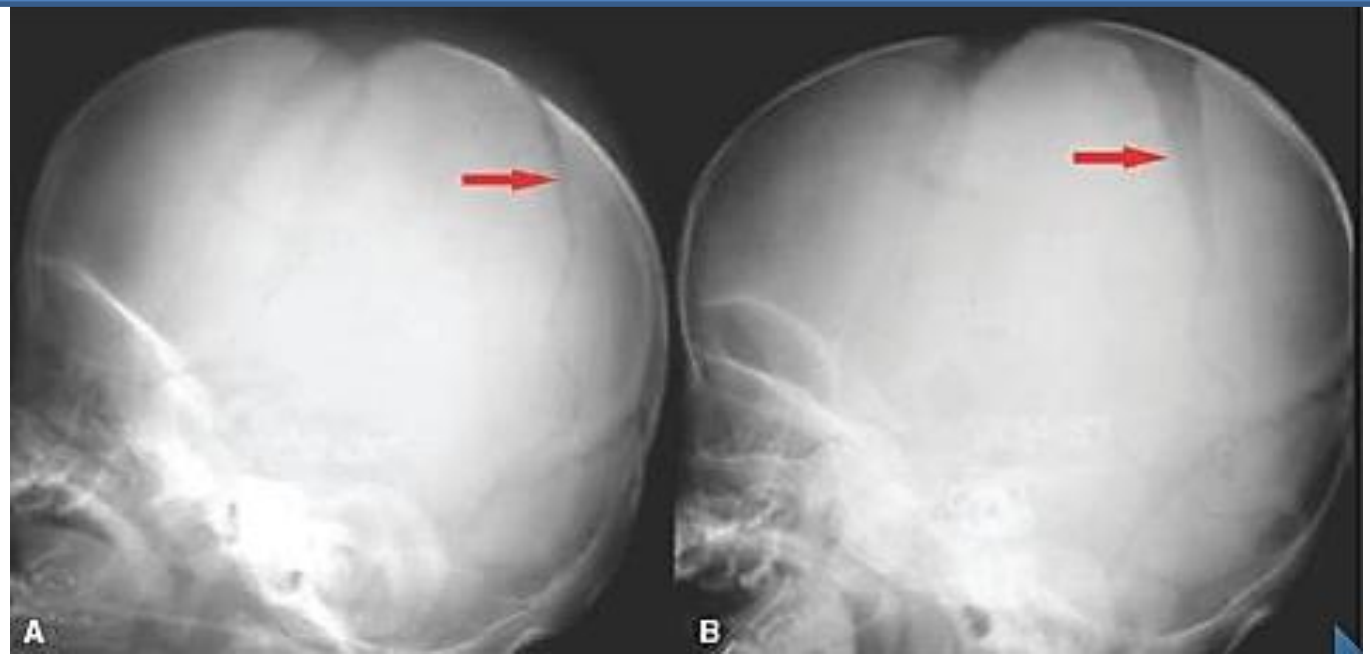

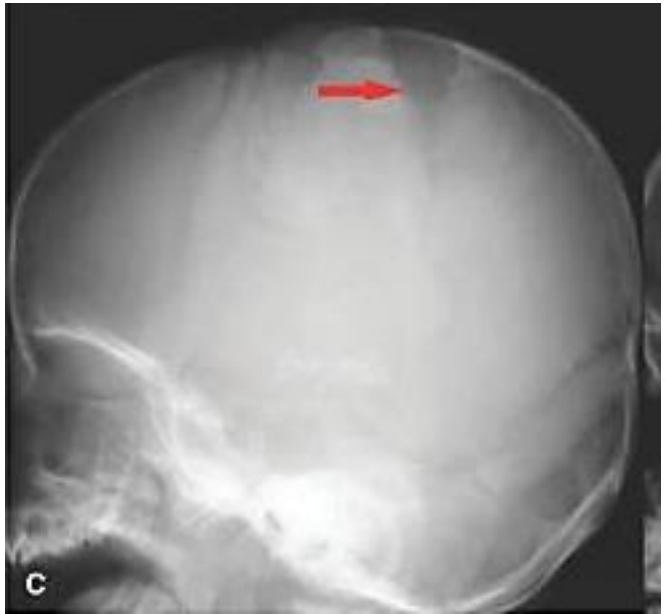

Cyst. A. Lateral skull radiograph from a 6-month old infant who presented with unconsciousness shows a slightly diastatic fracture (*arrow*) of the parietal bone. Follow-up radiographs at 2 weeks (B) and 6 weeks (C) show progressive widening of the fracture (*arrows*).

MRI and CT in Traumatic Brain Injury

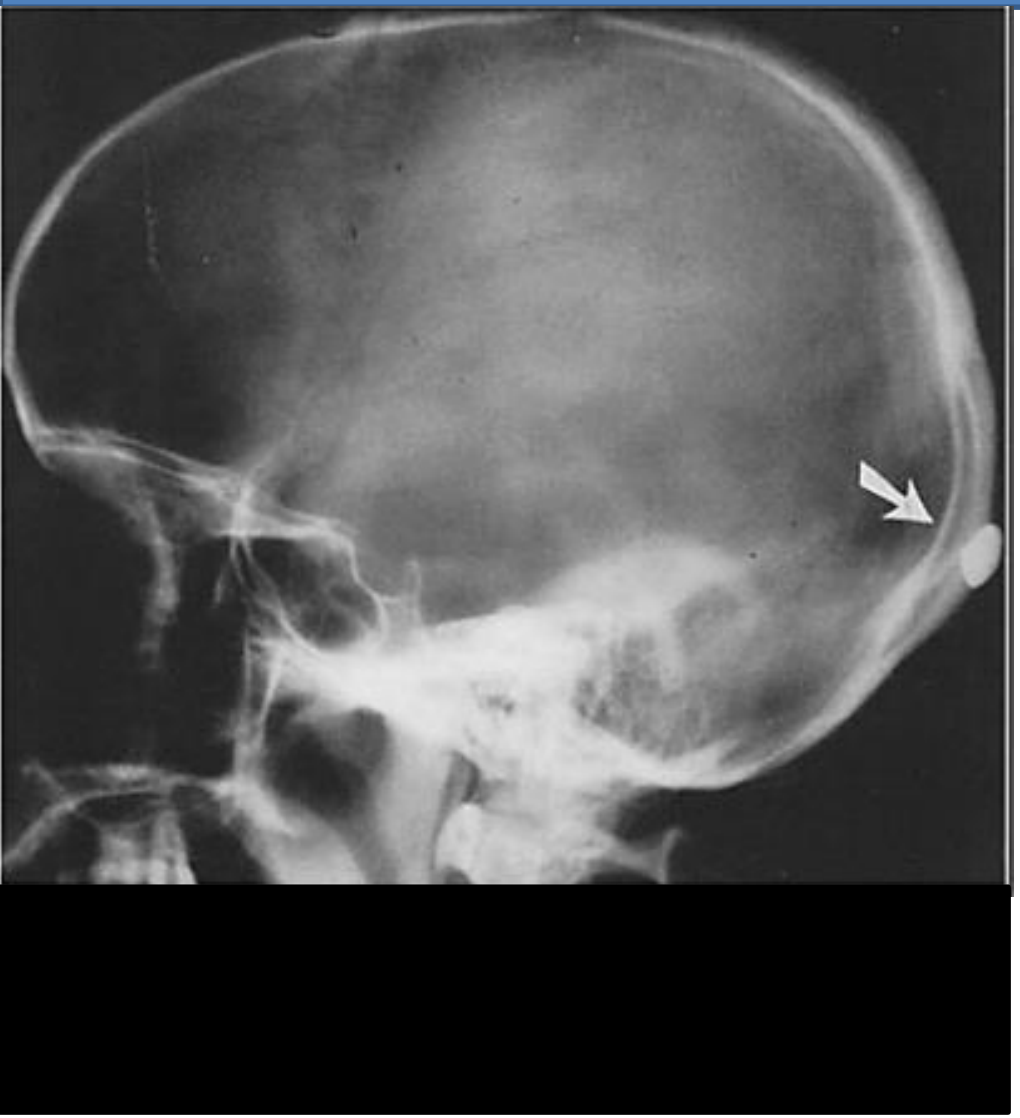

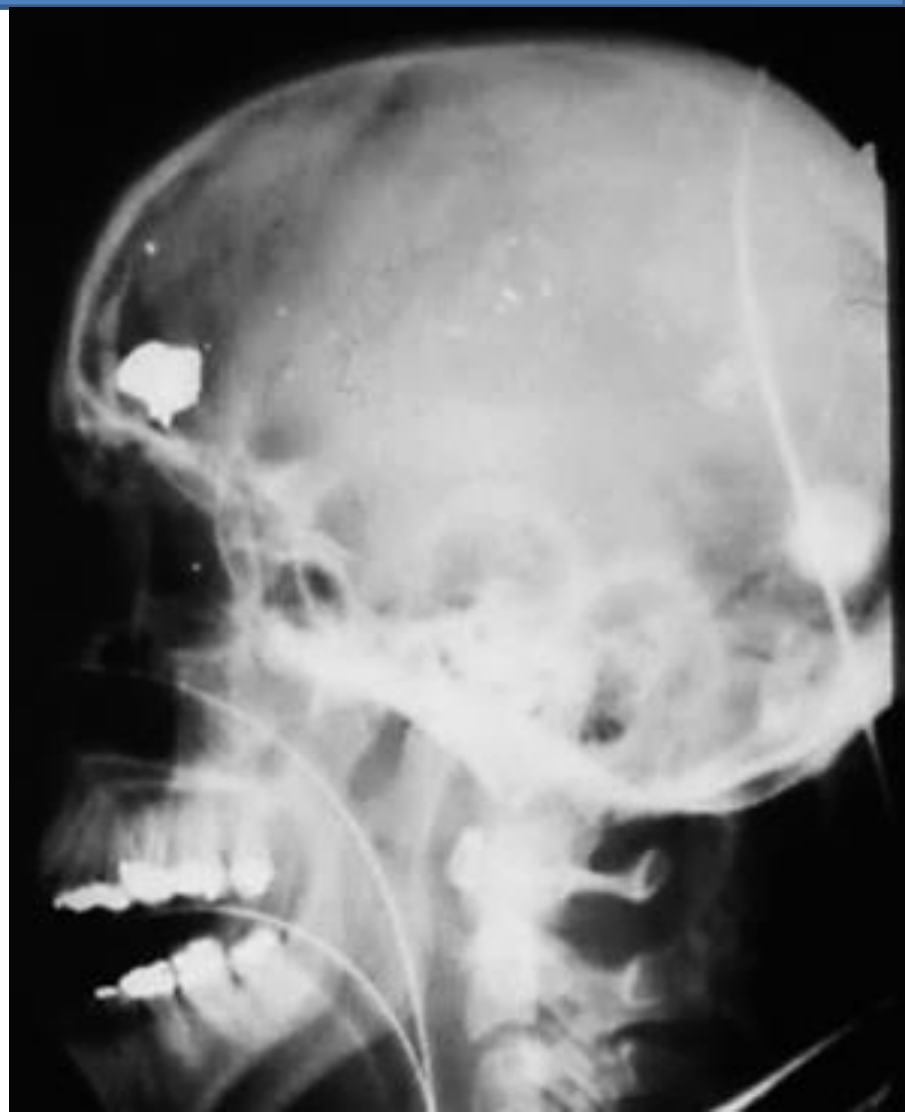

MRI and CT in Traumatic Brain Injury

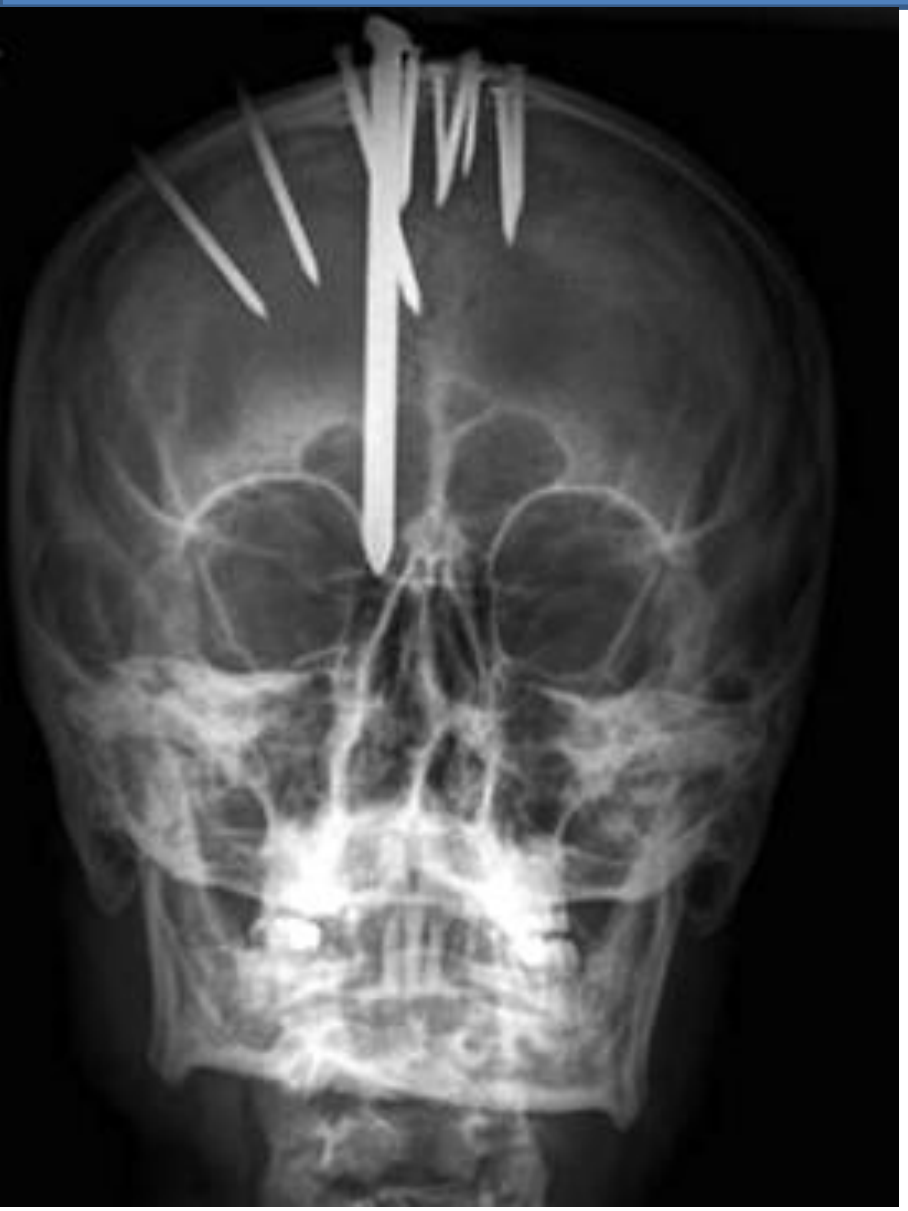

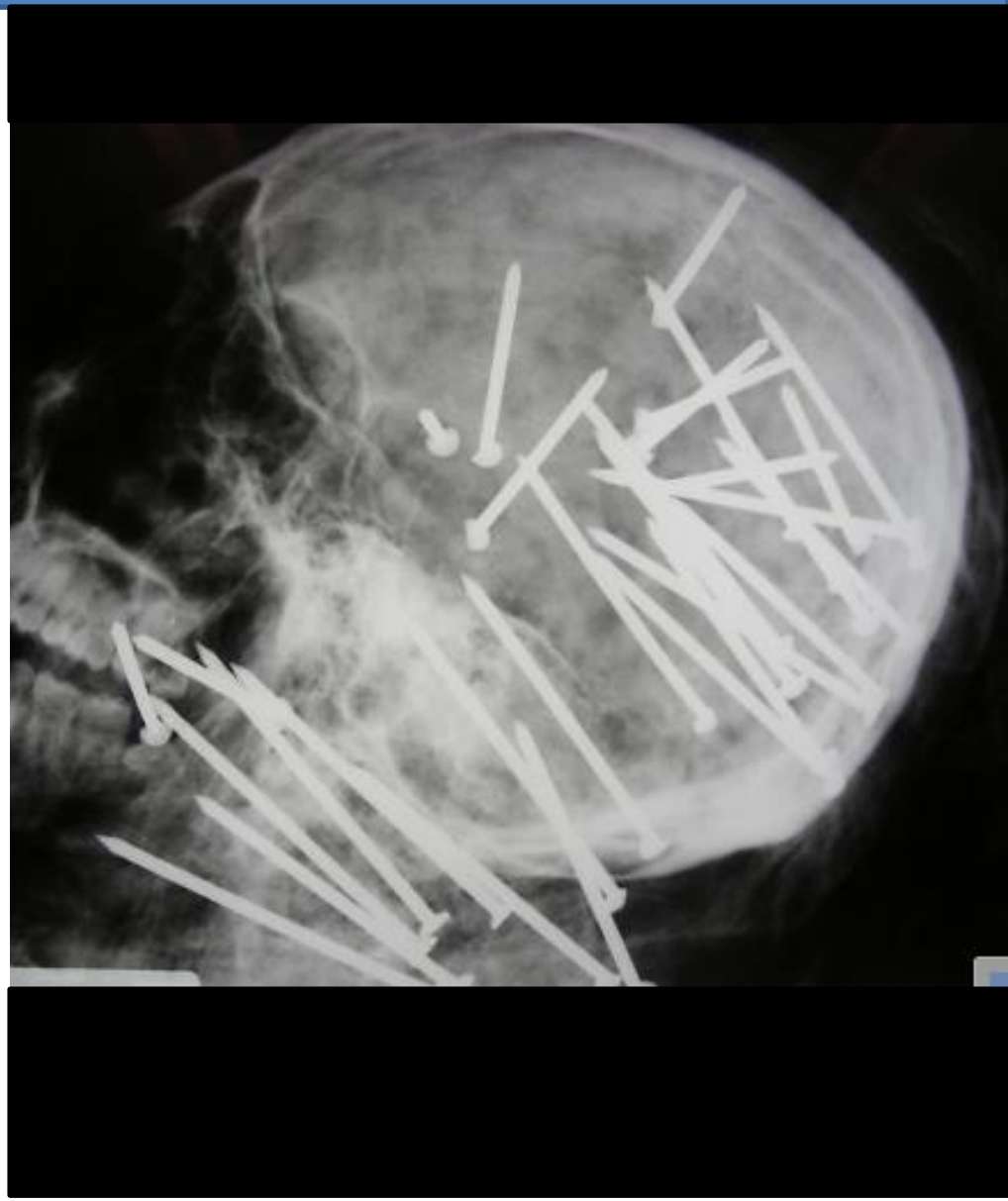

MRI and CT in Traumatic Brain Injury

CT Scanning in TBI Patients

Journal of Neuroradiology

Available online 4 April 2019

Comparison between postmortem computed tomography and autopsy in the detection of traumatic head injuries

L. Legrand [a, b, c], T. Delabarde [b, d, e], R. Souillard-Scemama [a, b], I. Sec [b, d, f], I. Plu [b, d, g], J-M. Laborie [b, d, f], Y. Delannoy [b, d, h], L. Hamza [b, d, i], M. Taccoen [b, d], L. De Jong [a, b, c], J. Benzakoun [a, b, c], M. Edjlali [a, b, c], J-F. Méder [a, b, c], C. Oppenheim [a, b, c], B. Ludes [b, d, e]

[a] Service d'Imagerie Morphologique et Fonctionnelle, Centre Hospitalier Sainte-Anne, 1 rue Cabanis, 75014 Paris, France

[b] Pôle Universitaire d'Imagerie Post-Mortem, Université Paris Descartes-Paris 5, Sorbonne Paris Cité, 12 rue de l'Ecole de Médecine, 75006 Paris, France

Abstract

Introduction. – The aim of this study was to assess the agreement between postmortem computed tomography (PMCT) and autopsy in detecting traumatic head injuries.

Materials and Methods. – Consecutive cases of death that underwent both unenhanced PMCT and conventional autopsy were collected from our institution database during a period of 3 years and reviewed retrospectively. PMCT images were reviewed for the presence of fractures (cranial vault, skull base, facial bones and atlas/axis) and intracranial hemorrhage. Kappa values were calculated to determine the agreement between PMCT and autopsy reports.

Results. – 73 cases were included, of which 44 (60%) had head trauma. Agreement between PMCT and autopsy was almost perfect ($\kappa = 0.95$) for fractures and substantial ($\kappa = 0.75$) for intracranial hemorrhage. PMCT was superior to autopsy in detecting facial bone and upper cervical spine fractures, and intraventricular hemorrhage. However, in some cases thin extra-axial blood collections were missed on PMCT.

Conclusions. – The agreement between PMCT and autopsy in detecting traumatic head injuries was good. Using a combination of both techniques increases the quality of postmortem evaluation because more lesions are detected.

Journal of Neuroradiology

Available online 4 April 2019

Comparison between postmortem computed tomography and autopsy in the detection of traumatic head injuries

L. Legrand [a, b, c], T. Delabarde [b, d, e], R. Souillard-Scemama [a, b], I. Sec [b, d, f], I. Plu [b, d, g], J-M. Laborie [b, d, f], Y. Delannoy [b, d, h], L. Hamza [b, d, i], M. Taccoen [b, d], L. De Jong [a, b, c], J. Benzakoun [a, b, c], M. Edjlali [a, b, c], J-F. Méder [a, b, c], C. Oppenheim [a, b, c], B. Ludes [b, d, e]

[a] Service d'Imagerie Morphologique et Fonctionnelle, Centre Hospitalier Sainte-Anne, 1 rue Cabanis, 75014 Paris, France

[b] Pôle Universitaire d'Imagerie Post-Mortem, Université Paris Descartes-Paris 5, Sorbonne Paris Cité, 12 rue de l'Ecole de Médecine, 75006 Paris, France

Results. – 73 cases were included, of which 44 (60%) had head trauma. Agreement between PMCT and autopsy was almost perfect ($\kappa = 0.95$) for fractures and substantial ($\kappa = 0.75$) for intracranial hemorrhage. PMCT was superior to autopsy in detecting facial bone and upper cervical spine fractures, and intraventricular hemorrhage. However, in some cases thin extra-axial blood collections were missed on PMCT.

HealthImaging

February 26, 2018 | Matt O'Connor

Emergency CT for head trauma may be overused

New research suggests emergency patients are often given unwarranted CT scans to check for skull fractures and brain hemorrhage, resulting in wasted healthcare dollars and increasing exposure to radiation, according to an American Roentgen Ray Society (ARRS) press release.

The study is set to be presented by Michaela Cellina, with the radiology department of Fatebenefratelli-Sacco Hospital in Italy, at the ARRS 2018 Annual Meeting April 22 to 27 in Washington, D.C.

In the study, the team evaluated head CT scans performed for minor head injury in patients aged 18 to 45 years old, who presented to the hospital's emergency department between Jan. 1 and June 30, 2016. Researchers determined whether CT scans met the criteria indicated by either the National Institute for Health and Care Excellence (NICE) and the Canadian CT Head Rule (CCHR).

Th study included 492 cases—260 were not indicated according to NICE and 376 did not meet CCHR requirements. The team noted no statistically significant difference between the specialty and seniority of the referring physician and over-referral. However, motor vehicle accidents were connected to a higher rate of non-indicated CT exams for both NICE and CCHR, and two-wheel vehicle driver accidents were associated with a higher rate of appropriated CT exams for both NICE and CCHR.

Only 15 of the 260 CT exams were positive for brain hemorrhage, subarachnoid hemorrhage or skull fracture, according to the release.

MRI and CT in Traumatic Brain Injury

Who Should Get a CT Scan?

Canadian CT Protocol

New Orleans CT Protocol

NICE UK CT Protocol

Neurosurgery Consensus 2017

J Neurol Surg A 2017;78:478–487.

Imaging after Head Injury

Computed tomography (CT) is currently considered the gold standard in patients who have suffered a head injury. CT after acute head injury is necessary, an absolute indication, in:

A

- Coma
- Impaired consciousness
- Amnesia
- Other neurologic disorders
- Vomiting in close temporal relation to the injury
- Seizure
- Clinical or radiologic signs of skull fracture
- Suspected depressed or perforating skull fracture
- Suspected CSF fistula
- Signs of a disorder of coagulation (history, prolonged bleedings, etc.)
- When in doubt, CT is optional, for example, in:

B

- History of head injury unclear
- Severe headache
- Intoxication with alcohol or drugs

B

- History of a high-energy injury such as motor vehicle accident of $>$ 60 km/hour, deformation of the vehicle, deformation of the passenger cabin of $>$ 30 cm, duration of rescue from the vehicle of $>$ 20 minutes, fall from height higher than 6 m, rolled-over injury, pedestrian or motorcycle collision of $>$ 30 km/hour, cyclist knocked off the cycle.[34]

CT, respectively repeat CT, is also necessary in deterioration of neurologic findings or when the patient fails to recover or is in a persisting coma after 4 to 8 hours.[34–37]

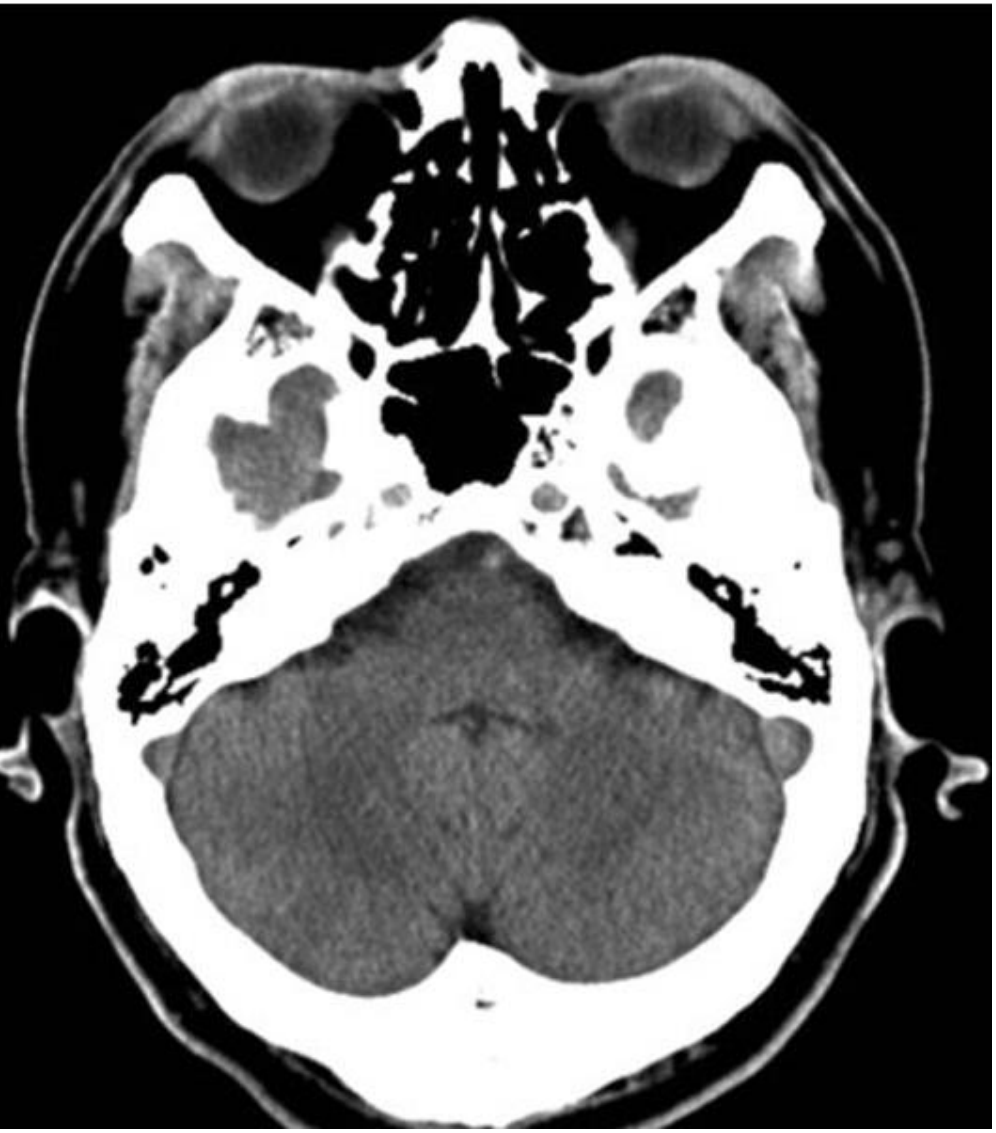

Fig. 2 The cranial CT scan of the brain and skull on the initial day was normal

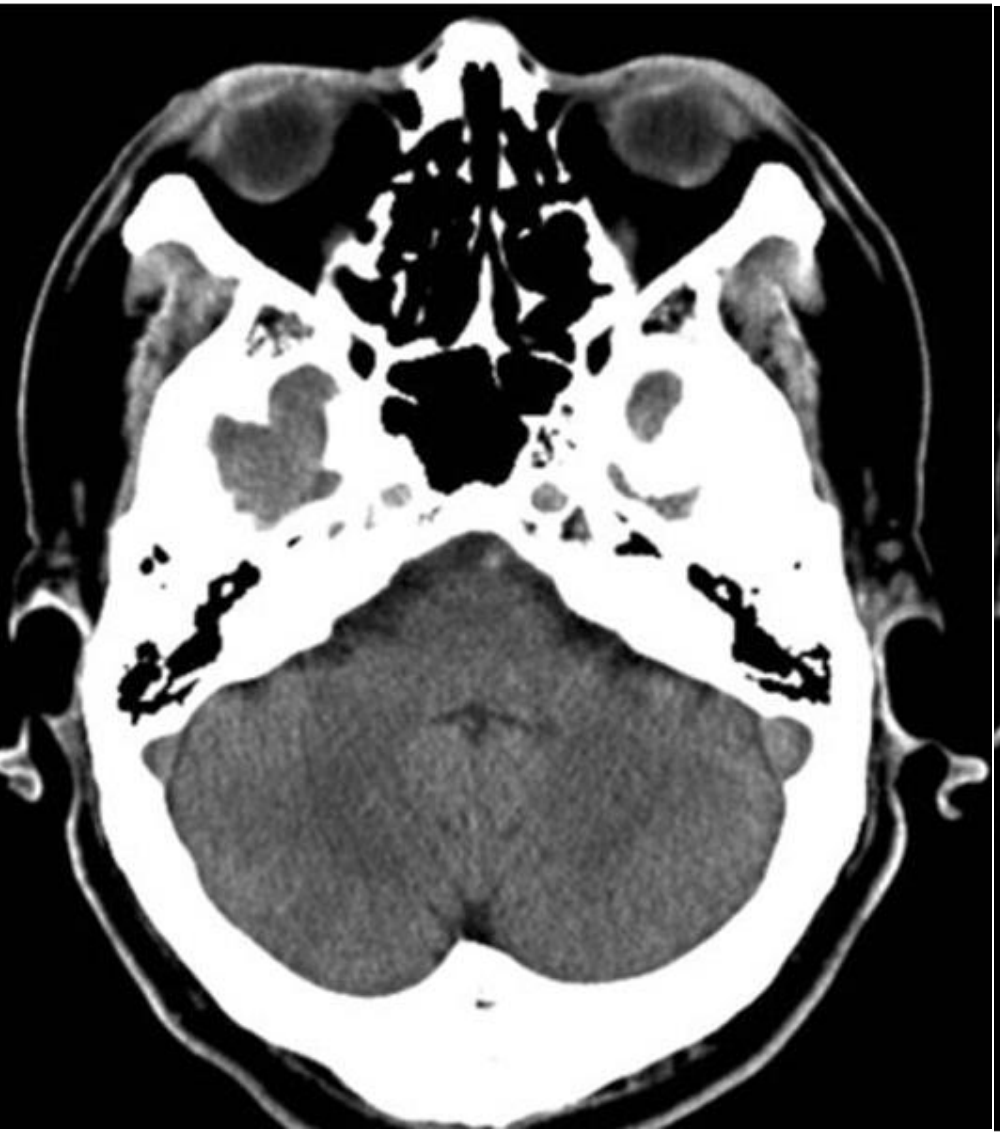

Fig. 2 The cranial CT scan of the brain and skull on the initial day was normal

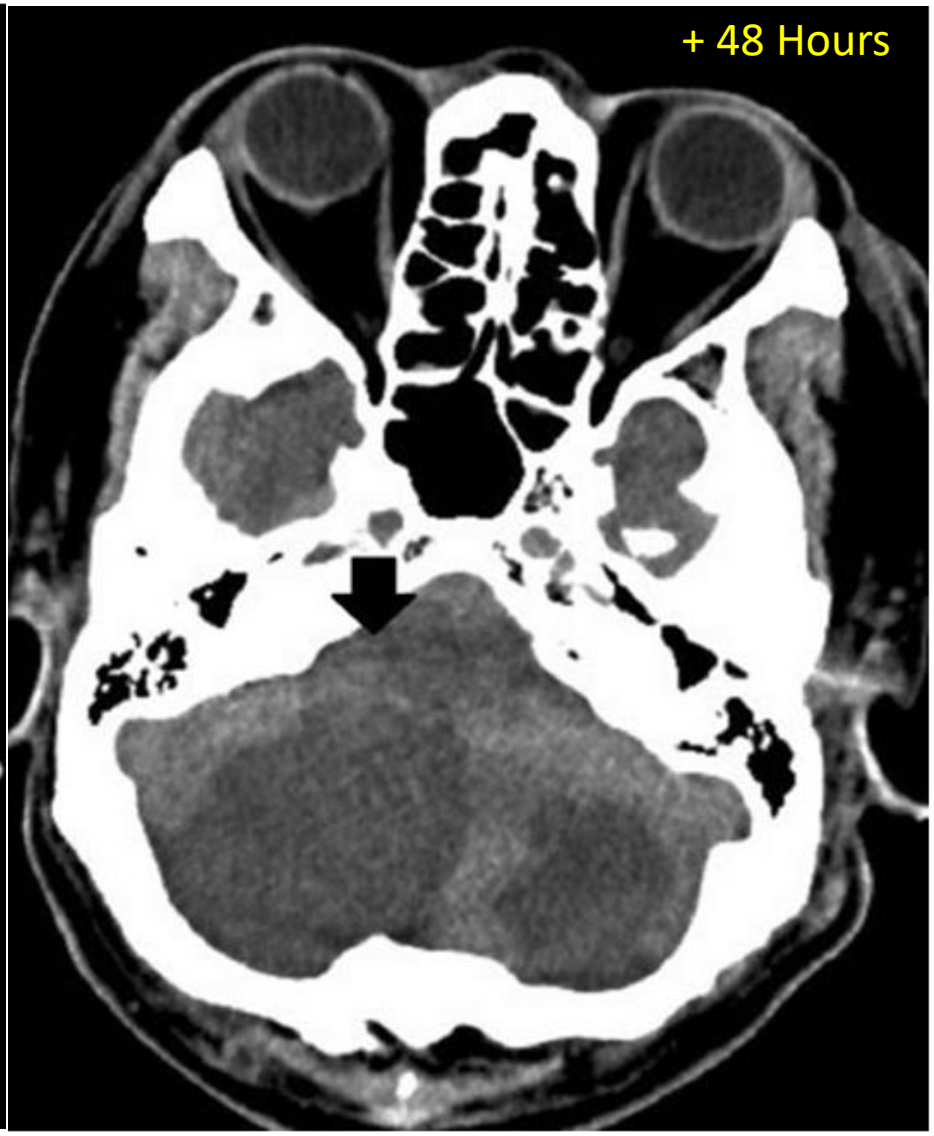

Fig. 5 The cranial CT scan 48 h after injury showed a massive low-density area on the bilateral cerebellar hemispheres and brain stem, suggesting bilateral cerebellar and brain stem infarction

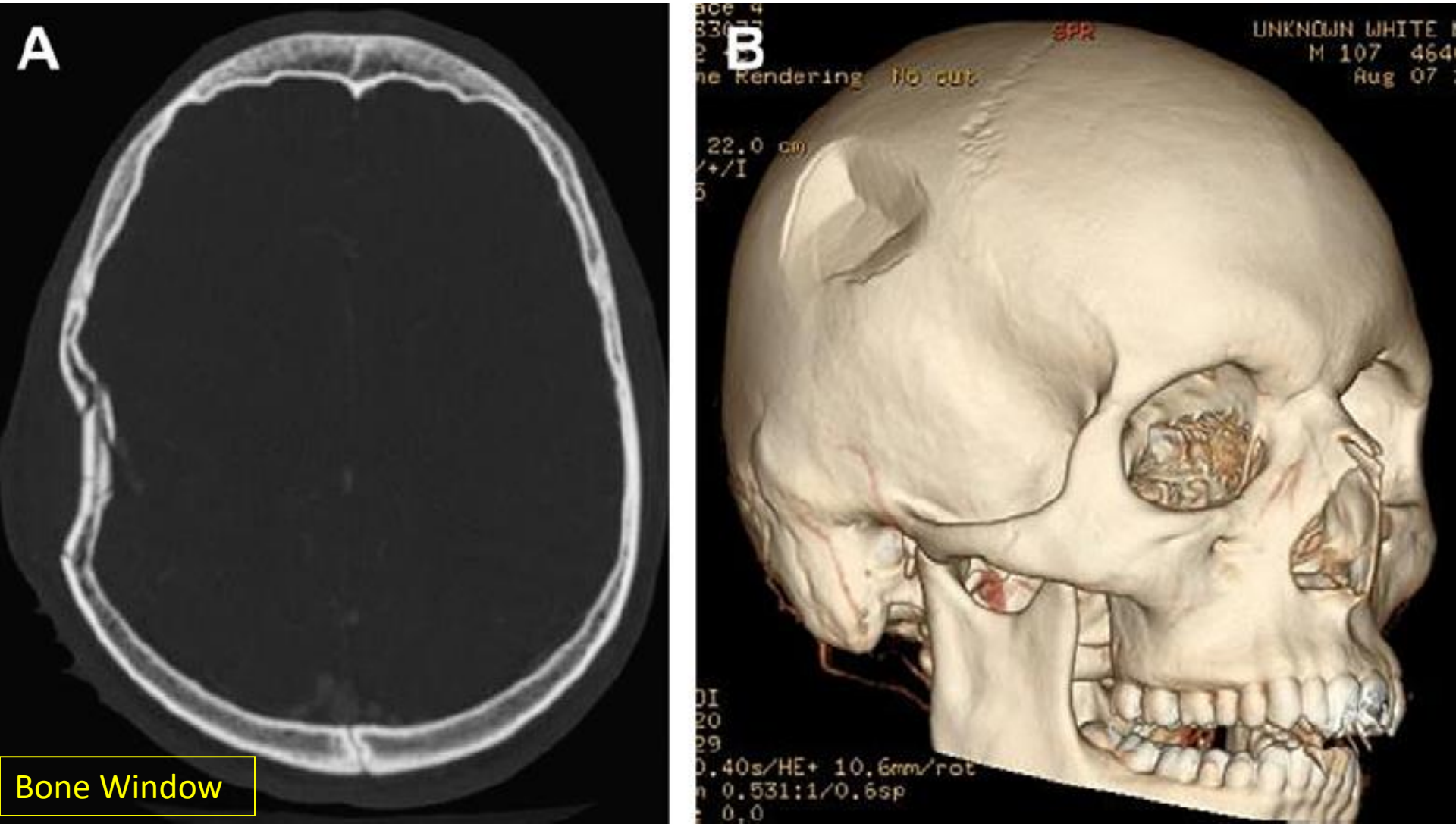

Fig. 4. (*A*) Axial CT image showing a comminuted, depressed calvarial fracture. (*B*) Surface shaded 3D volume-rendered CT image of a comminuted, depressed calvarial fracture.

MRI and CT in Traumatic Brain Injury

What Can You See with a CT Scan in TBI Patients ?

Skull Fractures

Brain Contusions

Acute Brain Hemorrhage

Extra-Axial Hemorrhage

Mass Effect/Midline Shift

Brain Herniations

Foreign Bodies

MRI and CT in Traumatic Brain Injury

Skull Fractures with Associated Hemorrhage

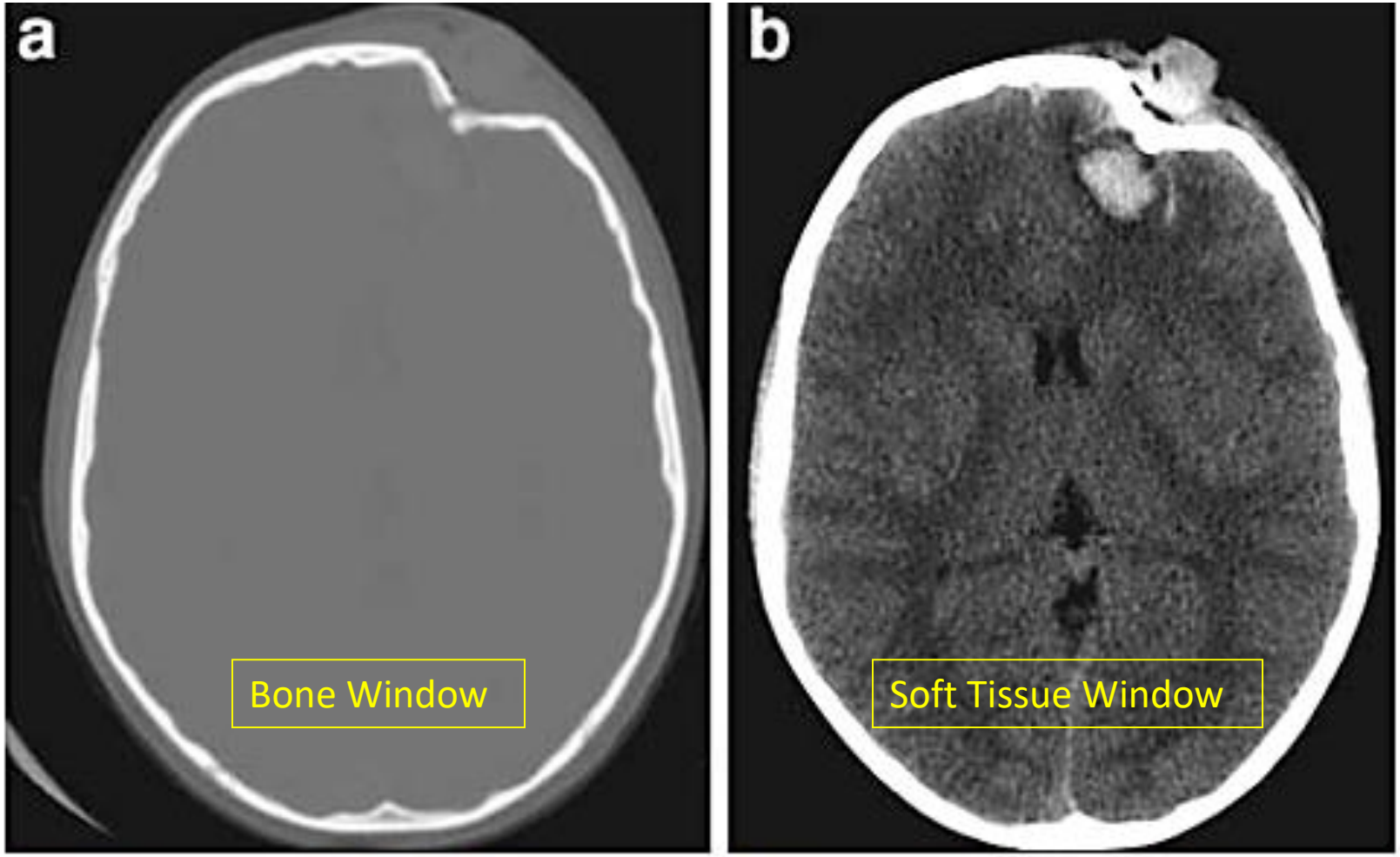

Fig. 2 Depressed skull fracture in a 16-year-old boy struck by a golf ball. **a** Axial CT image using bone window settings shows depressed fracture in left frontal bone. **b** Unenhanced axial CT image at same level as **a** using soft tissue window settings shows hemorrhagic contusion subjacent to depressed skull fracture

MRI and CT in Traumatic Brain Injury

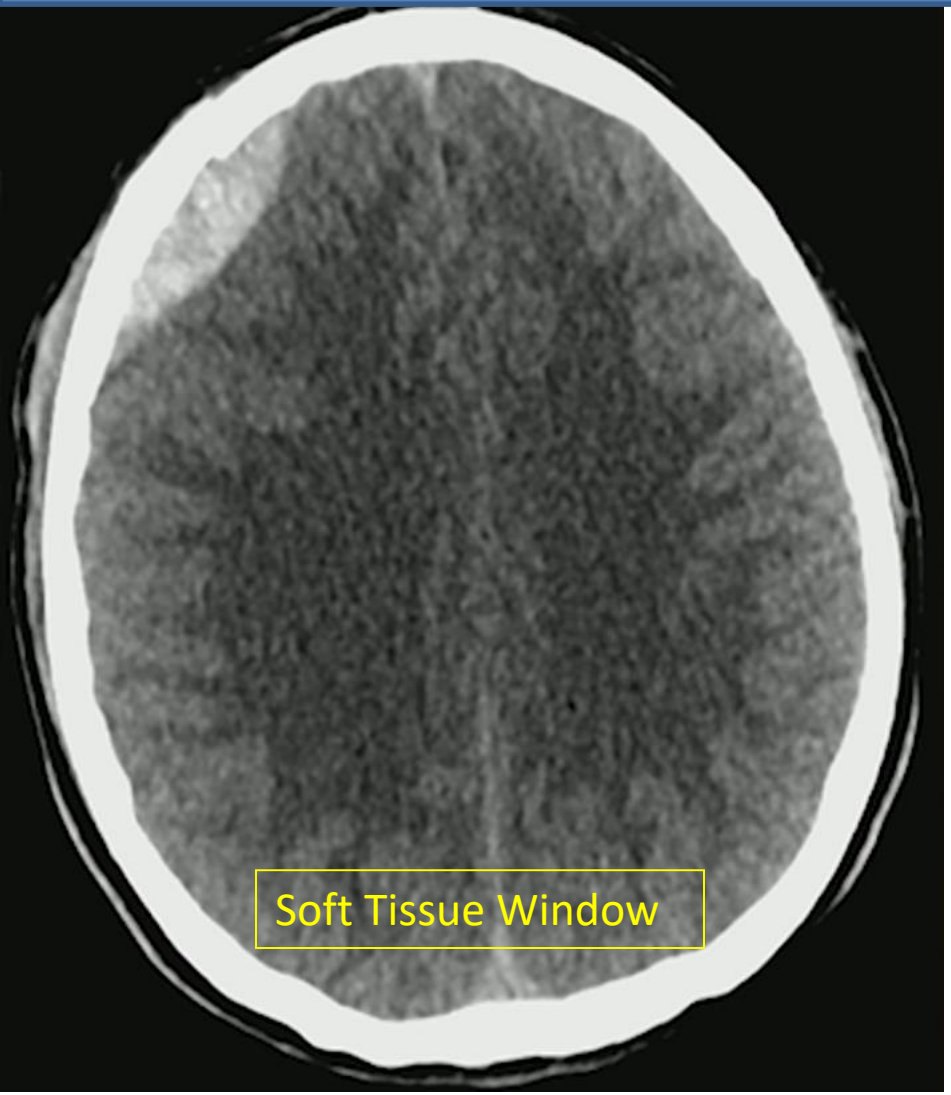

MRI and CT in Traumatic Brain Injury

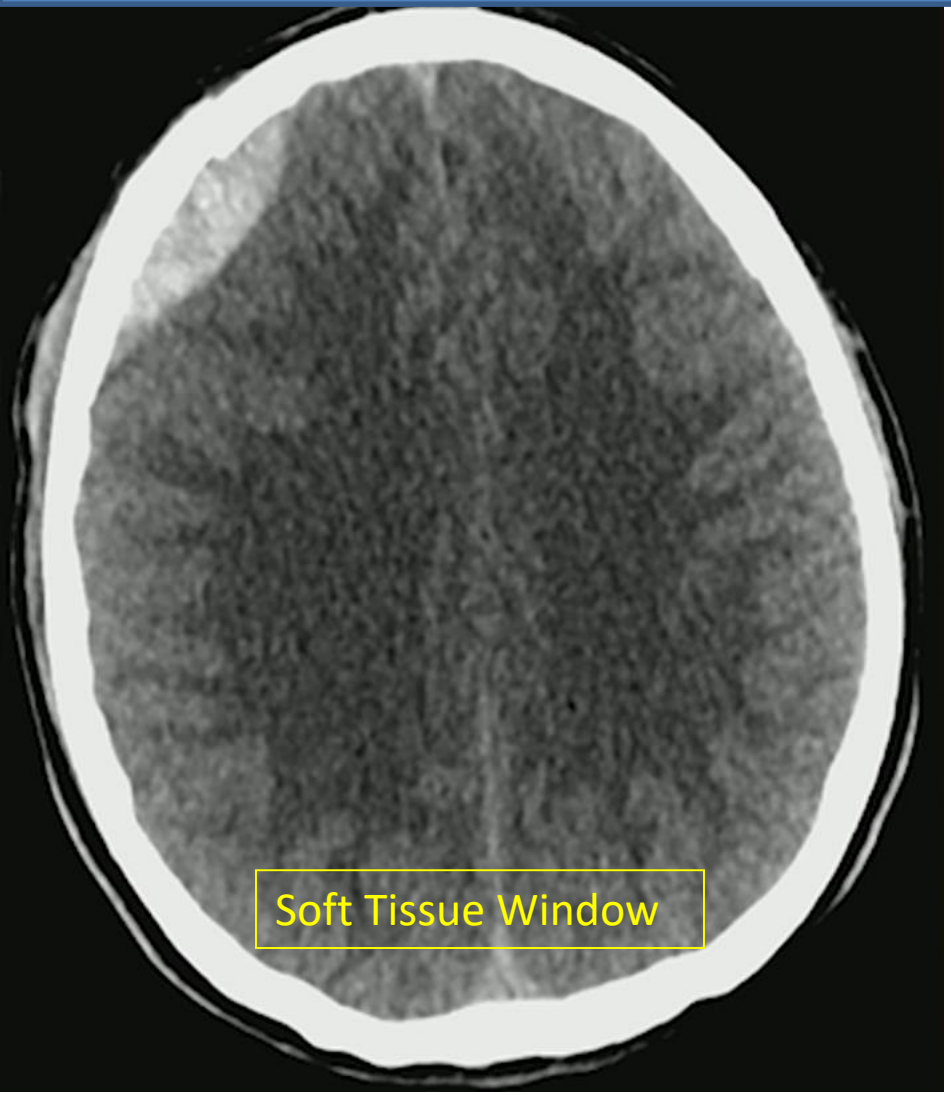

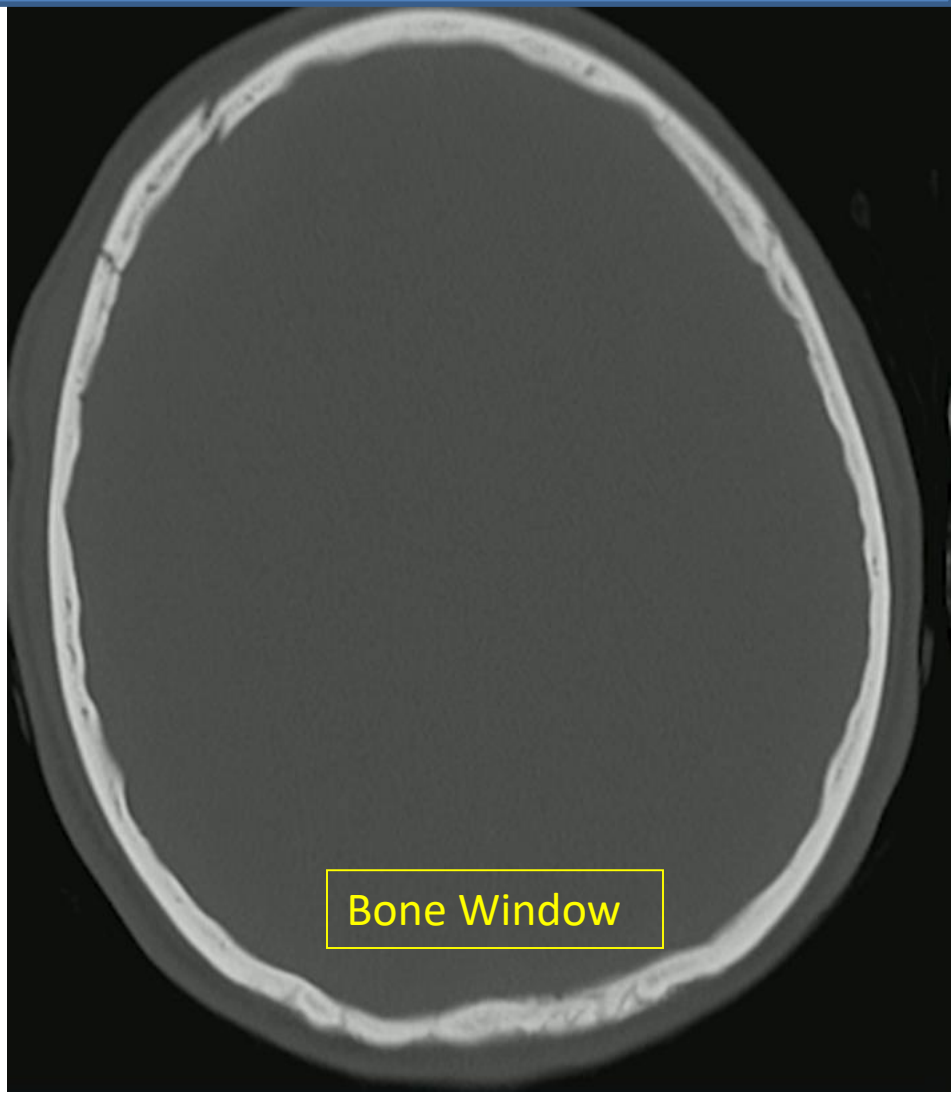

MRI and CT in Traumatic Brain Injury

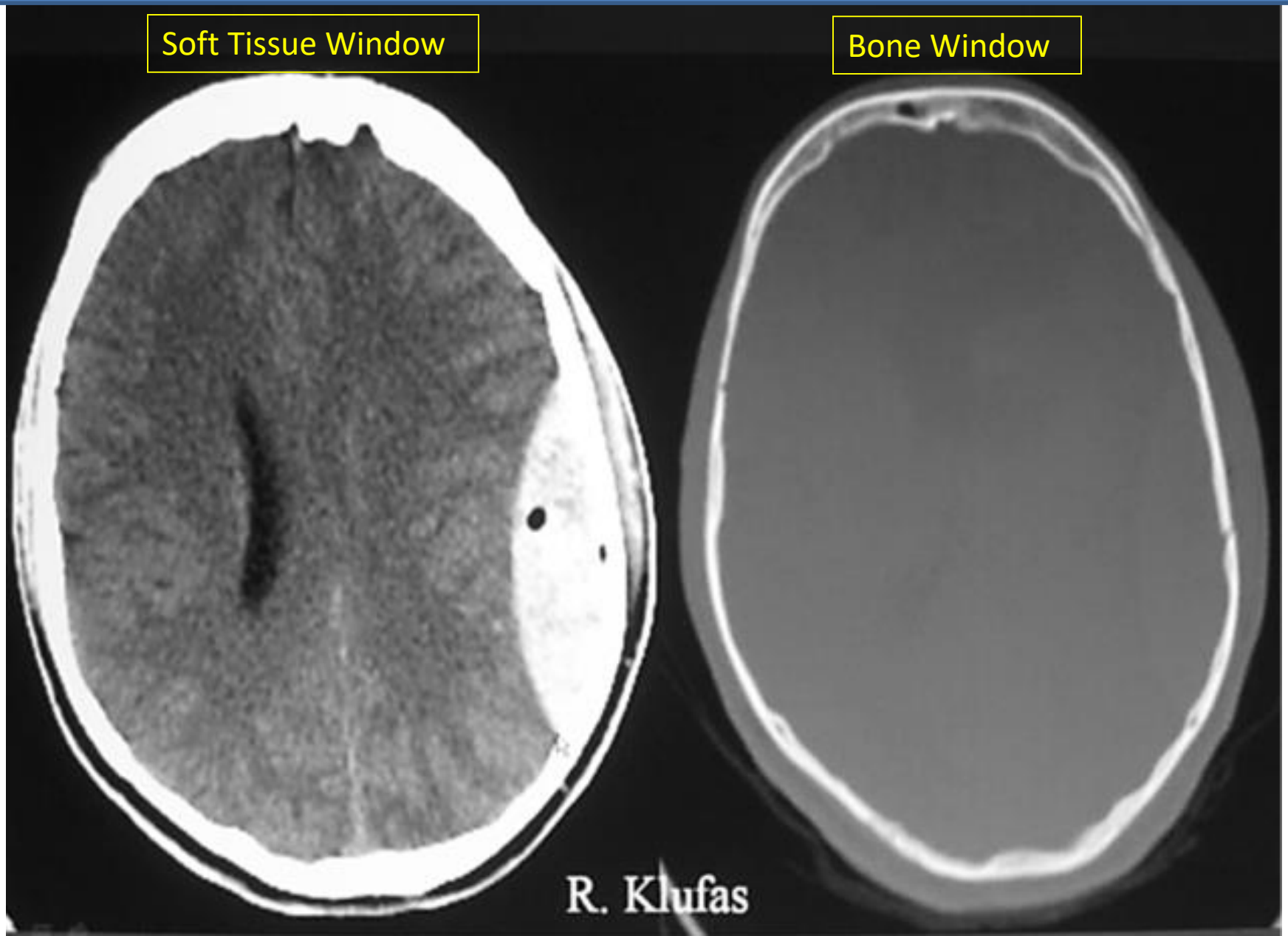

MRI and CT in Traumatic Brain Injury

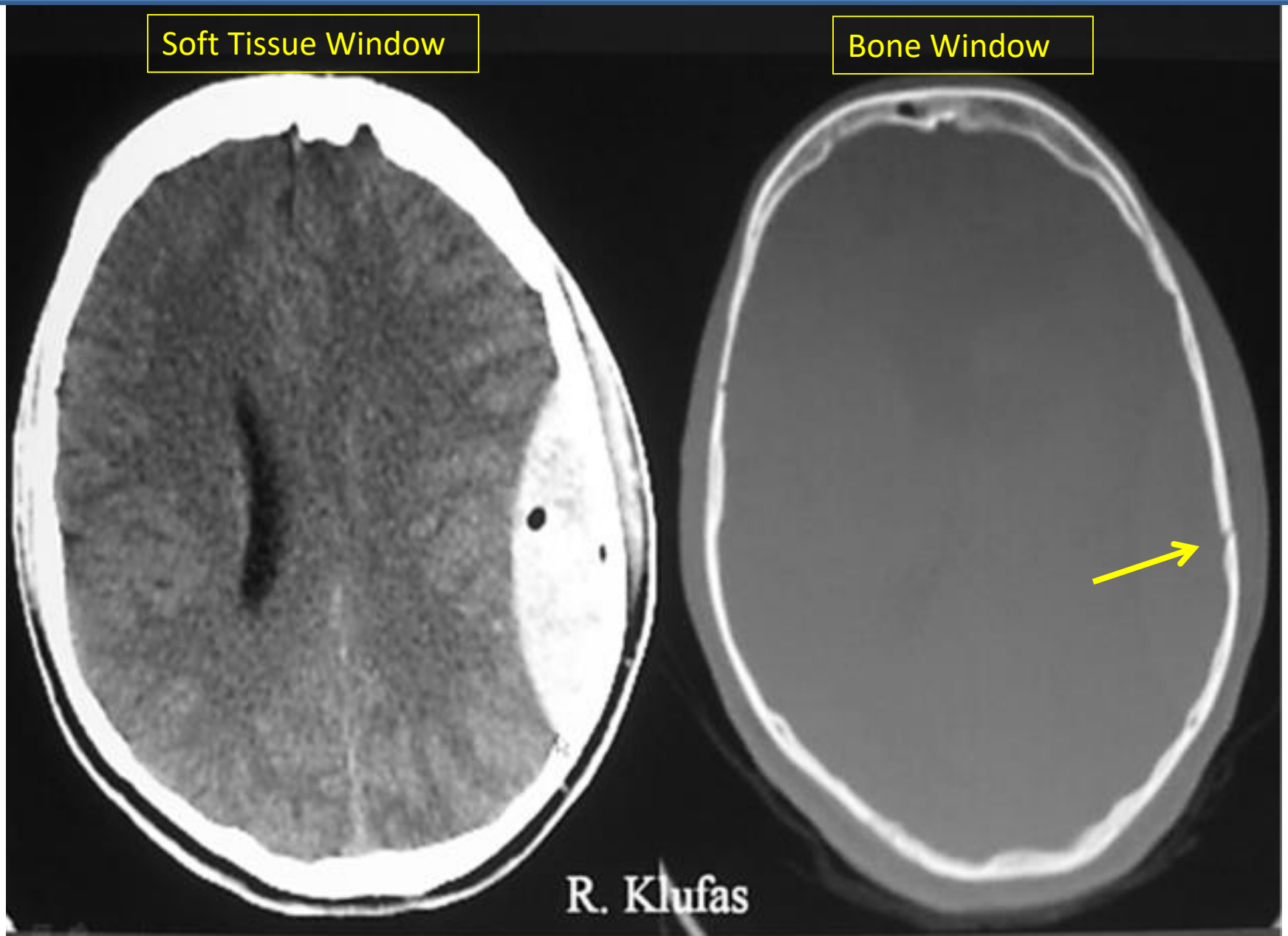

MRI and CT in Traumatic Brain Injury

Epidural vs. Subdural Hematoma

BJA British Journal of Anaesthesia

BJA › Volume 99, Issue 1 › Pp. 49-60.

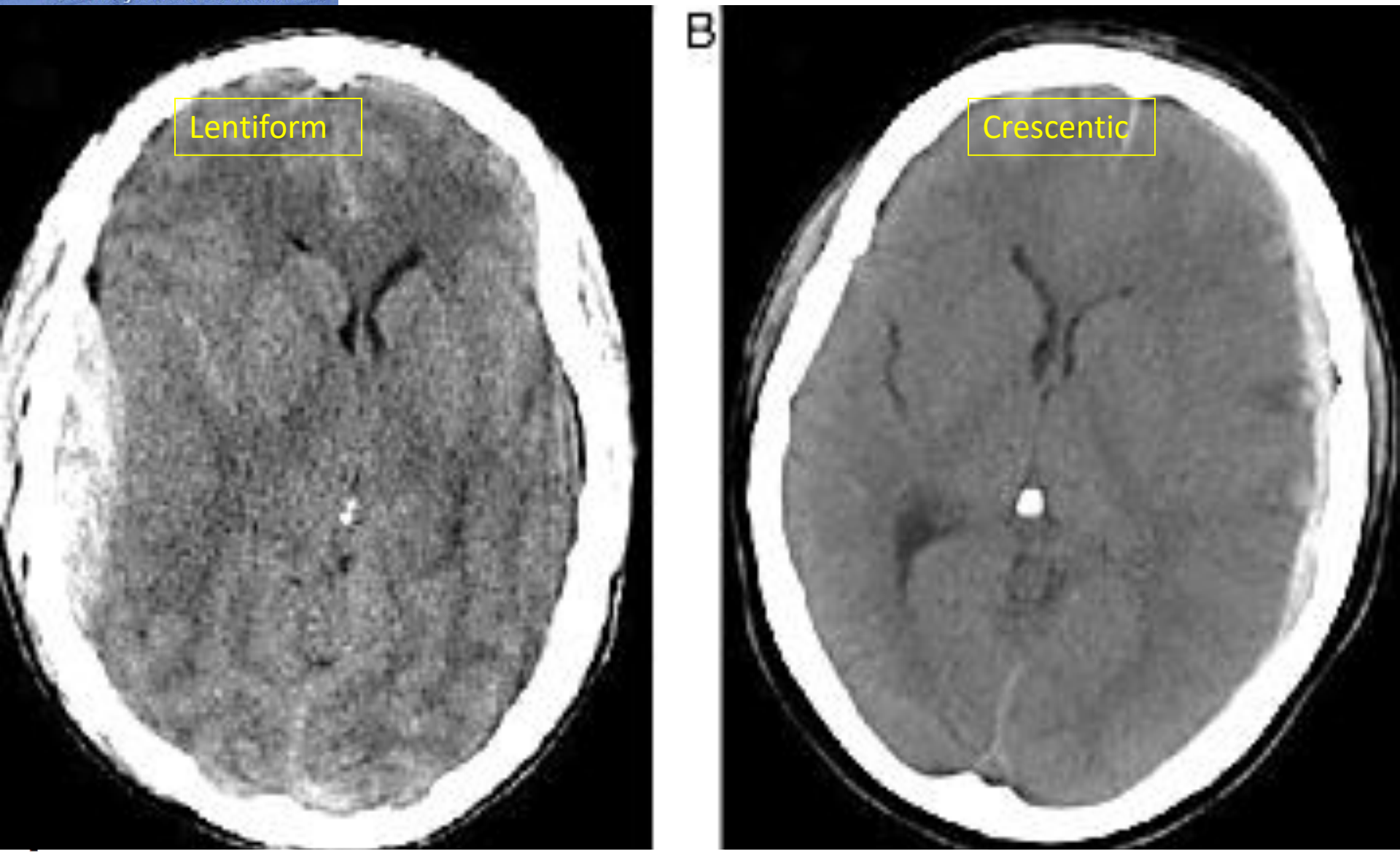

CT imaging of space-occupying lesions. (A) Right extradural haematoma. Bleeding occurs within the potential epidural space and is usually associated with a fracture. The expanding lesion has resulted in compression of the ipsilateral ventricle and midline shift. (B) Left subdural haematoma. Bleeding occurs between the arachnoid and inner meningeal layer of the dura. The underlying brain is swollen with cortical haemorrhagic contusion, compression of the ipsilateral ventricle, and midline shift. In

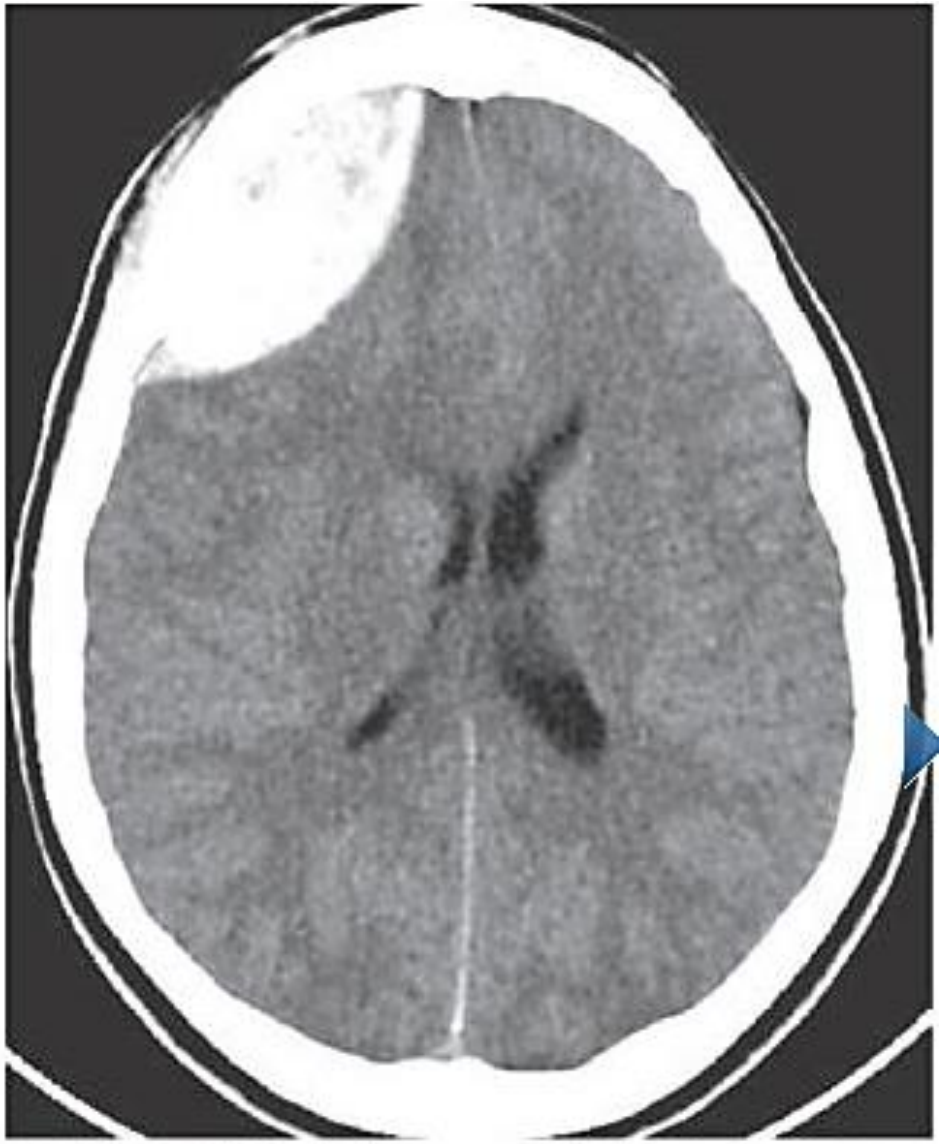

FIGURE 3.3. **Epidural Hematoma.** Axial CT scan demonstrates a biconvex high-attenuation extra-axial collection causing mass effect on the right frontal lobe and mild midline shift (subfalcine herniation). Note how the epidural hematoma does not extend beyond the right coronal suture.

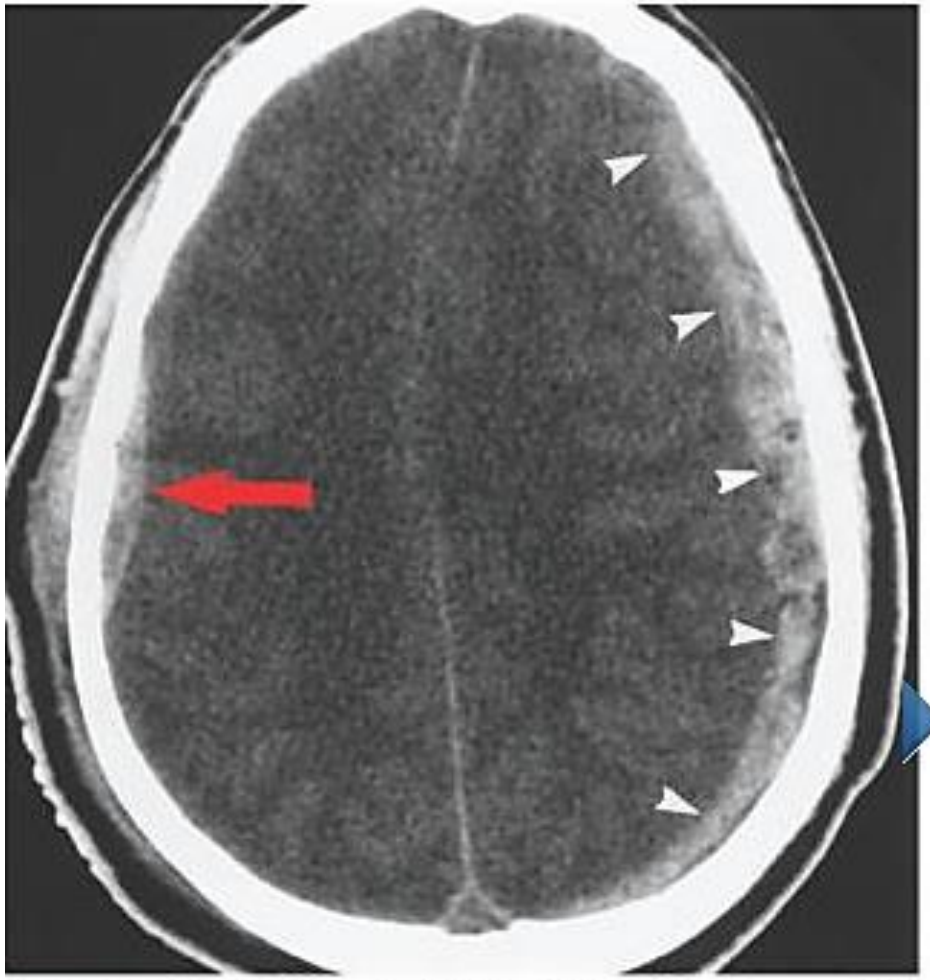

FIGURE 3.5. **Left Subdural and Right Epidural Hematomas.** Axial CT scan demonstrates a crescent-shaped high-attenuation collection extending along the entire left hemisphere consistent with a subdural hematoma (*arrowheads*). Compare the appearance with that of a small epidural hematoma seen on the right (*arrow*), where overlying scalp soft-tissue swelling is also present. (Reprinted with permission from Gean AD. Imaging of Head Trauma. Philadelphia: Lippincott Williams & Wilkins, 1994:120.)

The NEW ENGLAND JOURNAL of MEDICINE

IMAGES IN CLINICAL MEDICINE

Volume 344:580 February 22, 2001 Number 8

A 71-year-old man was pushed onto his back by a slow-moving vehicle. Initially, he was alert and fully oriented. In the emergency department, the patient was disoriented to place; the examination revealed no signs of injury, and coagulation studies were normal. Within 30 minutes after the initial evaluation, his neurologic status deteriorated. The axial section of a computed tomographic (CT) scan of the head, obtained without the addition of contrast

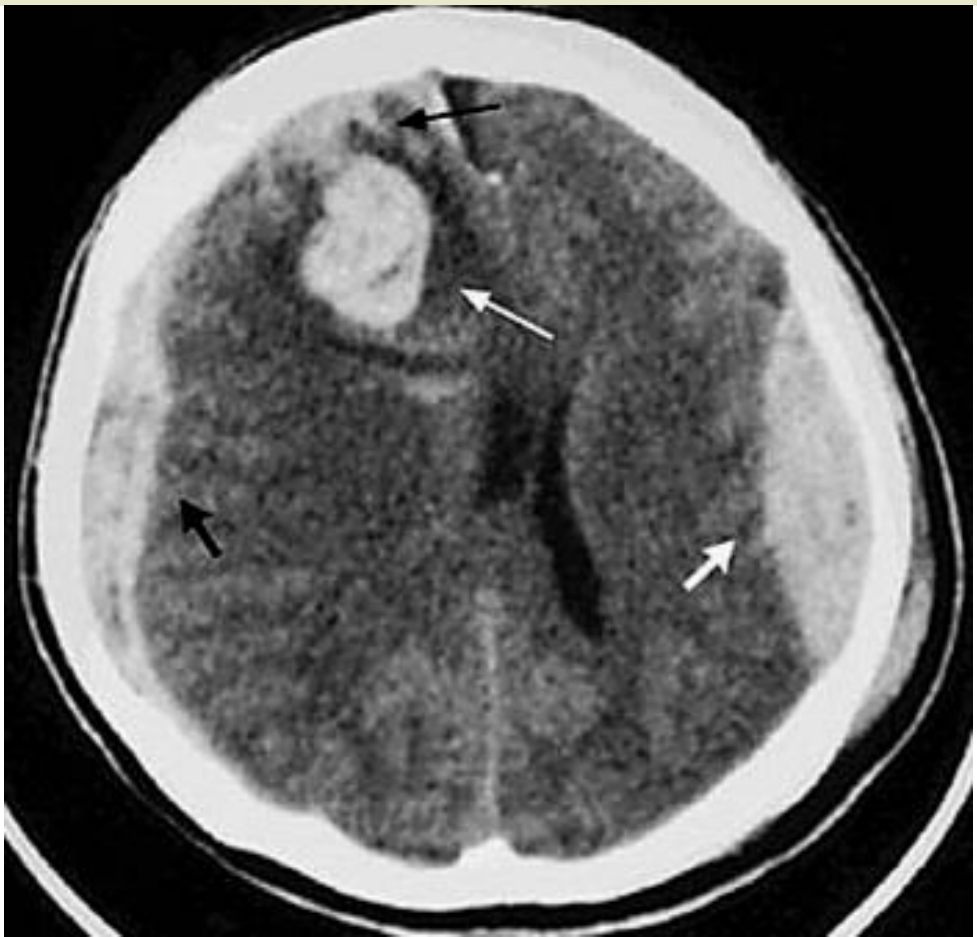

The NEW ENGLAND JOURNAL of MEDICINE

IMAGES IN CLINICAL MEDICINE

Volume 344:580 February 22, 2001 Number 8

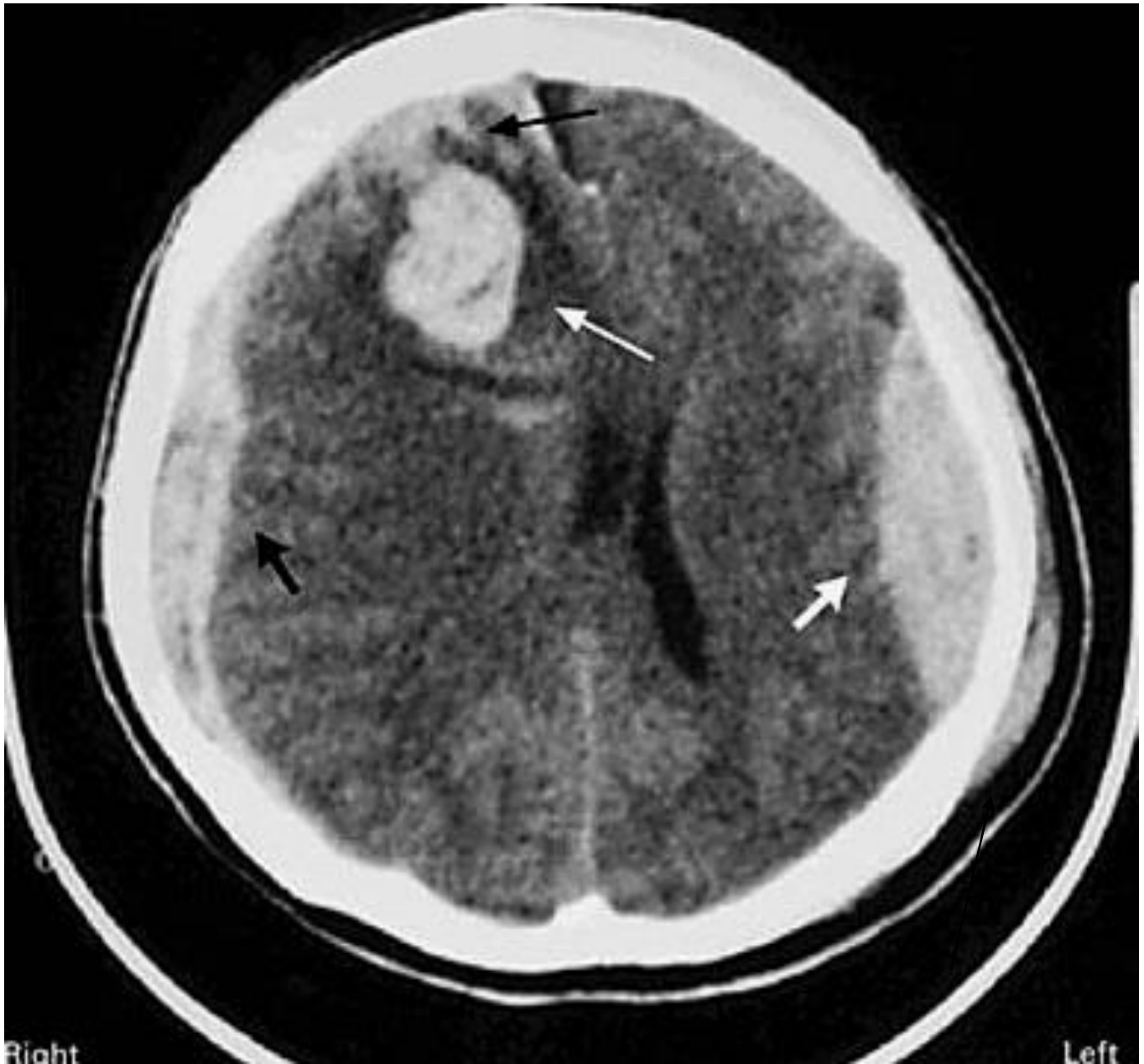

MRI and CT in Traumatic Brain Injury

Skull Base Fractures

MRI and CT in Traumatic Brain Injury

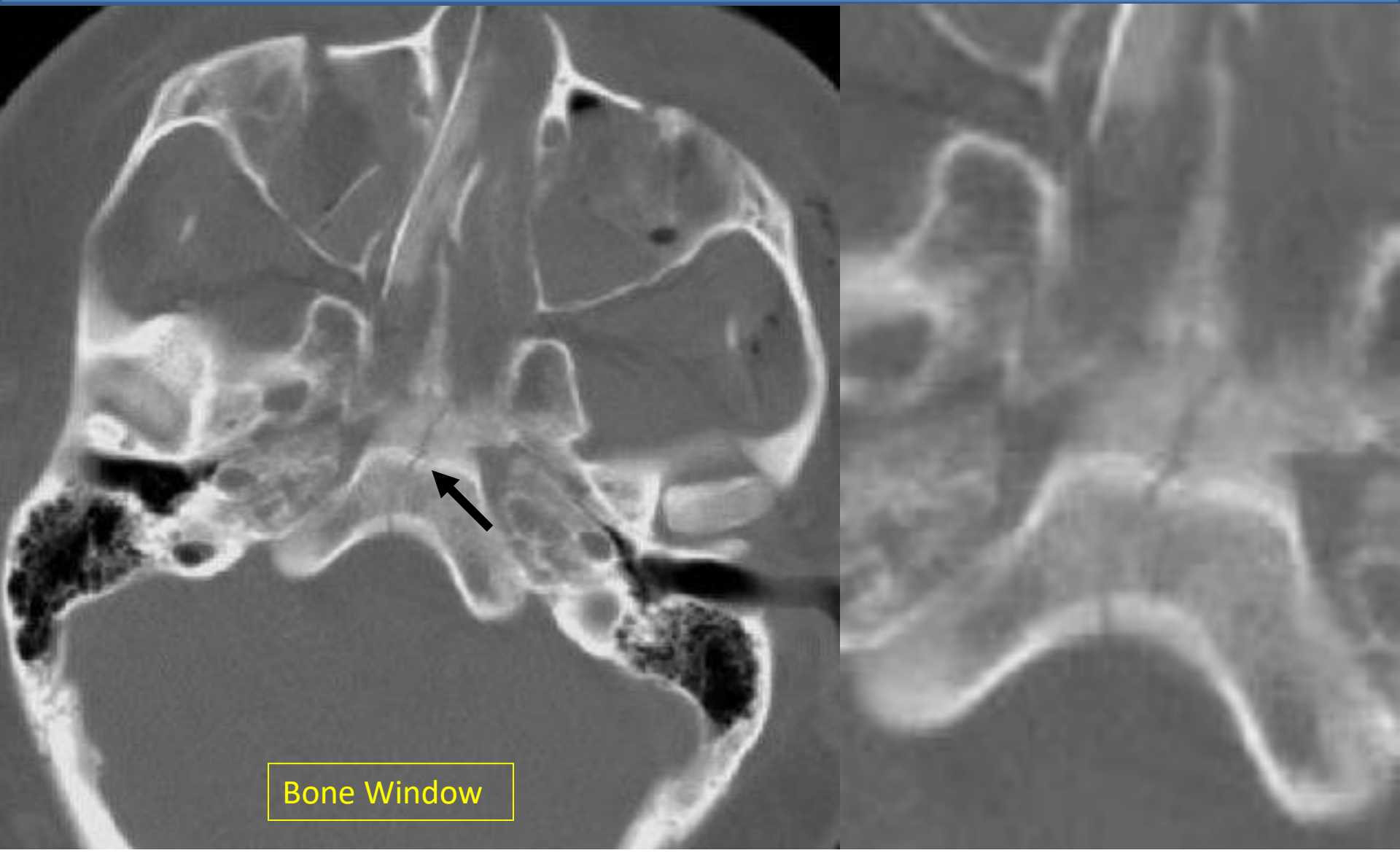

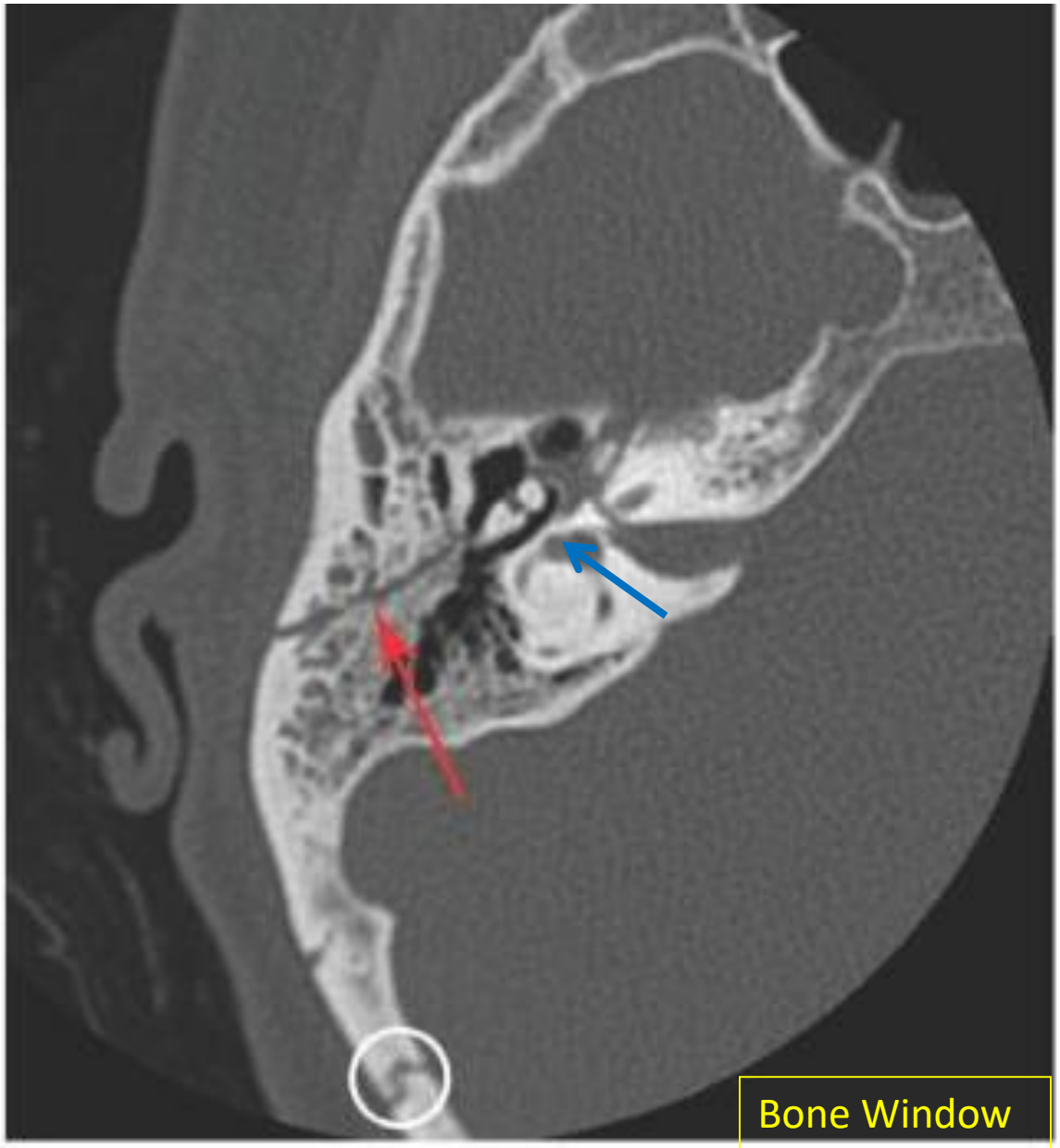

FIGURE 3.2. **Longitudinal Temporal Bone Fracture.** Axial CT image shows a right longitudinal temporal bone fracture (*arrow*) with associated incudomalleal dislocation. Diastasis of the right lambdoid suture (*circle*) is also present.

MRI and CT in Traumatic Brain Injury

Diffuse Axonal Injury (DAI)

- Due to acceleration/deceleration of the white matter + hypoxia
- Patients have severe LOC at impact
- Grade 1: axonal damage in WM only - 67%
- Grade 2: WM + corpus callosum (posterior > anterior) - 21%
- Grade 3: WM + CC + brainstem - 12%

MRI and CT in Traumatic Brain Injury

Diffuse Axonal Injury (DAI)

- Rarely detected on CT (20% of DAI lesions are hemorrhagic)
- MRI: T1, T2, DWI, T2 GRE, SWI

MRI and CT in Traumatic Brain Injury

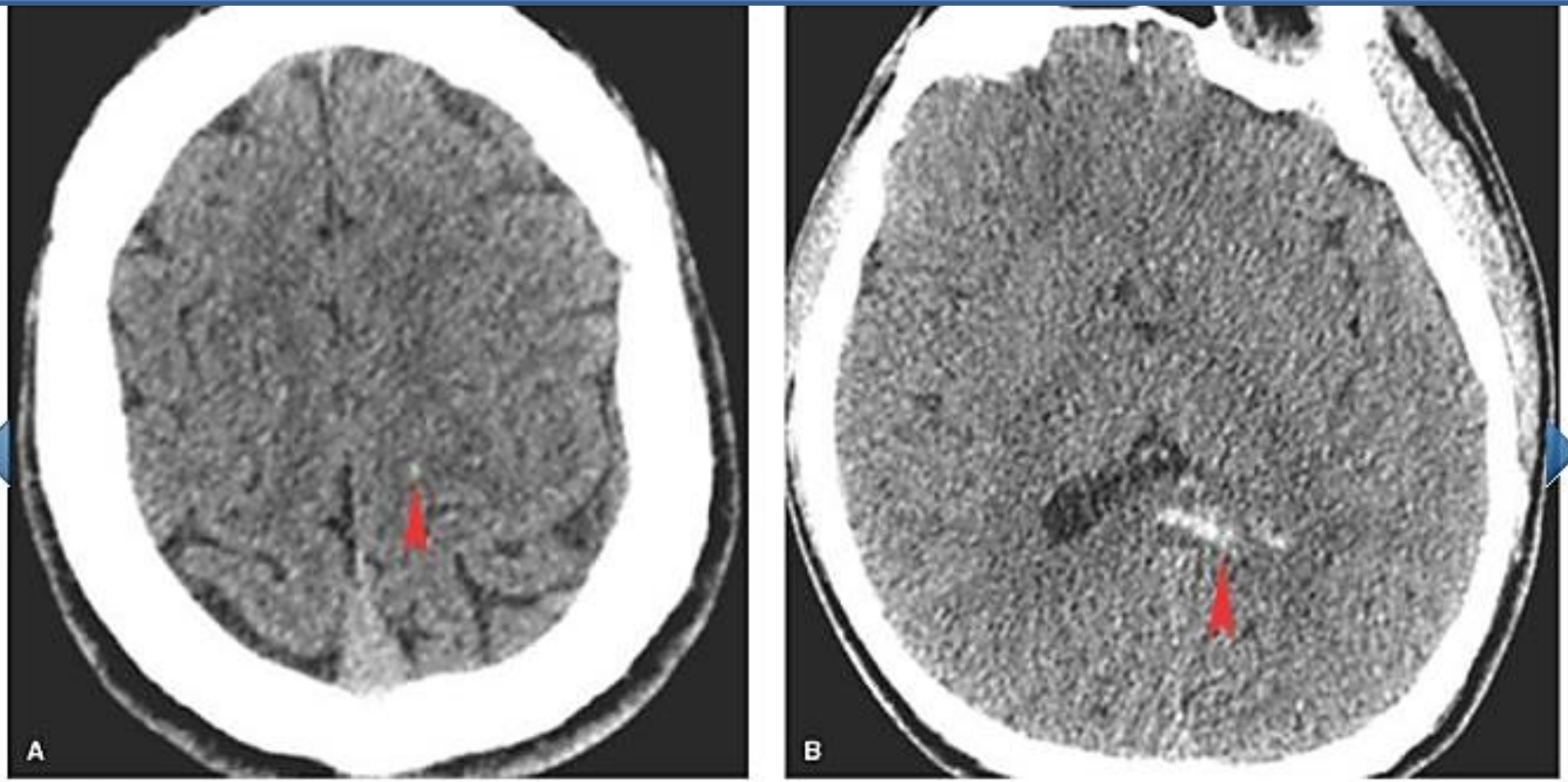

FIGURE 3.13. **The CT Appearance of Diffuse Axonal Injury.** Noncontrast CT images show a punctate high attenuation focus (*arrowhead*) within the left frontal subcortical white matter (A) and mixed linear and amorphous high attenuation (*arrowhead*) within the left splenium of the corpus callosum (B), consistent with hemorrhagic diffuse axonal injury.

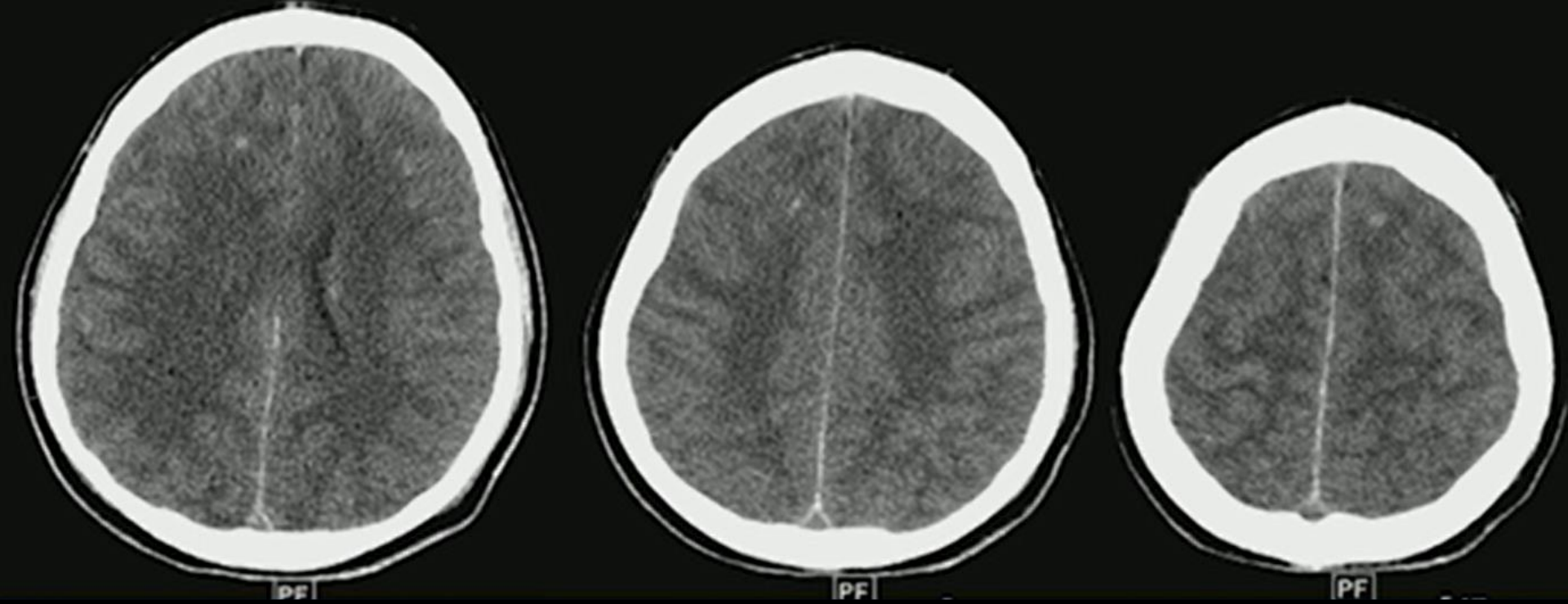
PF
PF
PF

MRI and CT in Traumatic Brain Injury

MRI in TBI Patients

Magnetic Resonance Imaging

Magnetic resonance imaging (MRI) is usually not feasible in acute injuries in terms of availability and time.[38] It is, however, far superior to CT in detecting lesions of brain tissue and is particularly recommended when CT offers no explanation for neurologic deficits.[39]

MRI and CT in Traumatic Brain Injury

MRI in TBI Patients

1983

- T1W Images
- PD/T2W Images

2019

- T1W Images
- PD/T2W Images
- Diffusion Weighted Images
- T2 FLAIR Images
- T1 FLAIR Images
- GRE/SWI
- DTI/FiberTracking
- NeuroQuant
- Arterial Spin Labeling
- MR Angiography

MRI and CT in Traumatic Brain Injury

What does MRI add to CT in TBI?

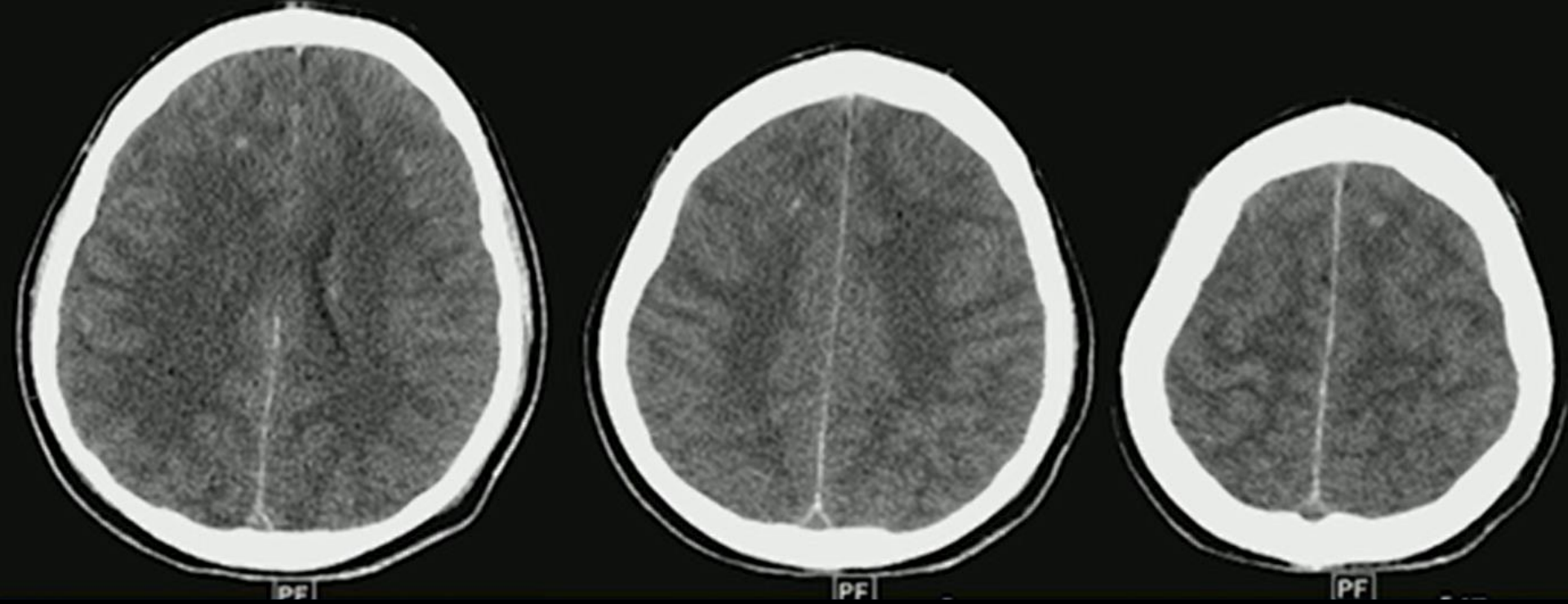
PF
PF
PF

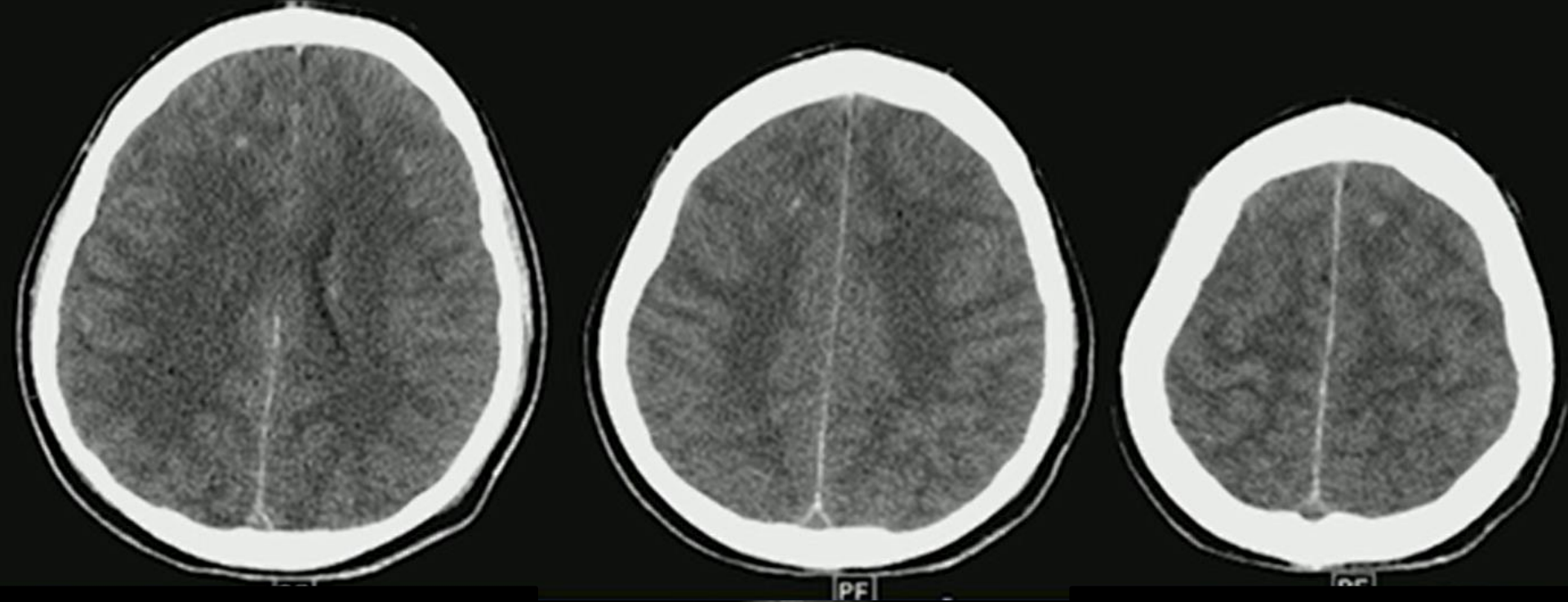

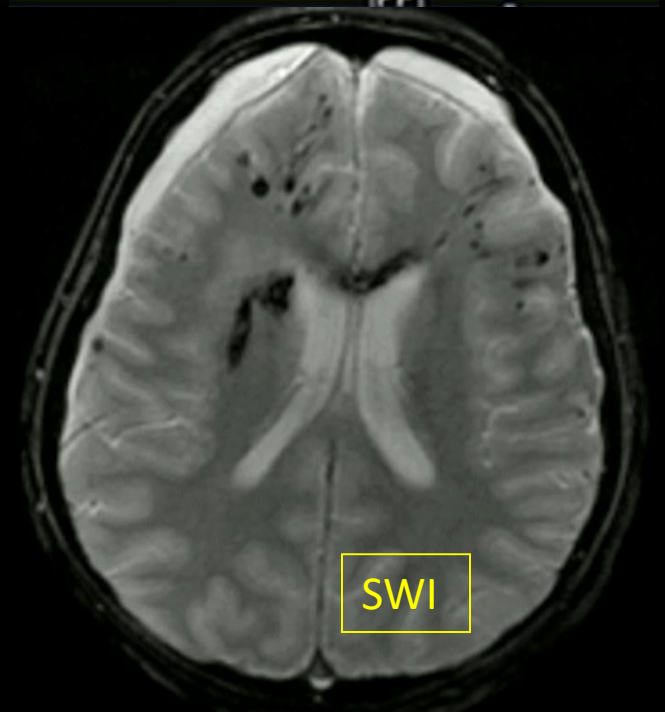
SWI

ANNALS of Neurology
THE OFFICIAL JOURNAL OF THE AMERICAN NEUROLOGICAL ASSOCIATION AND THE CHILD NEUROLOGY SOCIETY
ANN NEUROL 2012;00:000–000

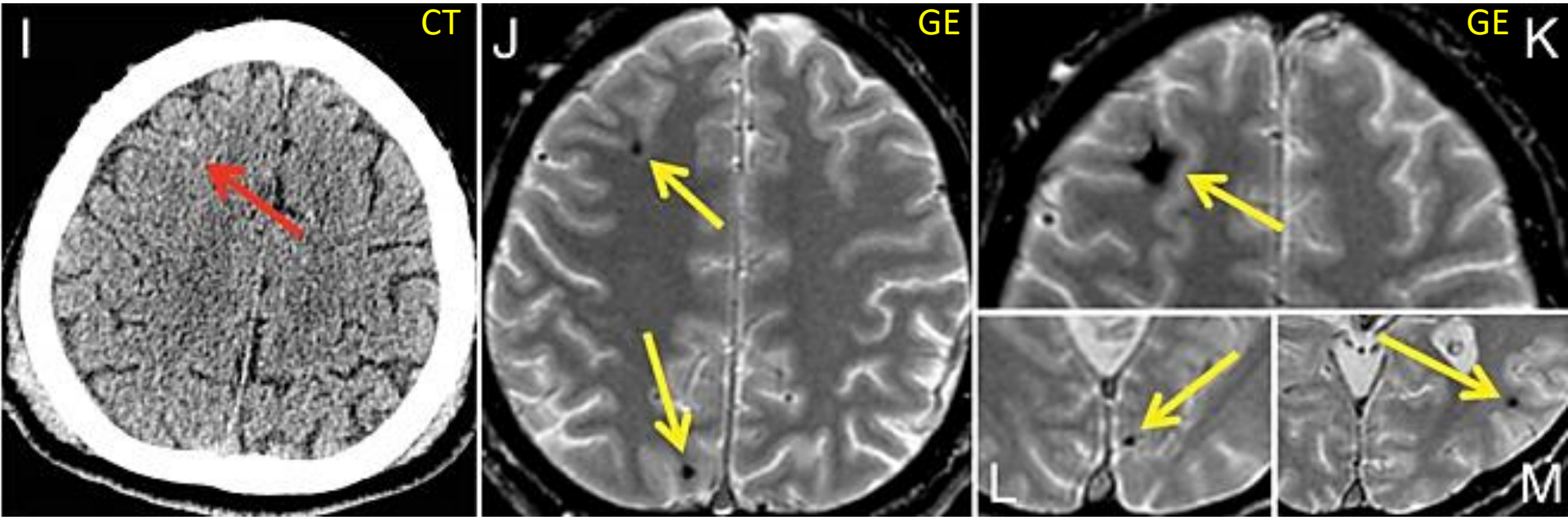

Fifty-four-year-old man after fall off bicycle. (I) CT was interpreted as demonstrating trace right frontal subarachnoid hemorrhage (*red arrow*). (J–M) T2*-weighted gradient echo MRI demonstrated numerous discrete foci of subcortical white matter signal loss (*yellow arrows*), consistent with hemorrhagic axonal injury and with the Traumatic Brain Injury Common Data Element (TBI-CDE) definition of diffuse axonal injury (≥4 visible discrete areas of axonal injury).

Stage	Areas Affected
I	- parasagittal regions of the frontal lobes - periventricular temporal lobes - internal and external capsules - cerebellum
II	Stage I areas + corpus callosum
III	Stage I + Stage II areas + dorsolateral quadrants of the rostral brain stem

MRI and CT in Traumatic Brain Injury

Diffusion Weighted Imaging (DWI)
in TBI

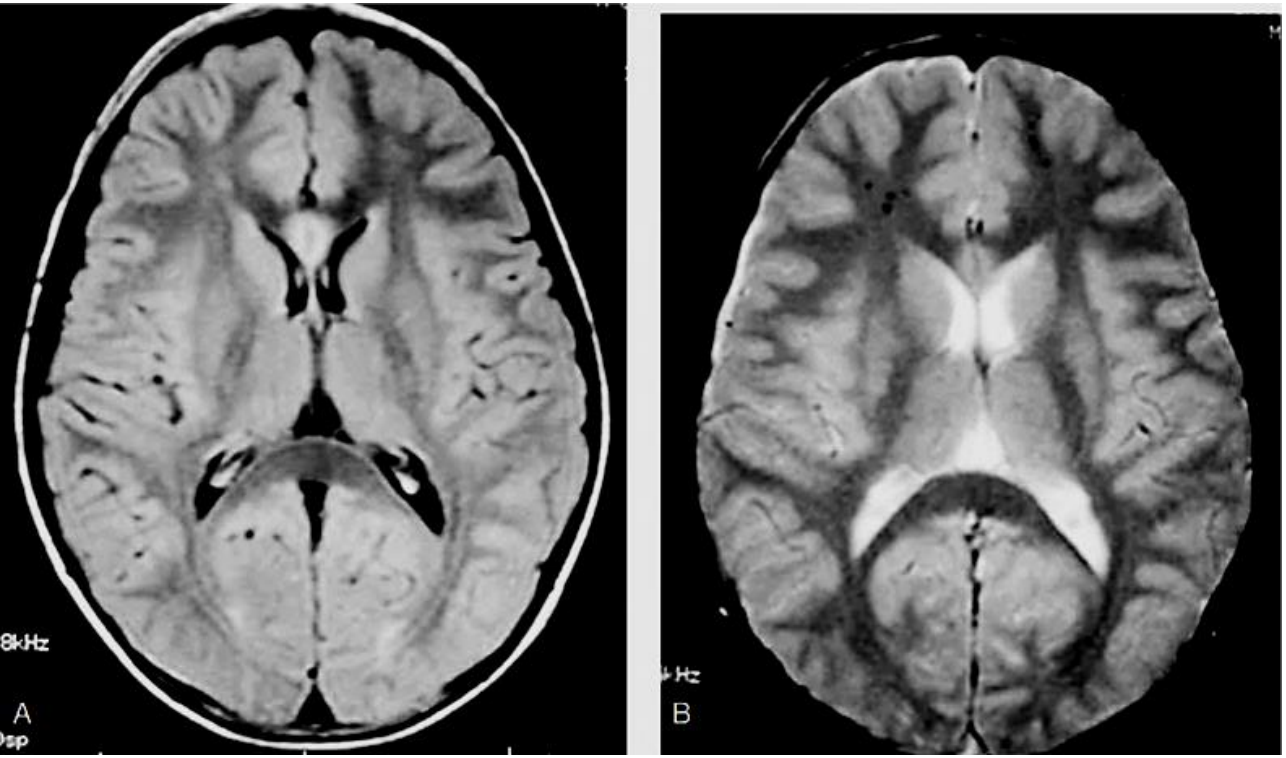

Fig. 1. A 42-year-old man who was a passenger in a traffic accident. MRI was performed 2 days after the accident.

Acta Radiol 2006;47:733–740.

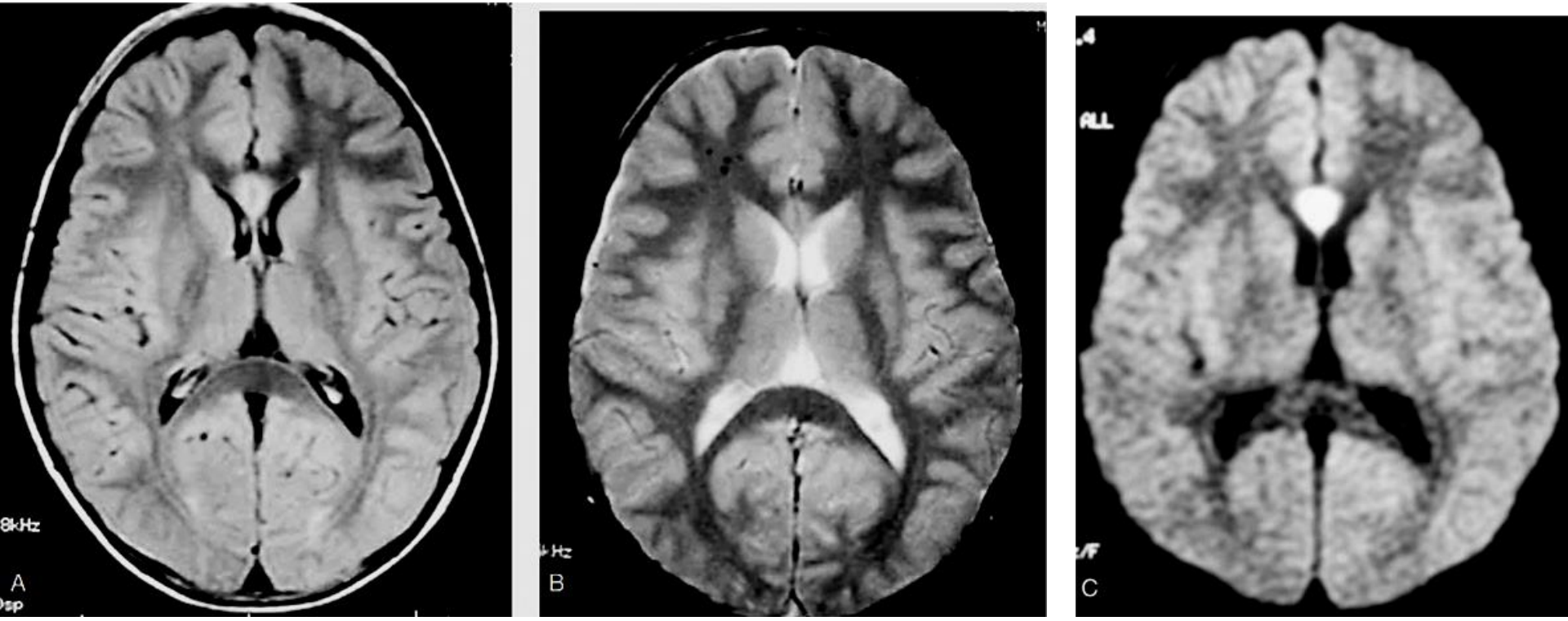

Fig. 1. A 42-year-old man who was a passenger in a traffic accident. MRI was performed 2 days after the accident. FLAIR and DWI (A and C) show hyperintensity within the corpus callosum. T2*-weighted GE imaging (B) shows no definite abnormality within the corpus callosum, but reveals hypointensities of bilateral frontal white matter.

MRI and CT in Traumatic Brain Injury

SWI vs. GRE

SW is 3-4x more sensitive than GRE for the detection of susceptibility effects.

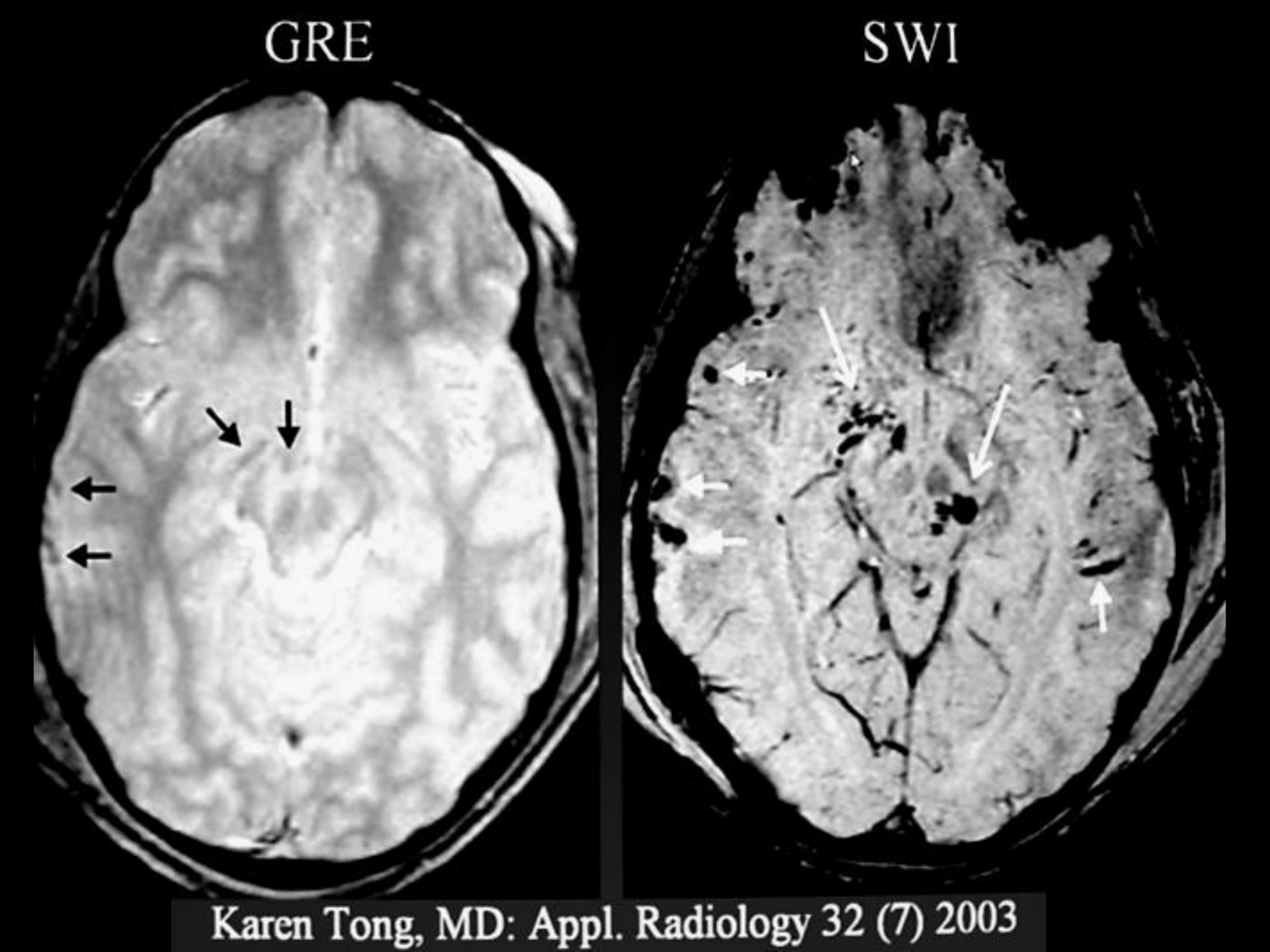
GRE
SWI
Karen Tong, MD: Appl. Radiology 32 (7) 2003

MRI and CT in Traumatic Brain Injury

1.5 SWI 3T

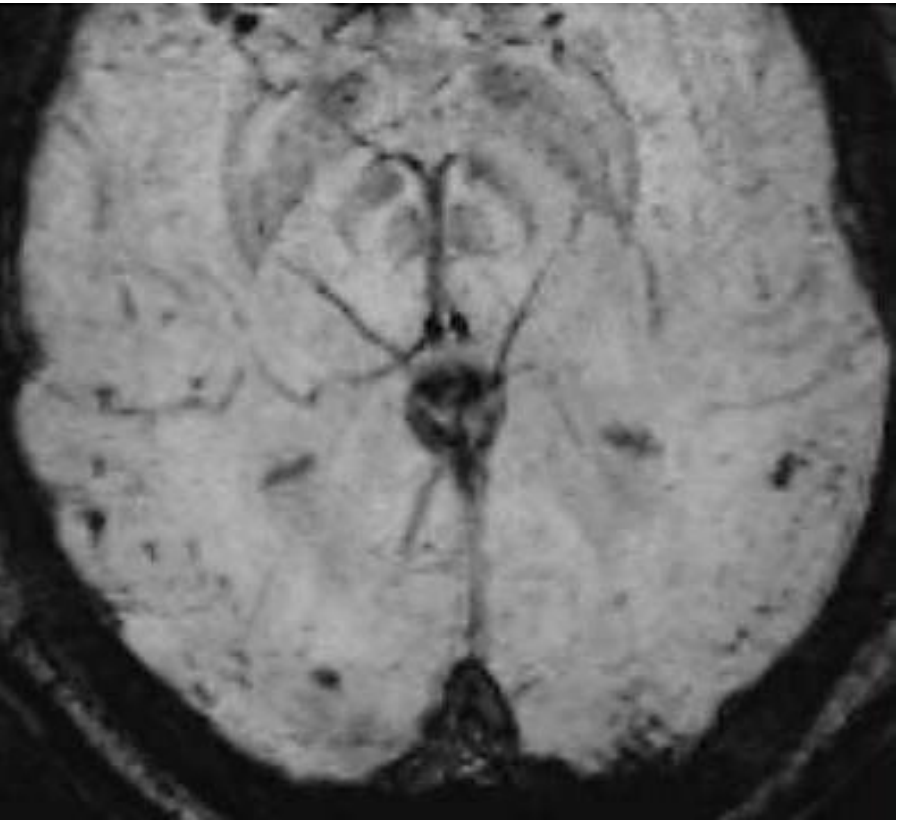

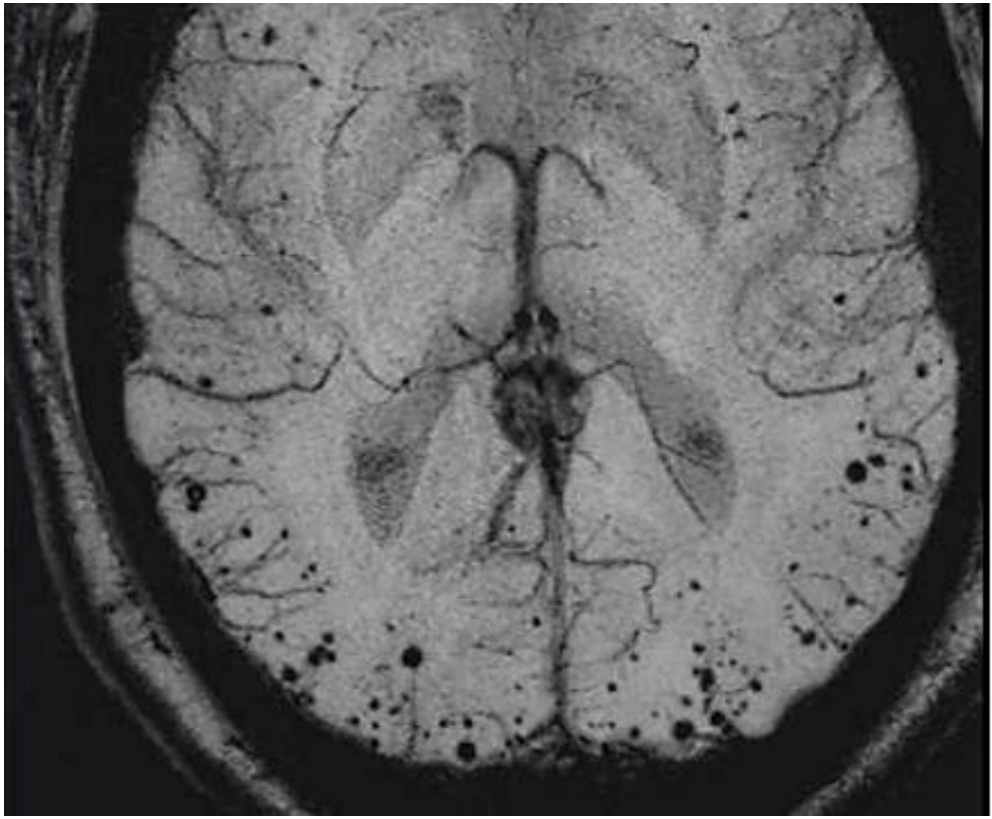

MRI and CT in Traumatic Brain Injury

38Y Male s/p Closed Head Trauma (Motorcycle Accident)

Insomnia, Altered Circadian Rhythms

T1 FLAIR

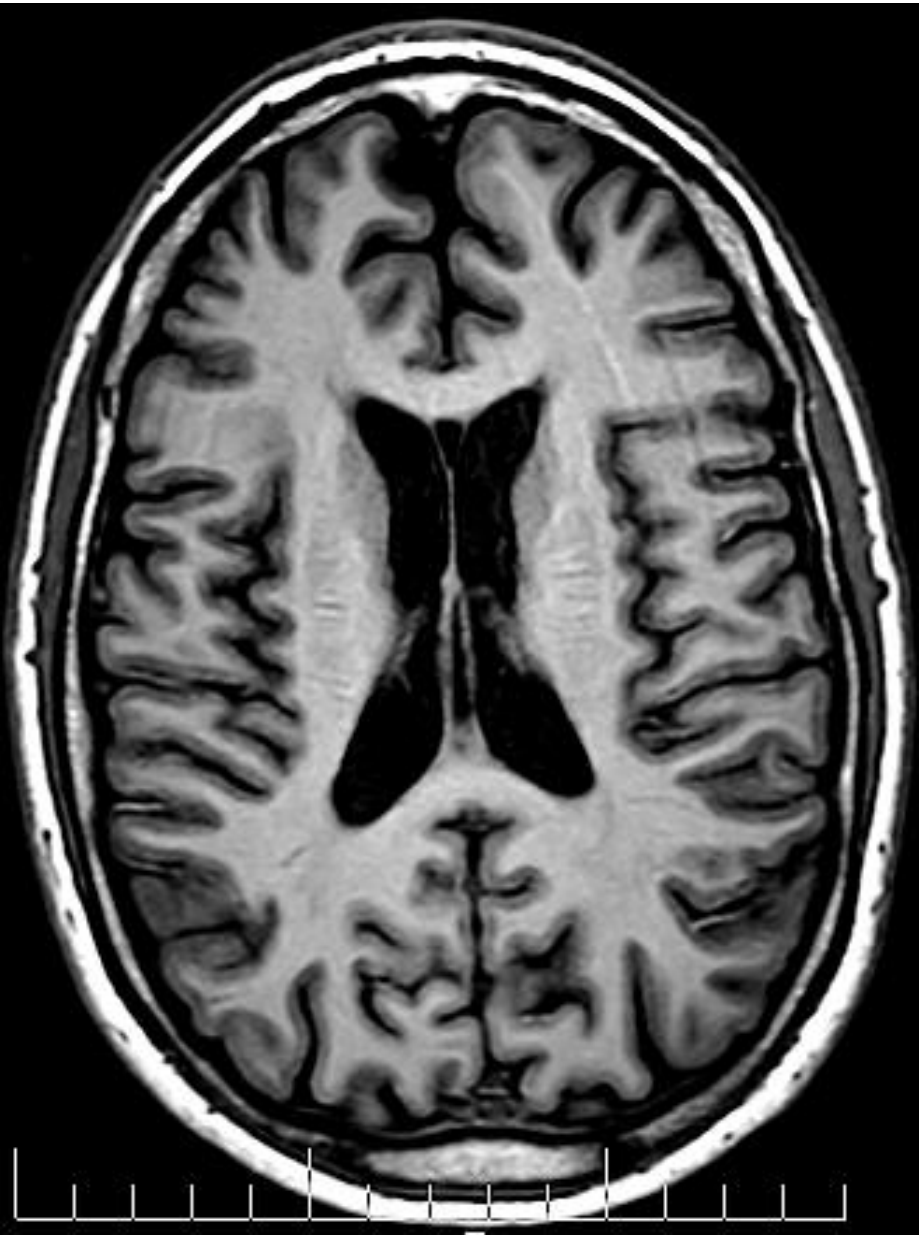

T2W

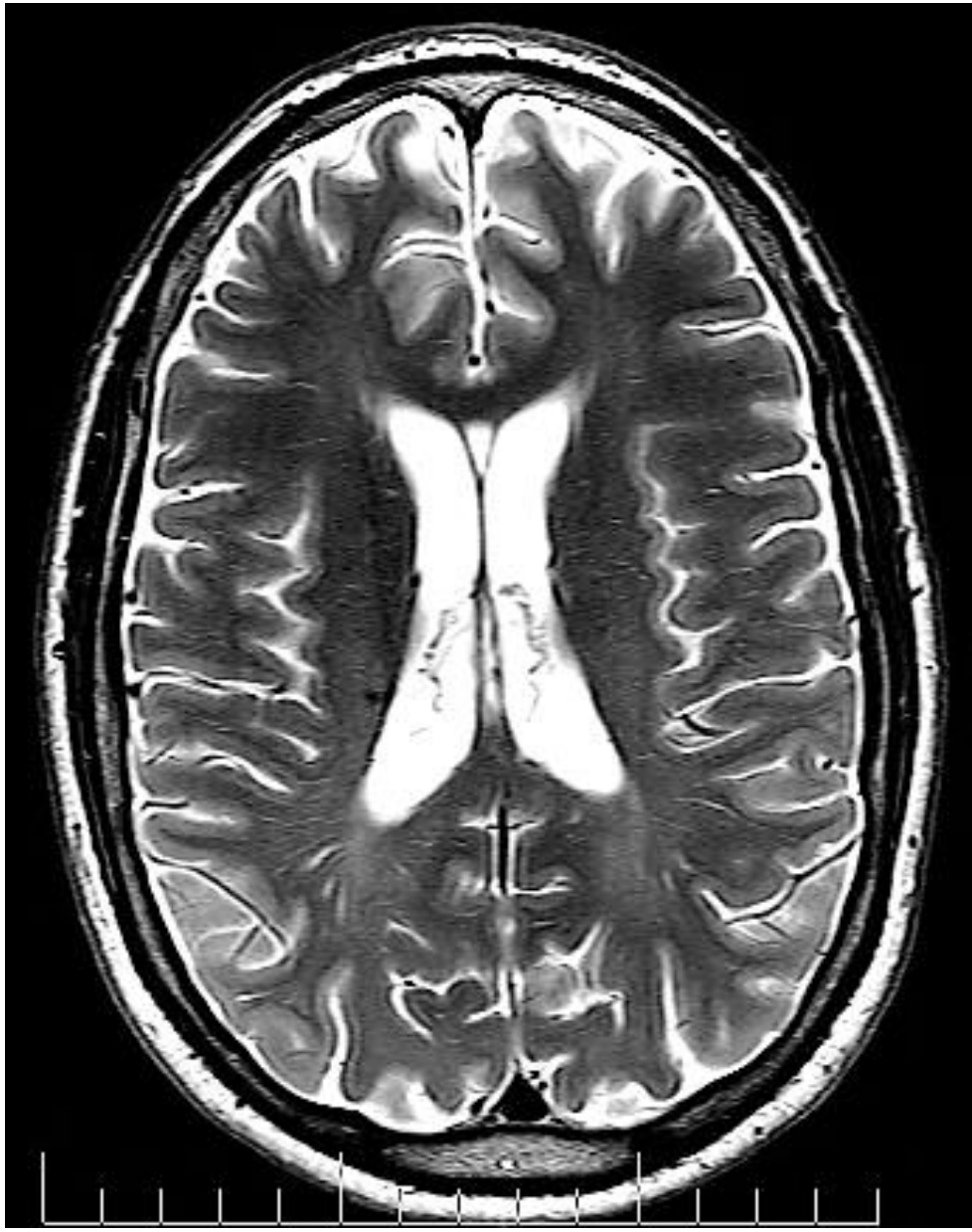

3T MRI Images

T1 FLAIR

T2W

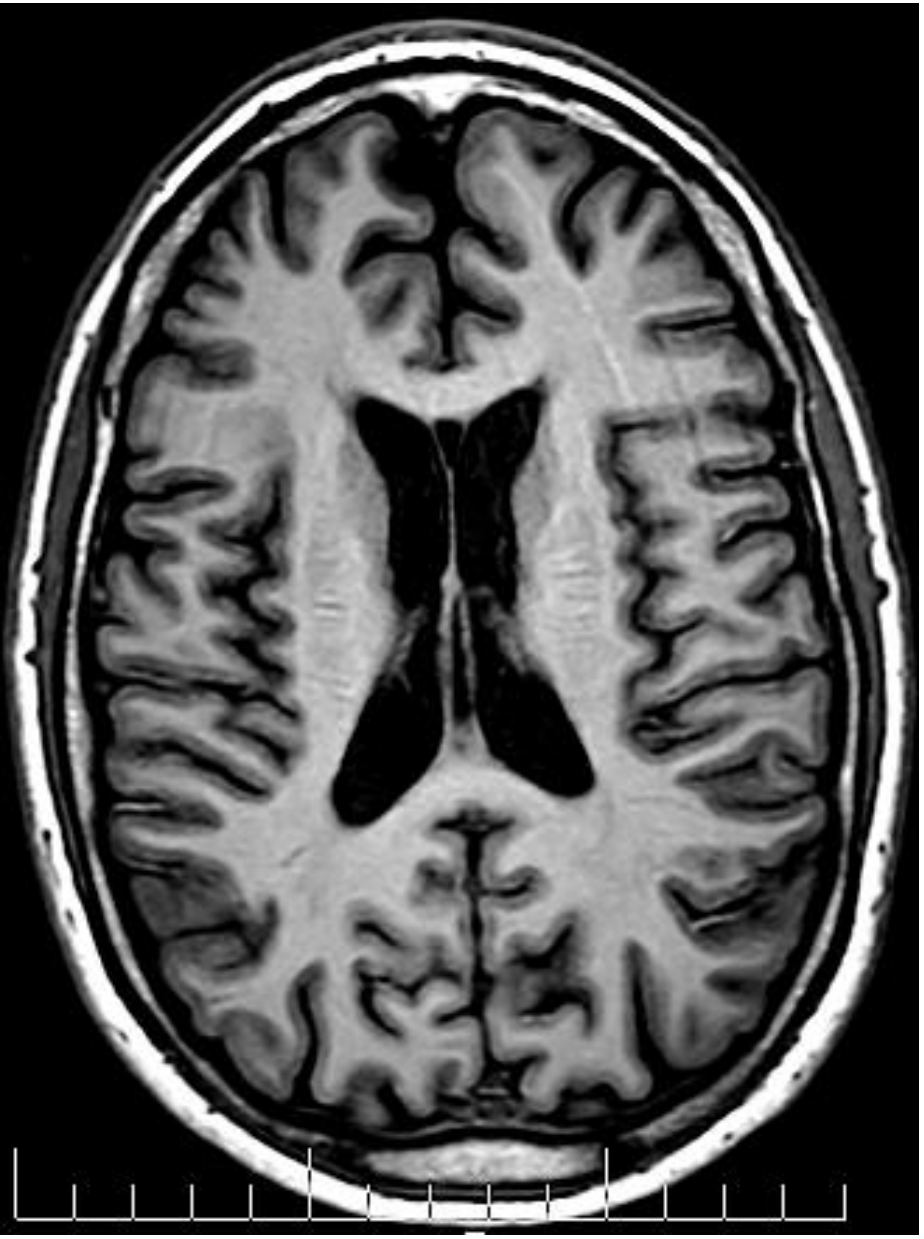

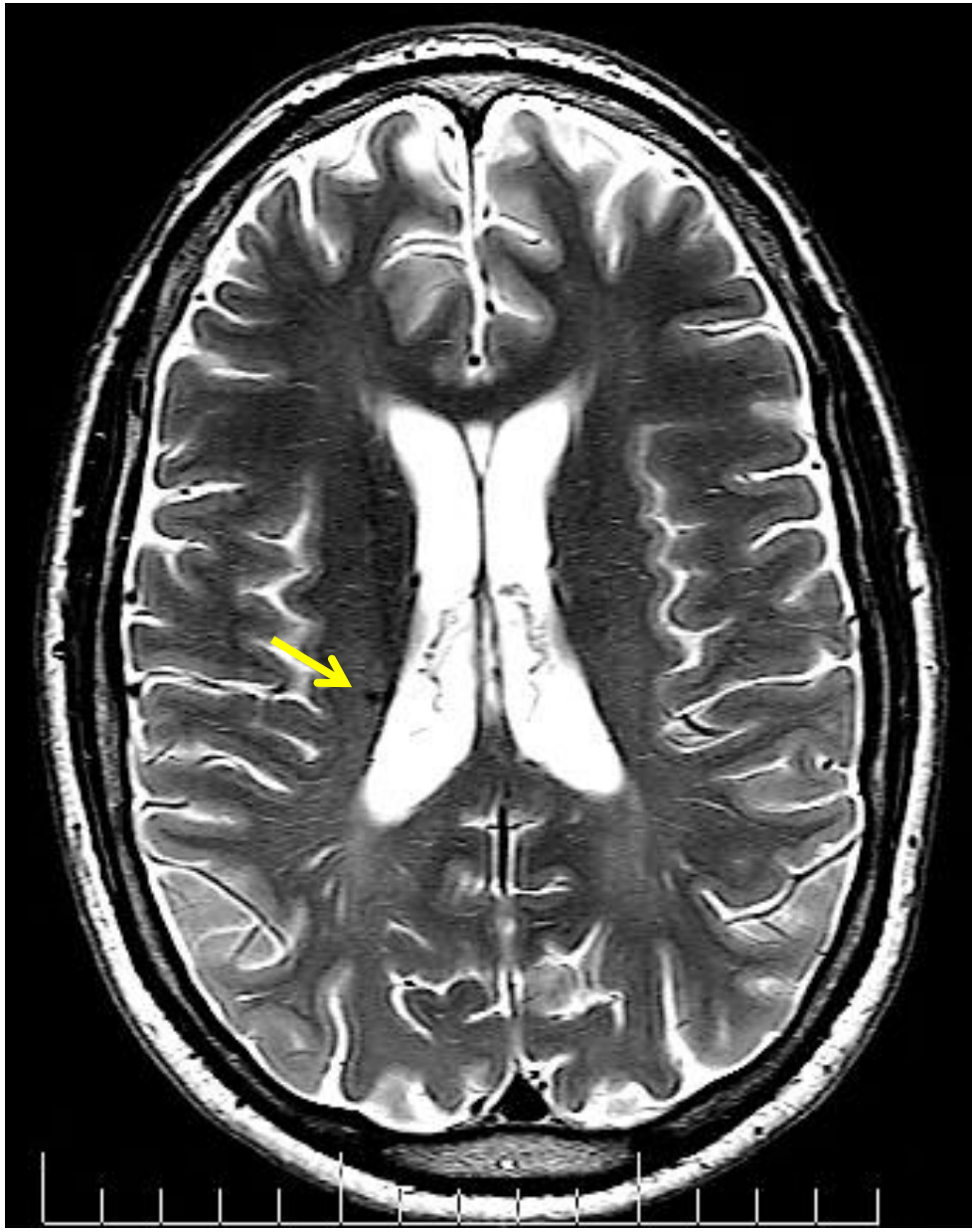

3T MRI Images

T2W

SWI

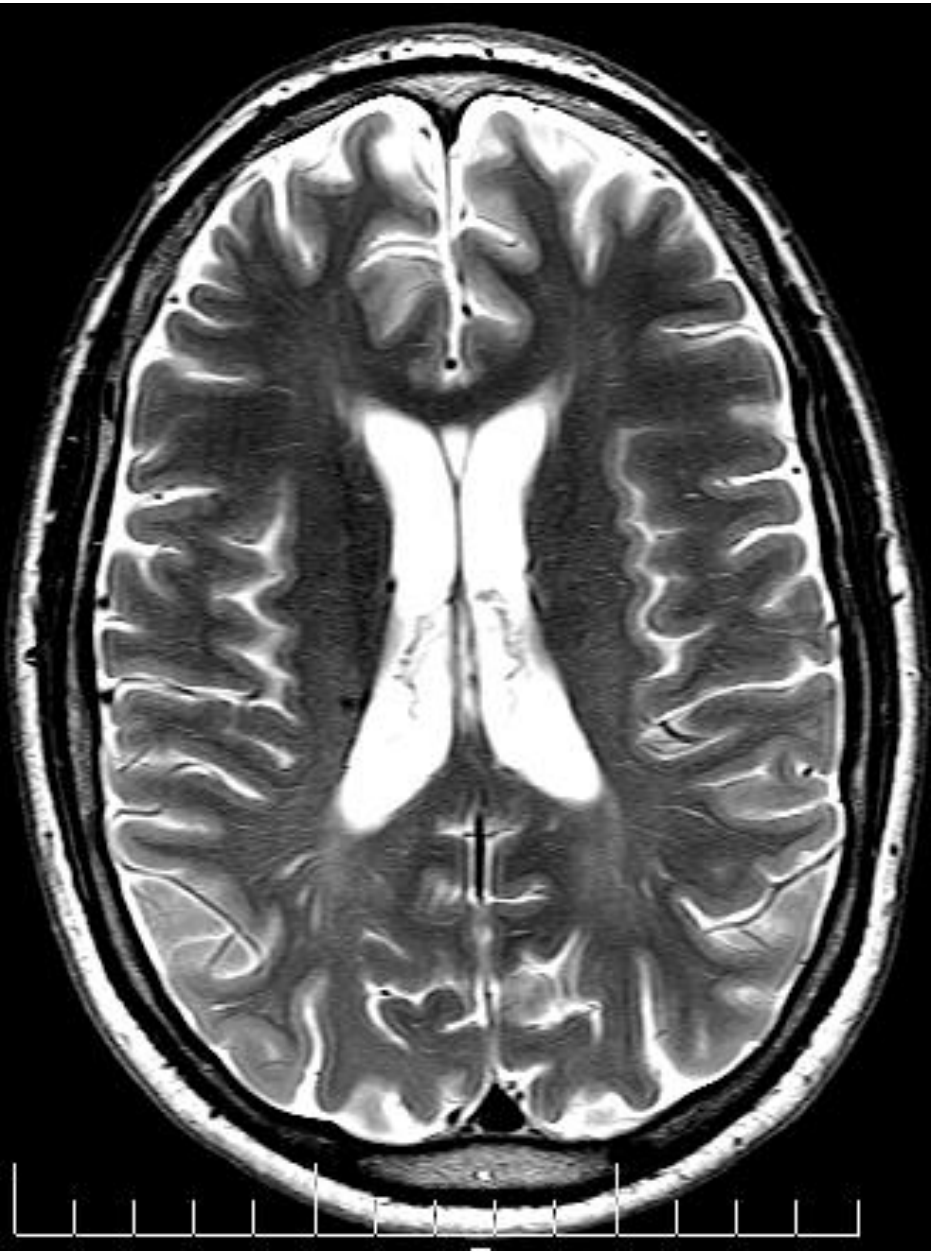

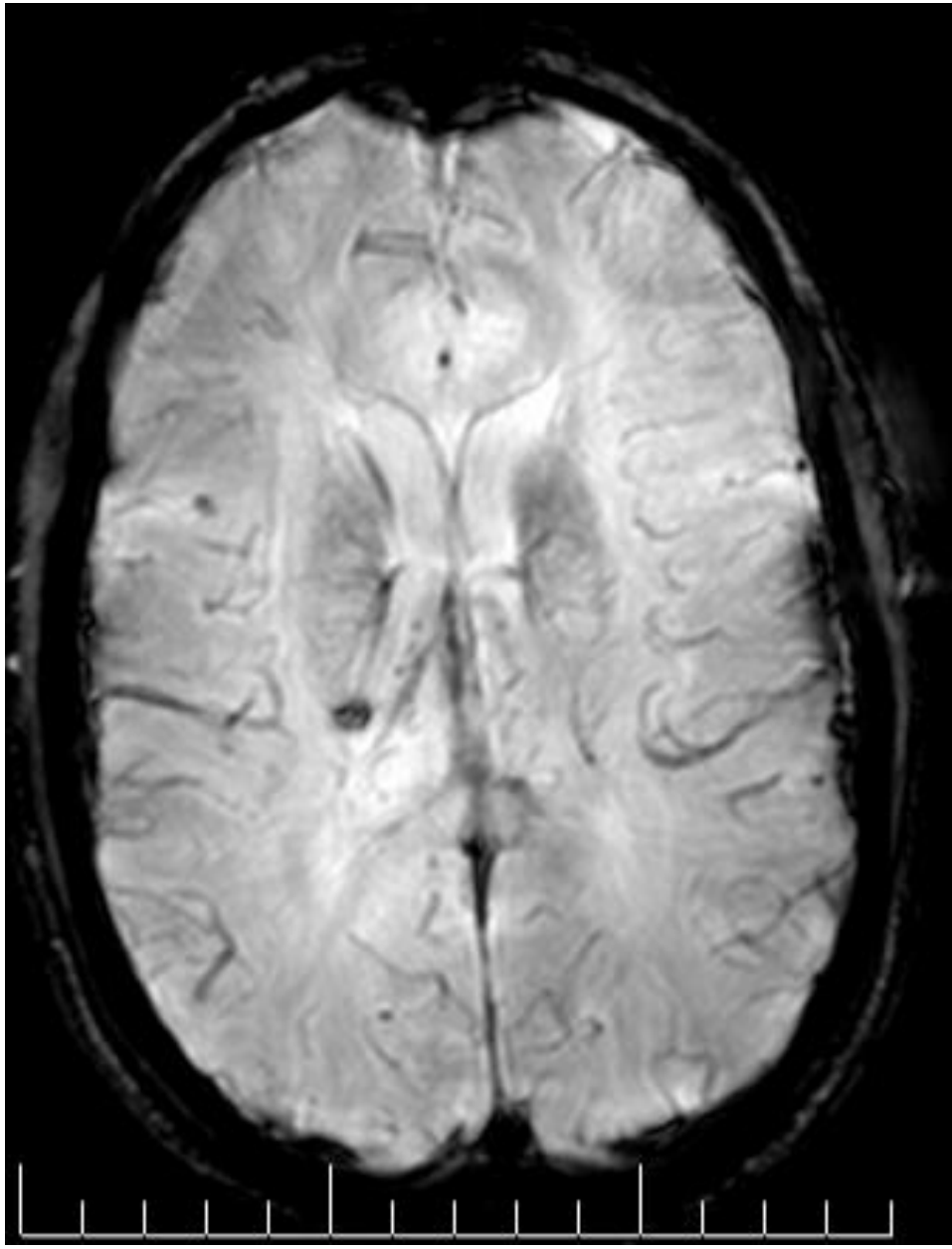

3T MRI Images

T2W

SWI

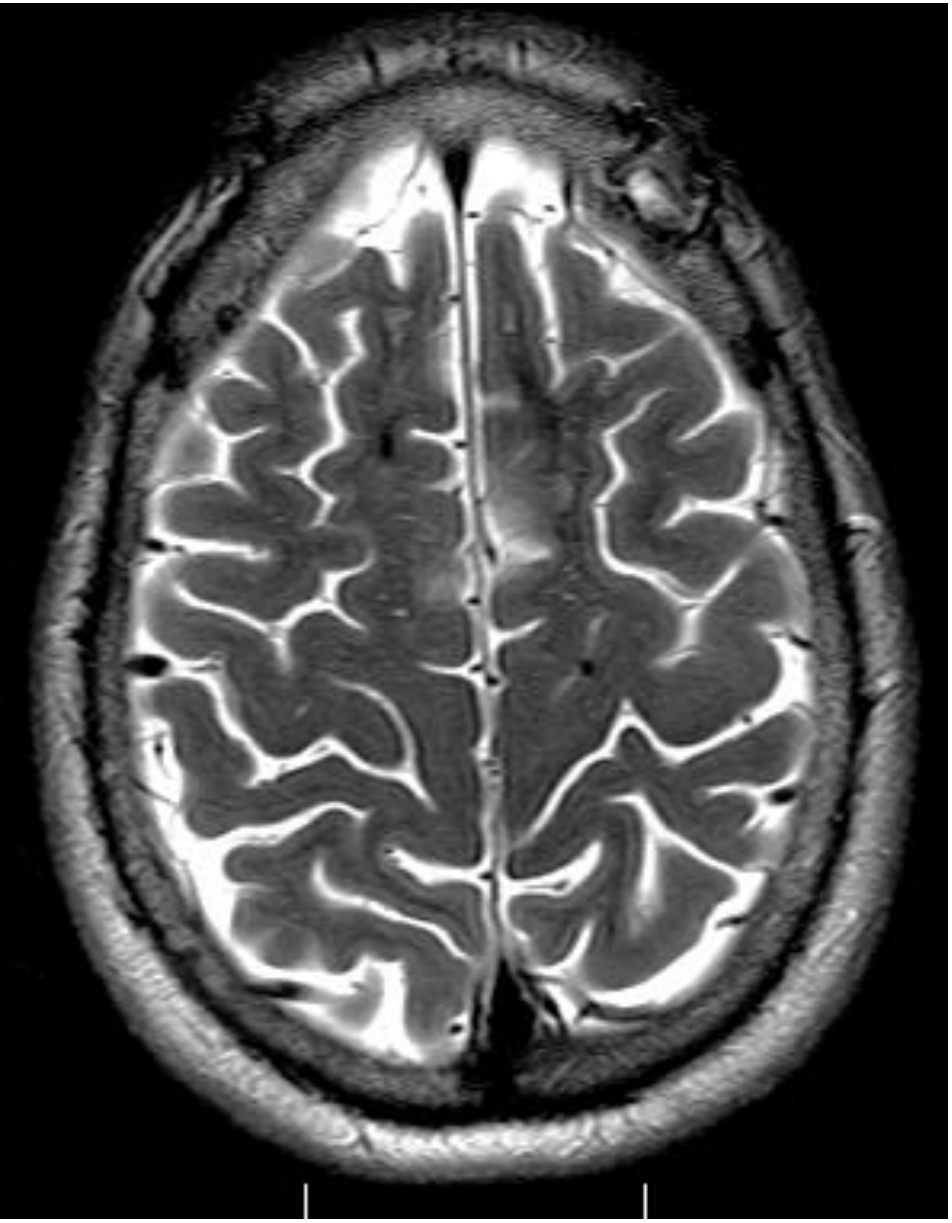

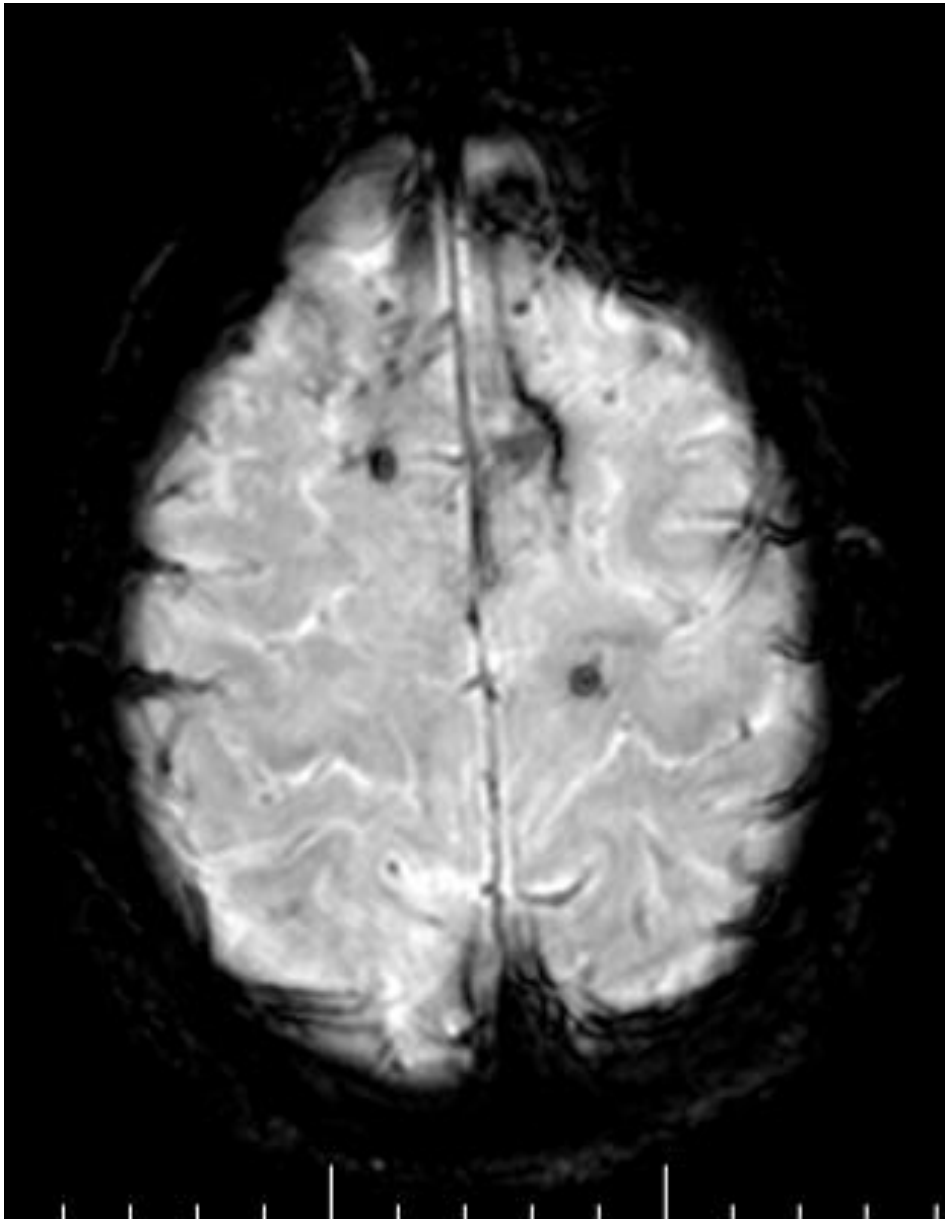

3T MRI Images

MRI and CT in Traumatic Brain Injury

3T DTI/FiberTracking in TBI

MRI and CT in Traumatic Brain Injury

Why do we need DTI/FiberTracking?

Conventional MRI cannot reveal detailed anatomy of the white matter. On routine MRI scans the white matter looks homogeneous because it is homogeneous with respect to chemical composition (water concentration, T1 and T2 values). Diffusion Tensor Imaging (DTI) can generate contrasts that are sensitive to fiber orientation.

MRI and CT in Traumatic Brain Injury

The diffusion of water molecules in biologic tissues can be measured using MR gradients and diffusion weighted sequences. Water molecules are “tagged” with a very short gradient pulse. The magnetization and phase of water molecules can measured and used for localization and therefore the determination of diffusion.

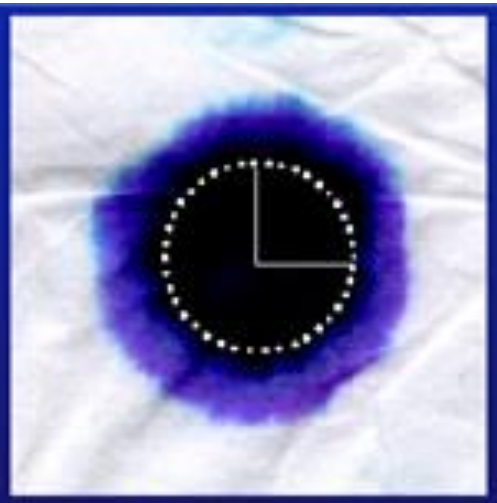

Kleenex

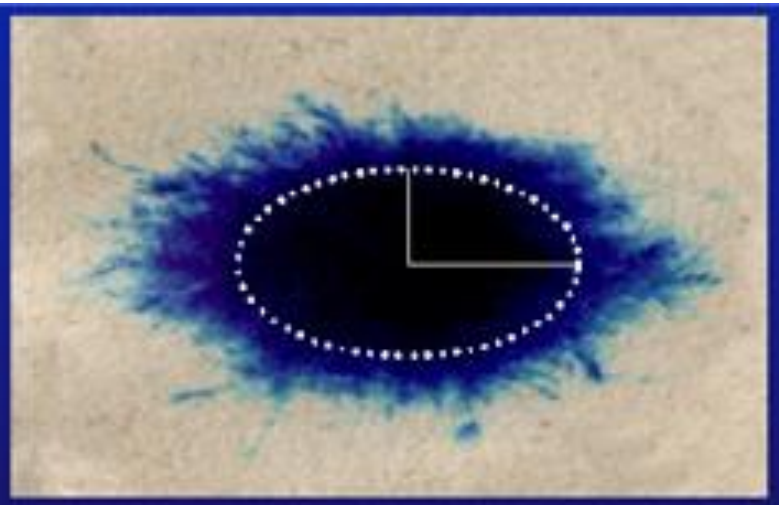

newspaper

- Anisotropy: diffusion rate depends on direction

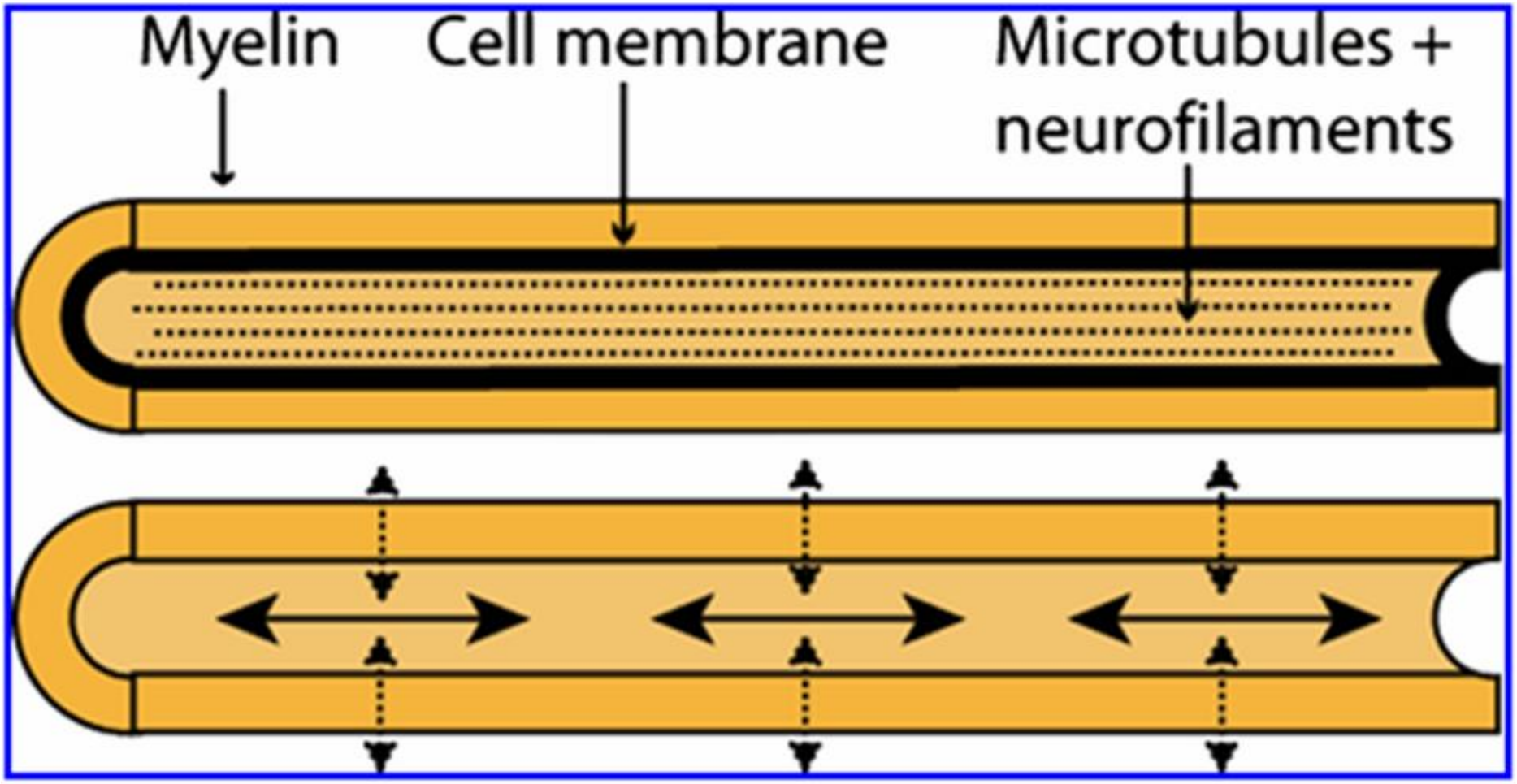

Diffusion perpendicular to axon bundles is hindered by axonal cell membranes and myelin sheaths whereas it is unrestricted along them. Within axons, the diffusion of water will be greater parallel to the fibers.

When diffusion exhibits a preferential direction, it is termed anisotropic.

Fractional Anisotropy (FA) is a measure of the degree of anisotropy.

MRI and CT in Traumatic Brain Injury

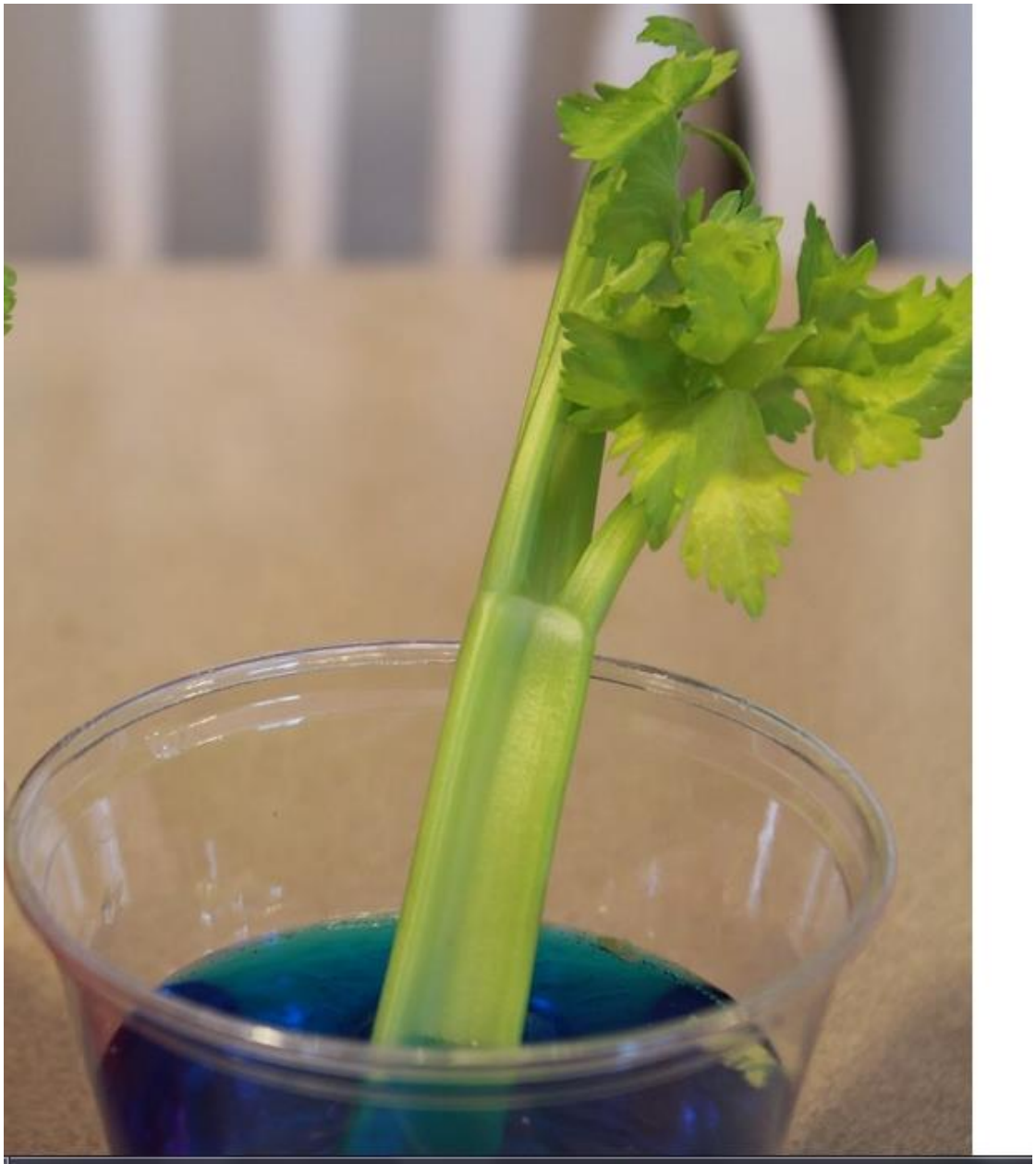

Anisotropic Diffusion in Celery

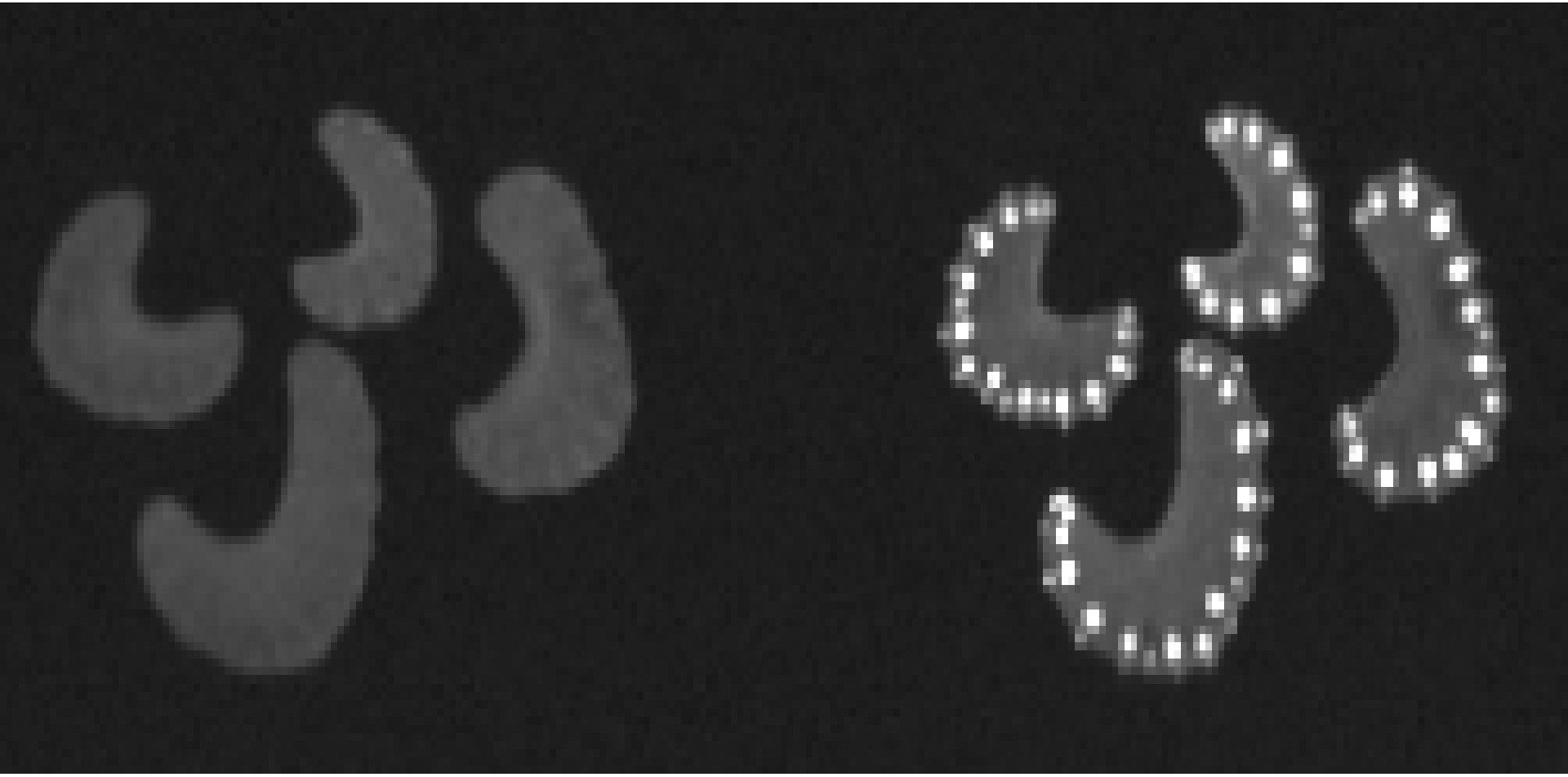

Courtesy of Tim Roberts & Mike Moseley

	Isotropic, unrestricted diffusion	Isotropic, restricted diffusion	Anisotropic, restricted diffusion
Diffusion Trajectory	 (free water)	 (random barriers present)	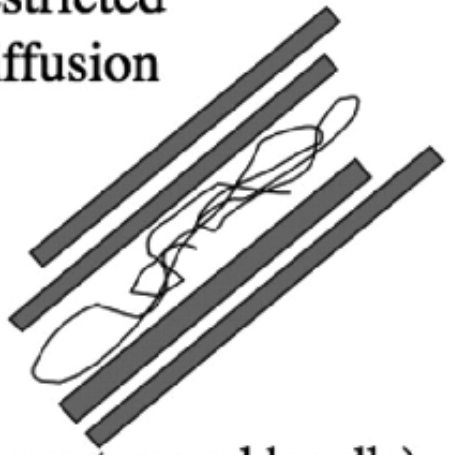 (coherent axonal bundle)
Diffusion Ellipsoid	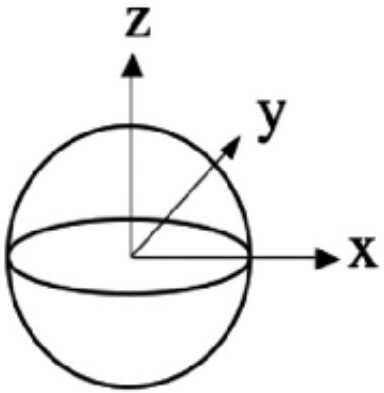	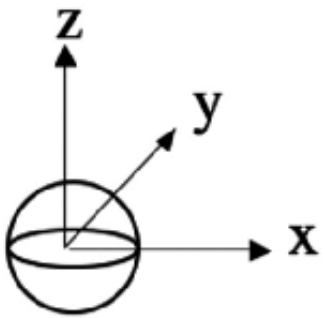	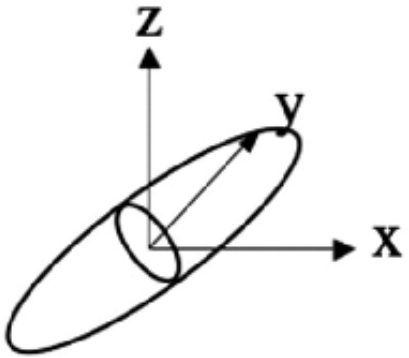
Diffusion Tensor	$\begin{bmatrix} D & 0 & 0 \\ 0 & D & 0 \\ 0 & 0 & D \end{bmatrix}$	$\begin{bmatrix} D_{eff} & 0 & 0 \\ 0 & D_{eff} & 0 \\ 0 & 0 & D_{eff} \end{bmatrix}$ $D_{eff} < D$	$\begin{bmatrix} D_{xx} & D_{xy} & D_{xz} \\ D_{yx} & D_{yy} & D_{yz} \\ D_{xz} & D_{yz} & D_{zz} \end{bmatrix}$

- Normalized variance of ellipsoid axis magnitudes
  - FA=0 for sphere
  - FA=1 for tube
  - FA is dimensionless

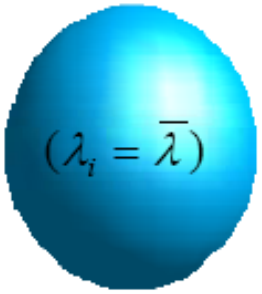

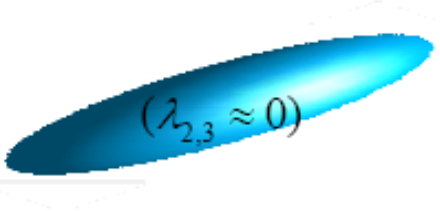

$$\sqrt{\frac{3}{2}}\sqrt{\frac{(\lambda_1-\bar{\lambda})^2+(\lambda_2-\bar{\lambda})^2+(\lambda_3-\bar{\lambda})^2}{\lambda_1^{\,2}+\lambda_2^{\,2}+\lambda_3^{\,2}}}, \quad \bar{\lambda}=\frac{\lambda_1+\lambda_2+\lambda_3}{3}$$

Multiple Sclerosis International
Volume 2013, Article ID 671730, 11 pages

Table 1: Schematic description of the main DTI parameters.

	Unit of measure	Formula	Object measured
FA	Scalar value ranging between 0-1	$\sqrt{\frac{1}{2}}\frac{\sqrt{(\lambda_1-\lambda_2)^2+(\lambda_2-\lambda_3)^2+(\lambda_3-\lambda_1)^2}}{\sqrt{\lambda_1^2+\lambda_2^2+\lambda_3^2}}$	Fibers directionality/axonal loss
MD	mm^2/sec	$(\lambda_1+\lambda_2+\lambda_3)/3$	Amount of water diffusion/myelin loss
AD	mm^2/sec	λ_1	Diffusivity parallel to the fibers/myelin and axonal content
RD	mm^2/sec	$(\lambda_2+\lambda_3)/2$	Diffusivity perpendicular to the fibers/myelin content

FA: fractional anisotropy; MD: mean diffusivity; AD: axial diffusivity; RD: radial diffusivity; mm: millimeters; sec: second.

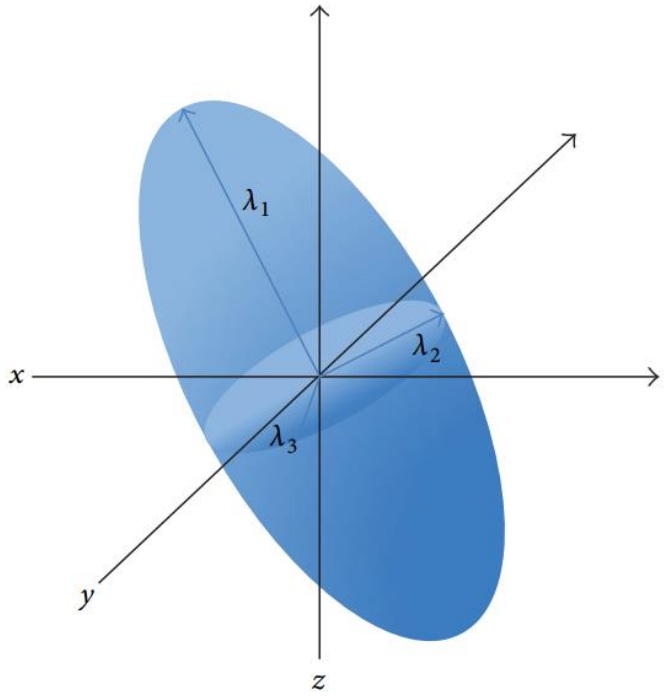

Figure 1: Elliptical representation of a diffusion tensor with the 3 main axes: the longest axis stands for the primary eigenvector (λ_1), reflecting the diffusion parallel to the fibers; the two shorter axes represent the second (λ_2) and third (λ_3) eigenvectors, whose average provides a measure of diffusivity perpendicular to the fibers.

Fractional Anisotropy (FA)

A measure of the degree of anisotropy in a tensor model of diffusion at a given voxel. FA values are bounded between zero (a perfect sphere) and one (an infinitely long cigar shape)

Diffusion through white matter probes:

- density of axons
- degree of myelination
- average fiber diameter
- directional similarity of axons

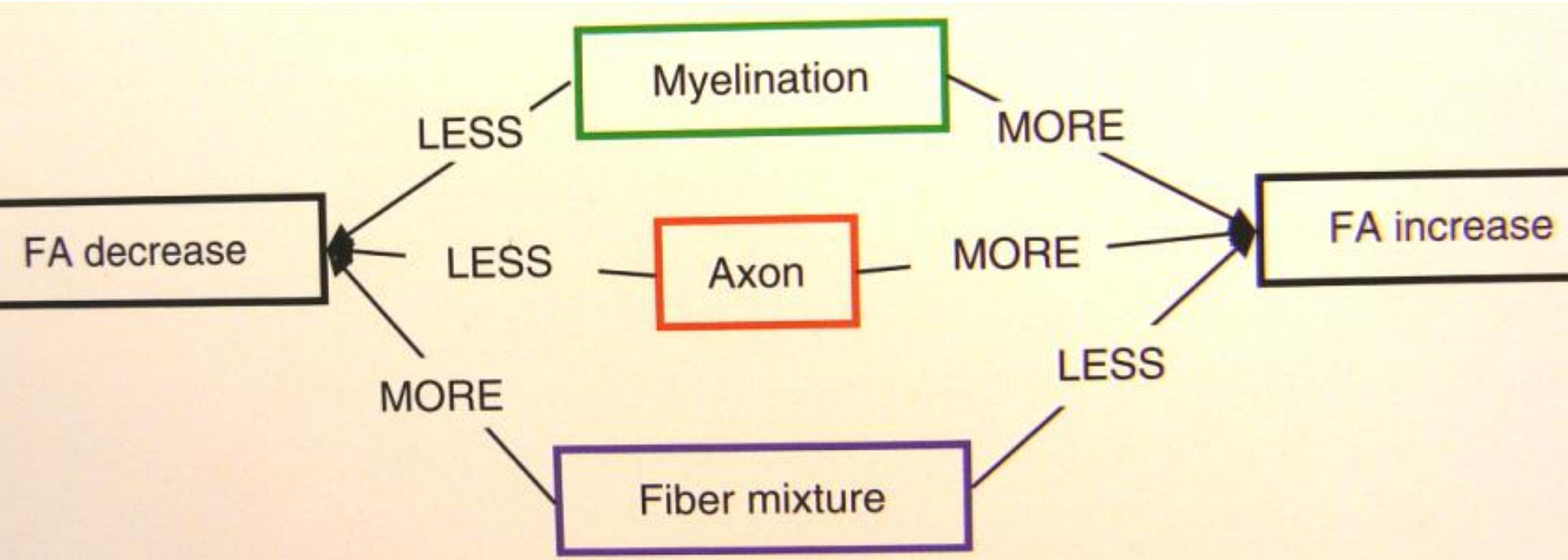

Modeling Tracts from Seed Points

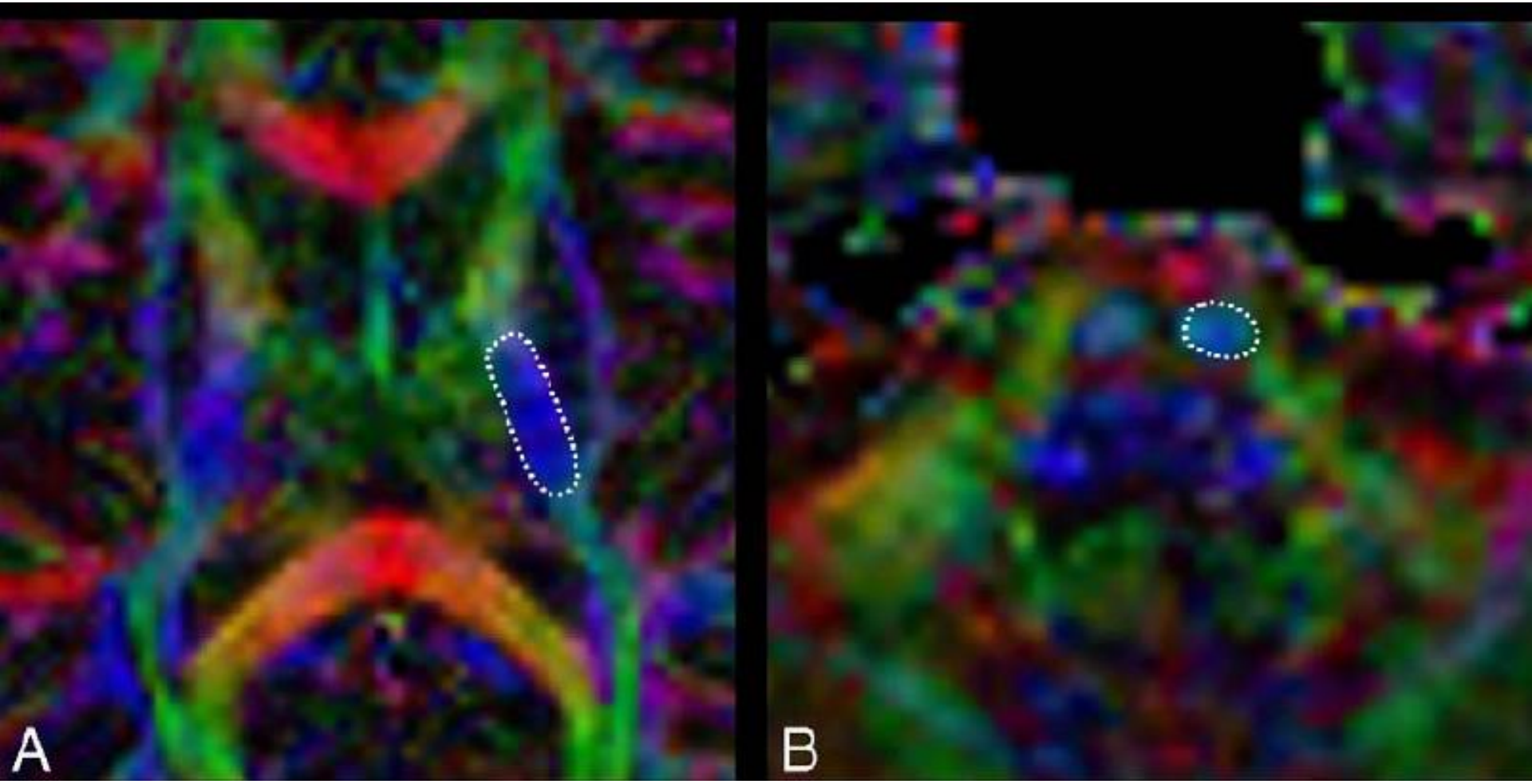

Fig. 1. Location of two regions of interest (ROIs) for tracking the corticospinal tract (CST). (A) Upper ROI including the posterior limb of the upper internal capsule and (B) lower ROI including the CST at the lower pons.

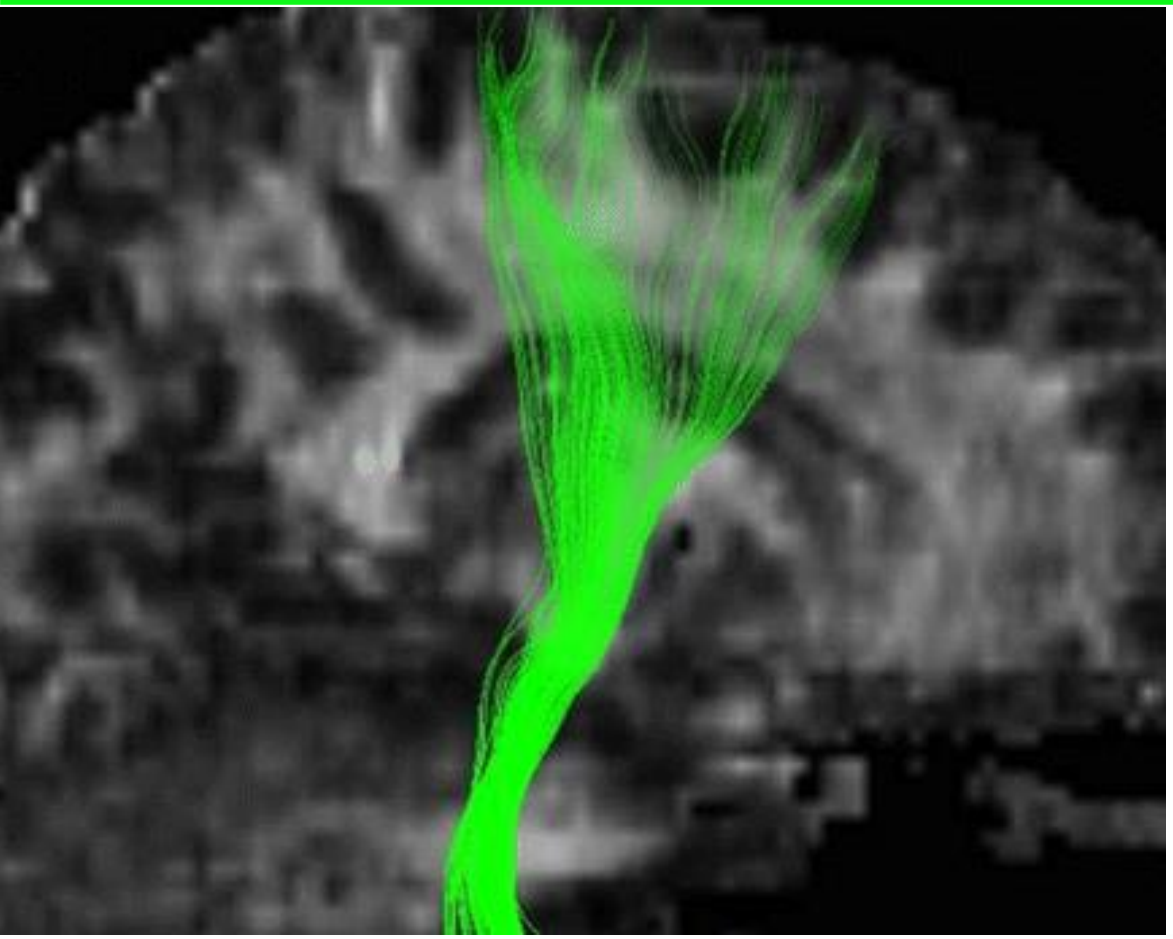

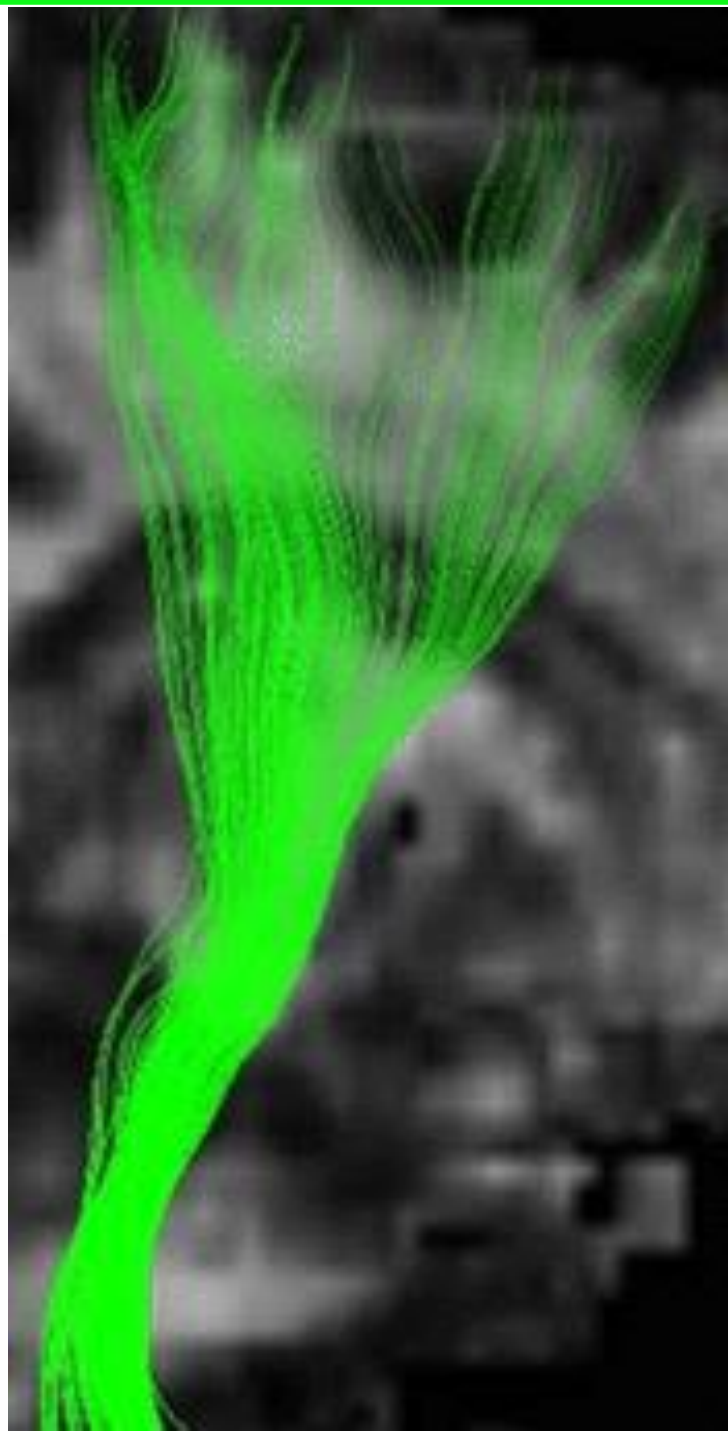

Figure 4a: (a) Tractography of corticospinal tract performed by iteratively extending streamlines (green) from a seed ROI in the direction of principal eigenvector by using the fiber assignment by continuous tracking, or FACT, algorithm (63,64). Images are superimposed on sagittal fractional anisotropy map. **(b)** Volume-rendered probability map of corticospinal tract produced by generating several thousand tracts from each seed voxel (69). Rather than follow the same path, since each track is extended it may overlap or depart from the rest at random. The probability of deviating from principal eigenvector in a traversed voxel reflects its diffusion properties, with increased divergence in voxels of low anisotropy. Probability map is formed from superposition of all tracts from all voxels in the seed ROI tract (color denotes index of probability that voxel is included in tract) (DT imaging: 12 directions; *b* value, 800 sec/mm^2; 6500/99; matrix, 128 x 128; FOV, 220 x 220 mm; section thickness, 3 mm).

The “tracts” created with fiber tracking are mathematical analogs (stream tubules) of the WM tracts representing fractional anisotropy values and not actual WM fibers or bundles.

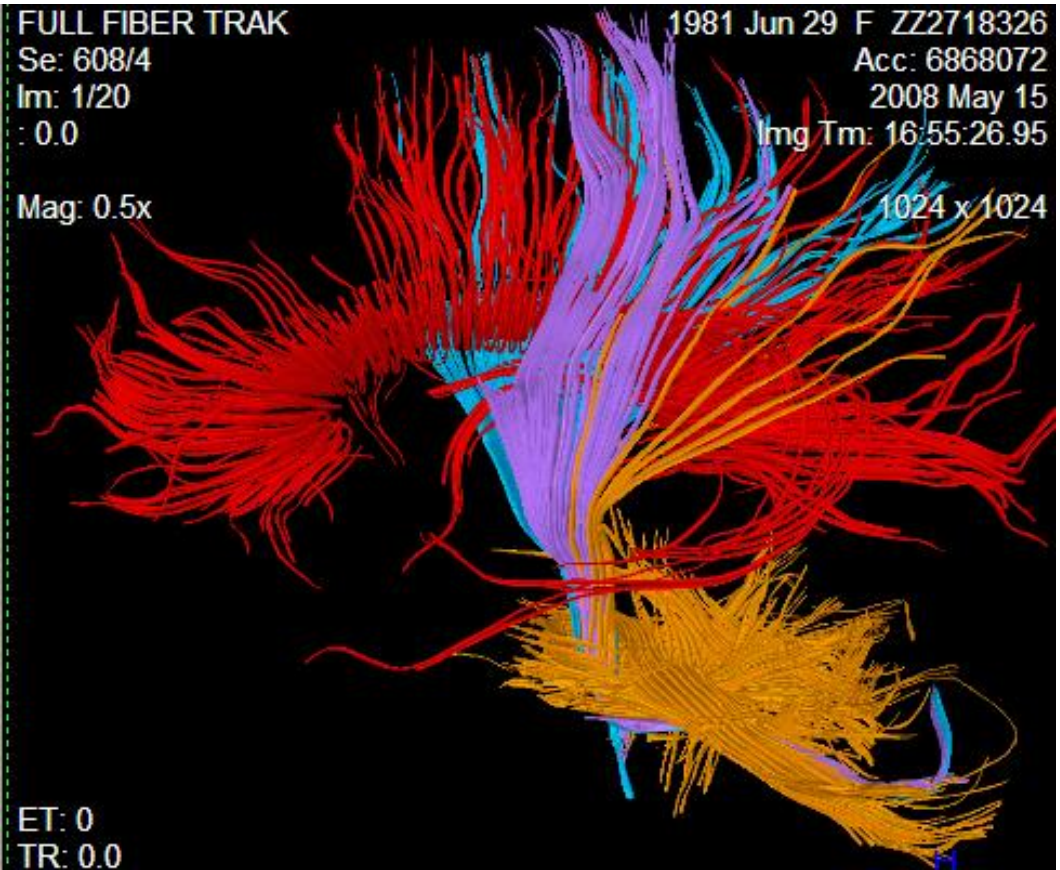

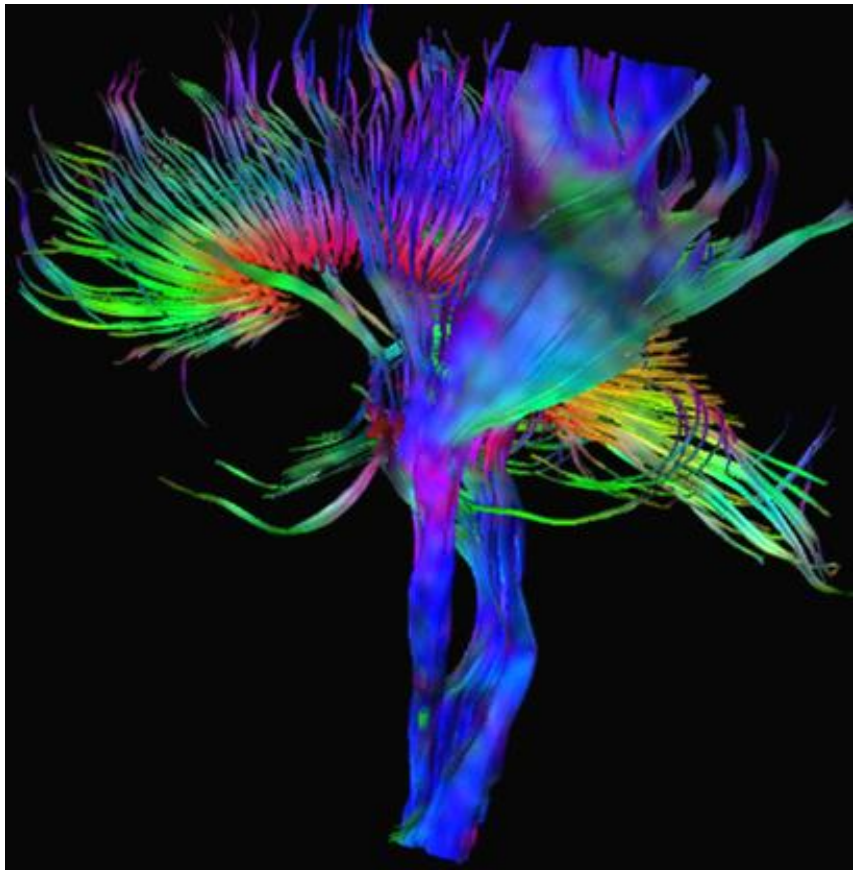

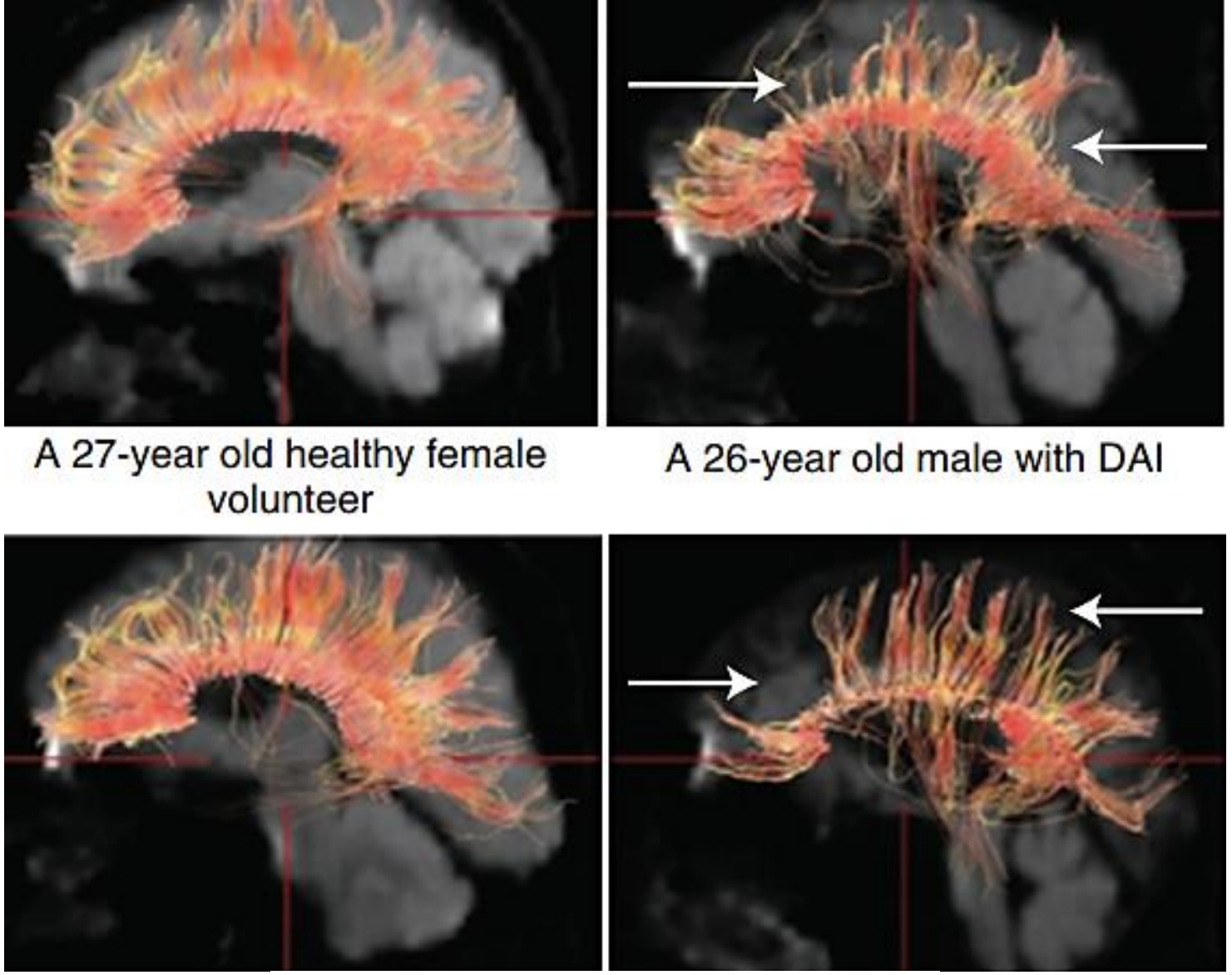

Fig. 50B.9 Two examples of patients with diffuse axonal injury. Diffusion tensor imaging (DTI) fiber tractography around the corpus callosum in a midsagittal plain. In the pictures on the left there were fewer fibers extending to the frontal, parietal, and occipital white matter, and they were even absent in some areas *(arrows)* in comparison with the normal volunteer image. *(From Sugiyama, K., Kondo, T., Higano, S., et al., 2007. Diffusion tensor imaging fiber tractography for evaluating diffuse axonal injury. Brain Inj 21, 413-419.)*

MRI and CT in Traumatic Brain Injury

54Y F M.D. Anesthesiologist involved in a severe MVA with head trauma. She was airlifted by helicopter and hospitalized at Stanford.

Mentation Changes after a Severe MVA

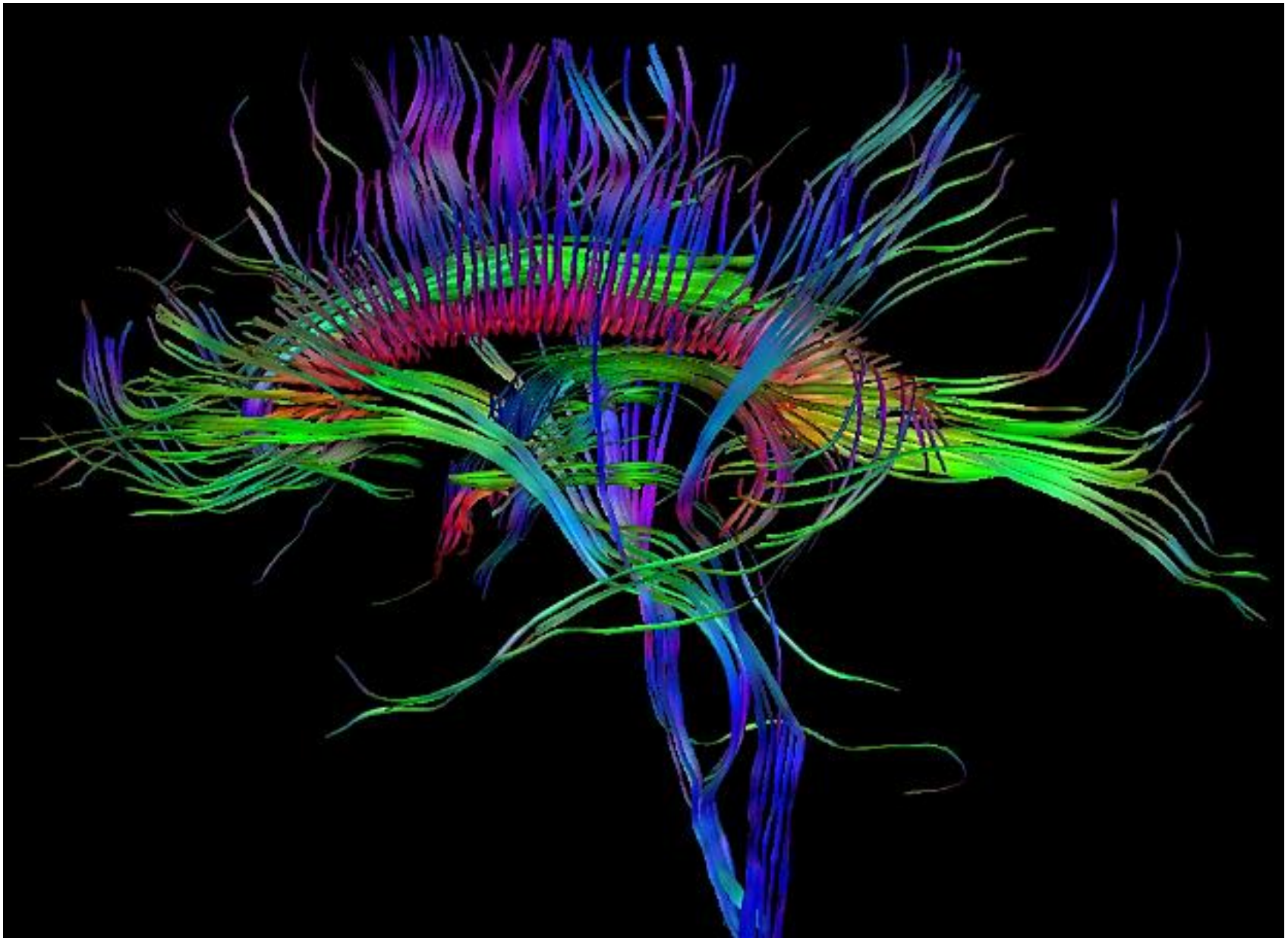

Severe MVA

Age Matched Normal

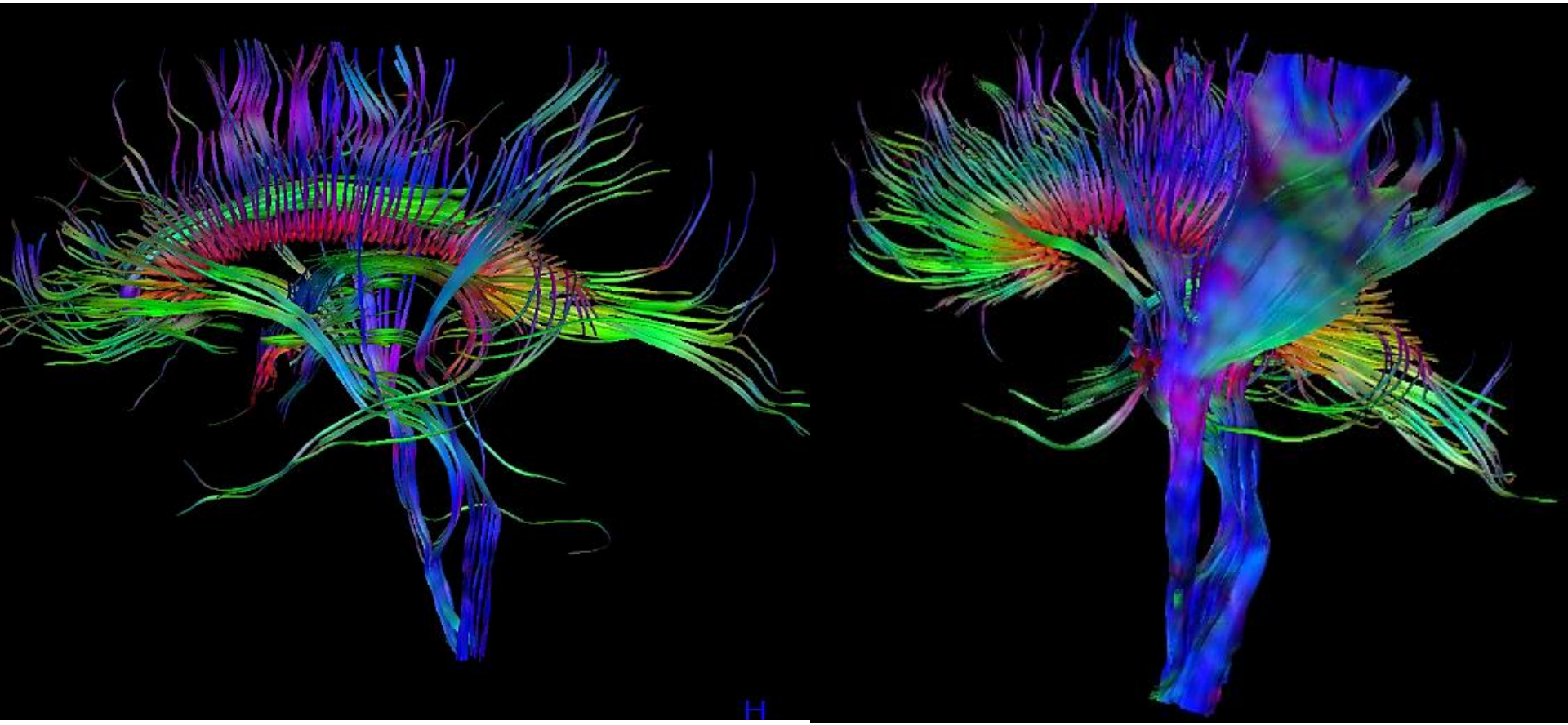

MRI and CT in Traumatic Brain Injury

54YF Fell Down Stairs 1.5M Prior to MRI Scan. Hit Head “Hard” Several Times Resulting in a Concussion

“Post-concussive Syndrome” with HA, Memory Loss, Difficulty with Concentration

MRI and CT in Traumatic Brain Injury

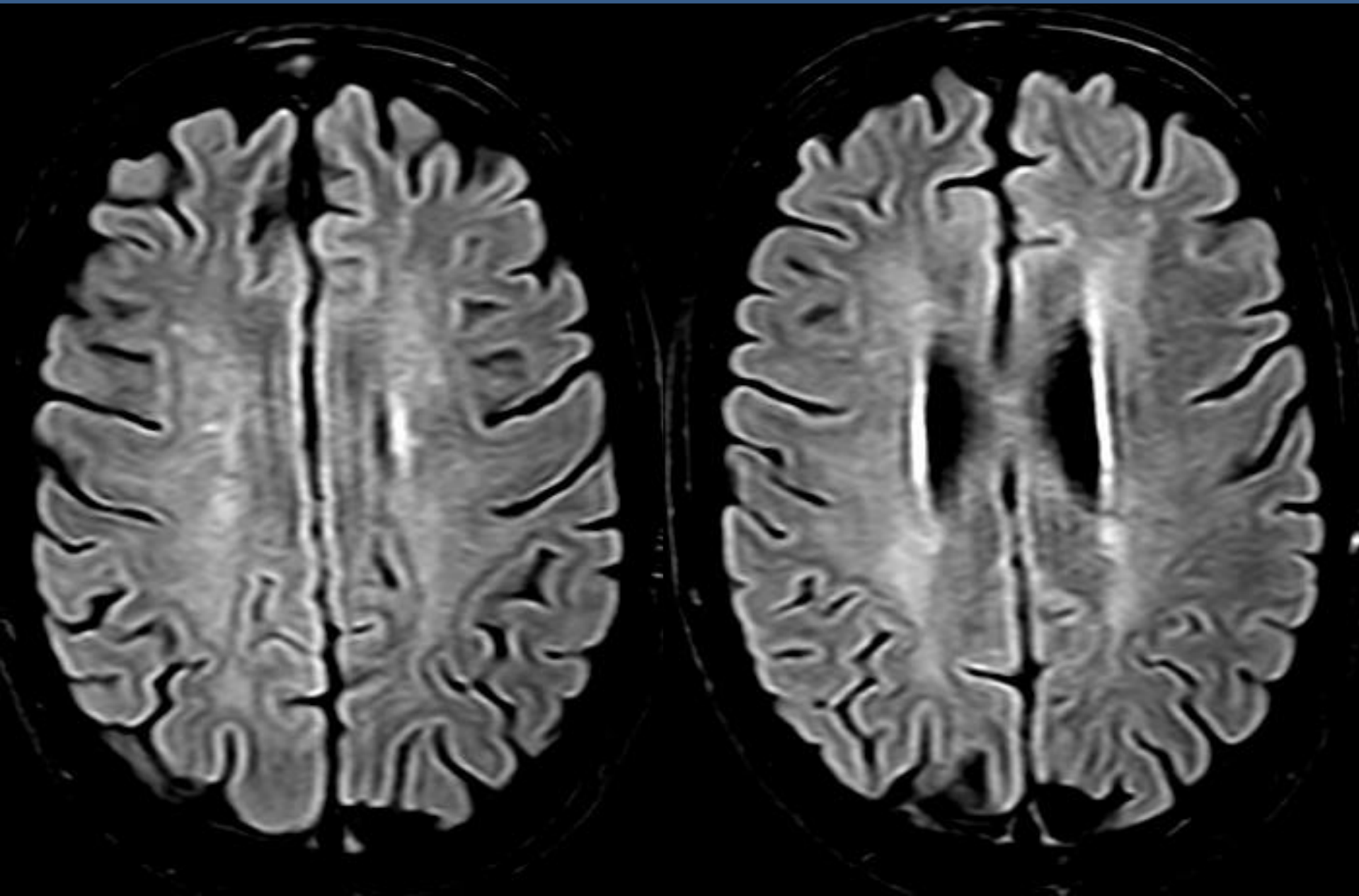

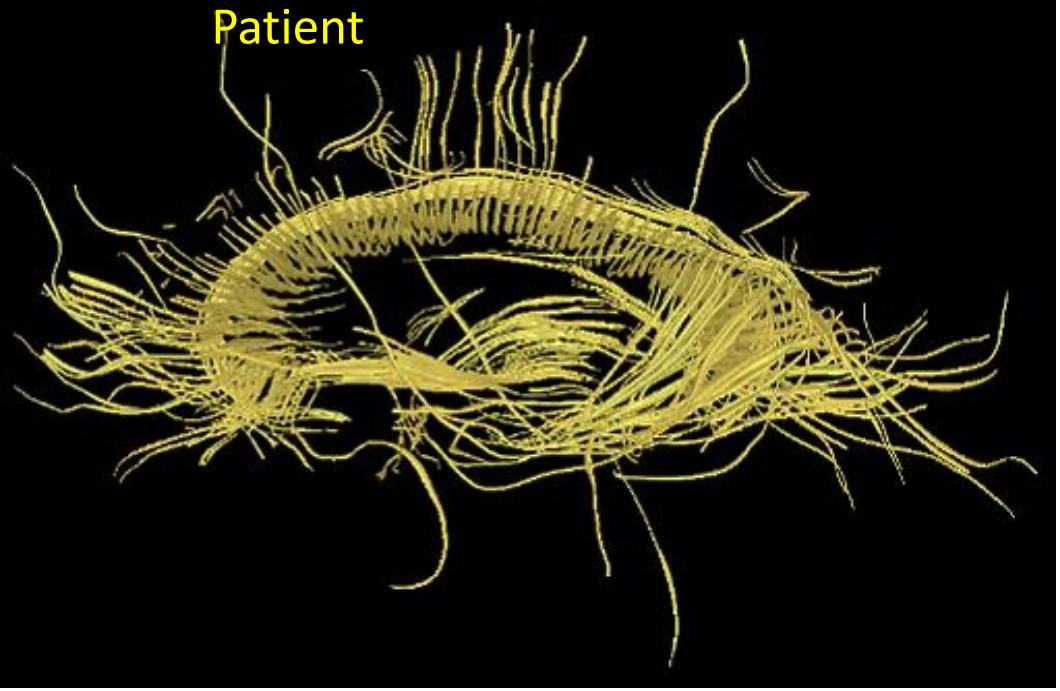
Patient

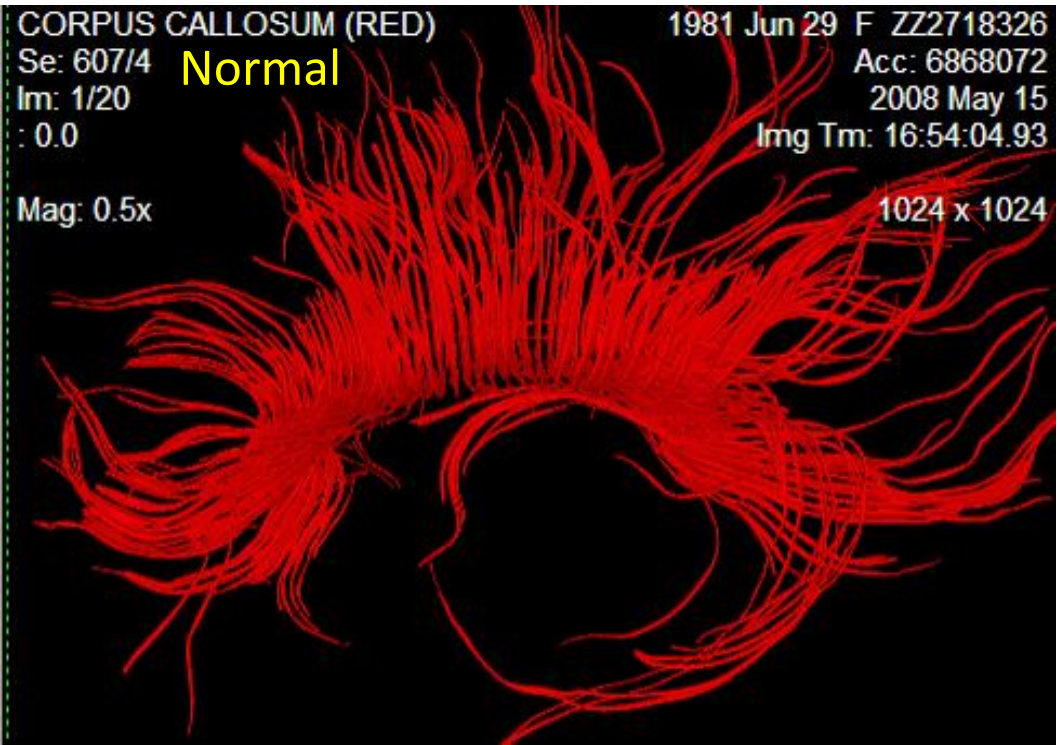
CORPUS CALLOSUM (RED)
Se: 607/4
Im: 1/20
: 0.0
Mag: 0.5x
Normal
1981 Jun 29 F ZZ2718326
Acc: 6868072
2008 May 15
Img Tm: 16:54:04.93
1024 x 1024

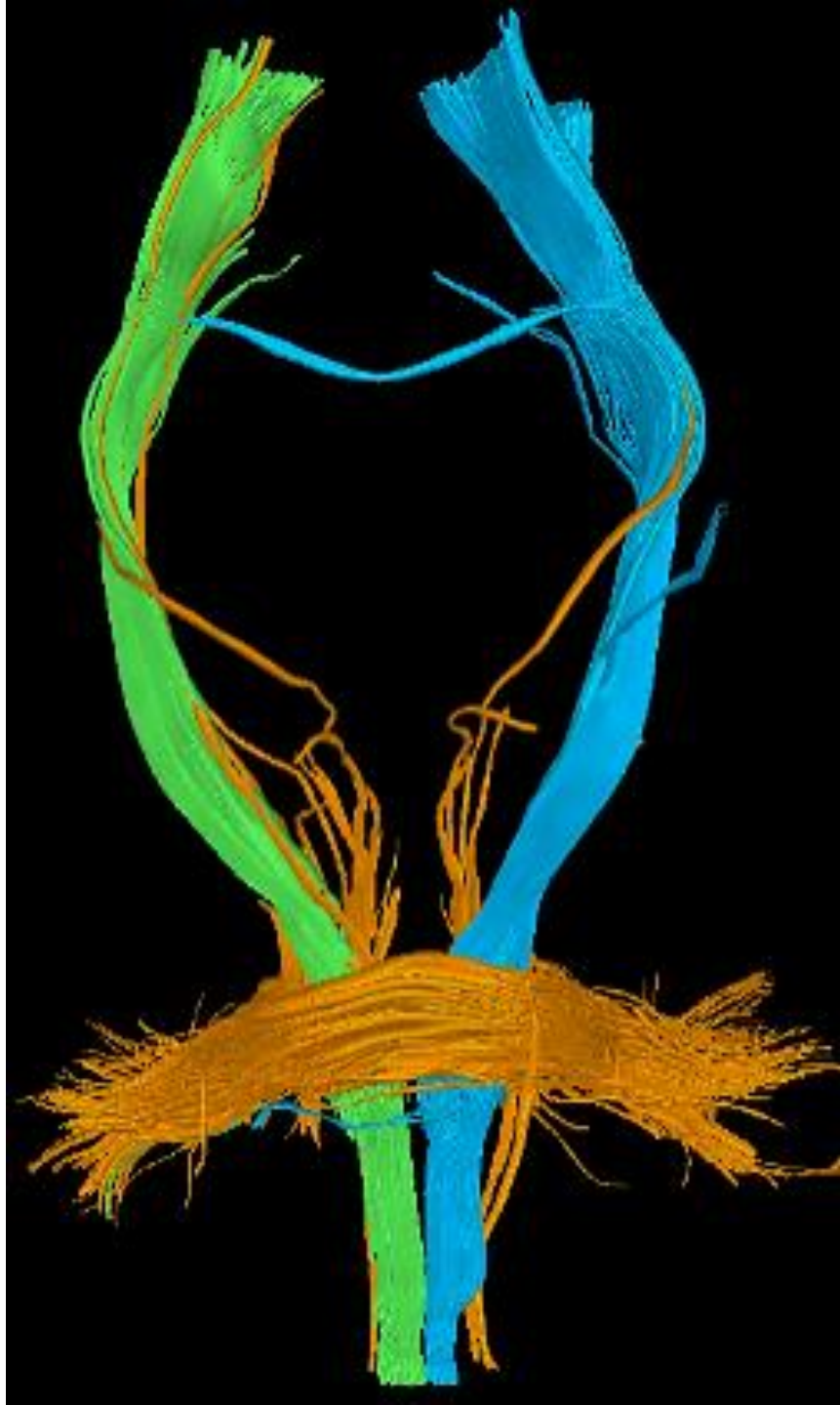

Numbers Don't Lie

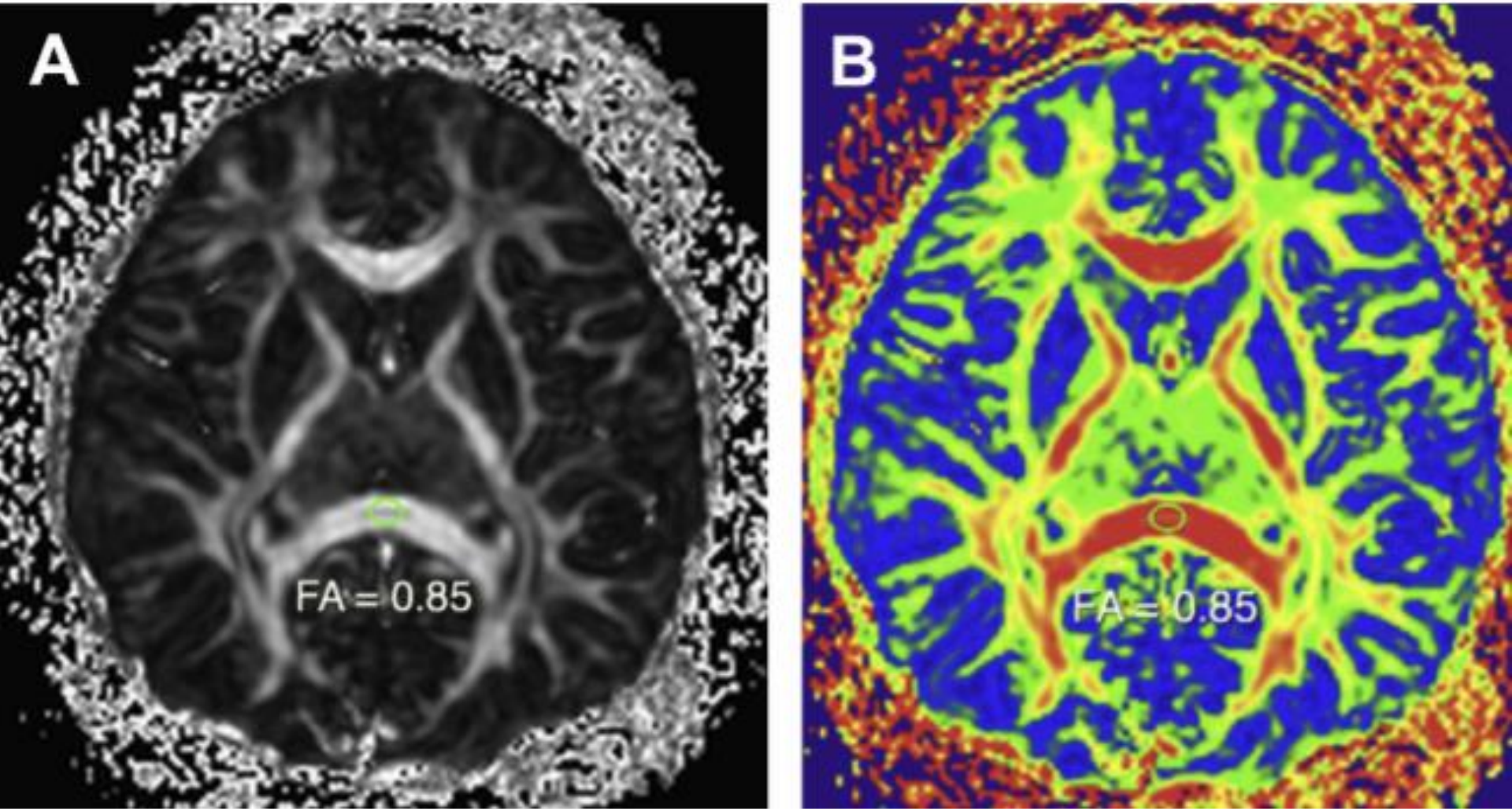
A
FA = 0.85
B
FA = 0.85

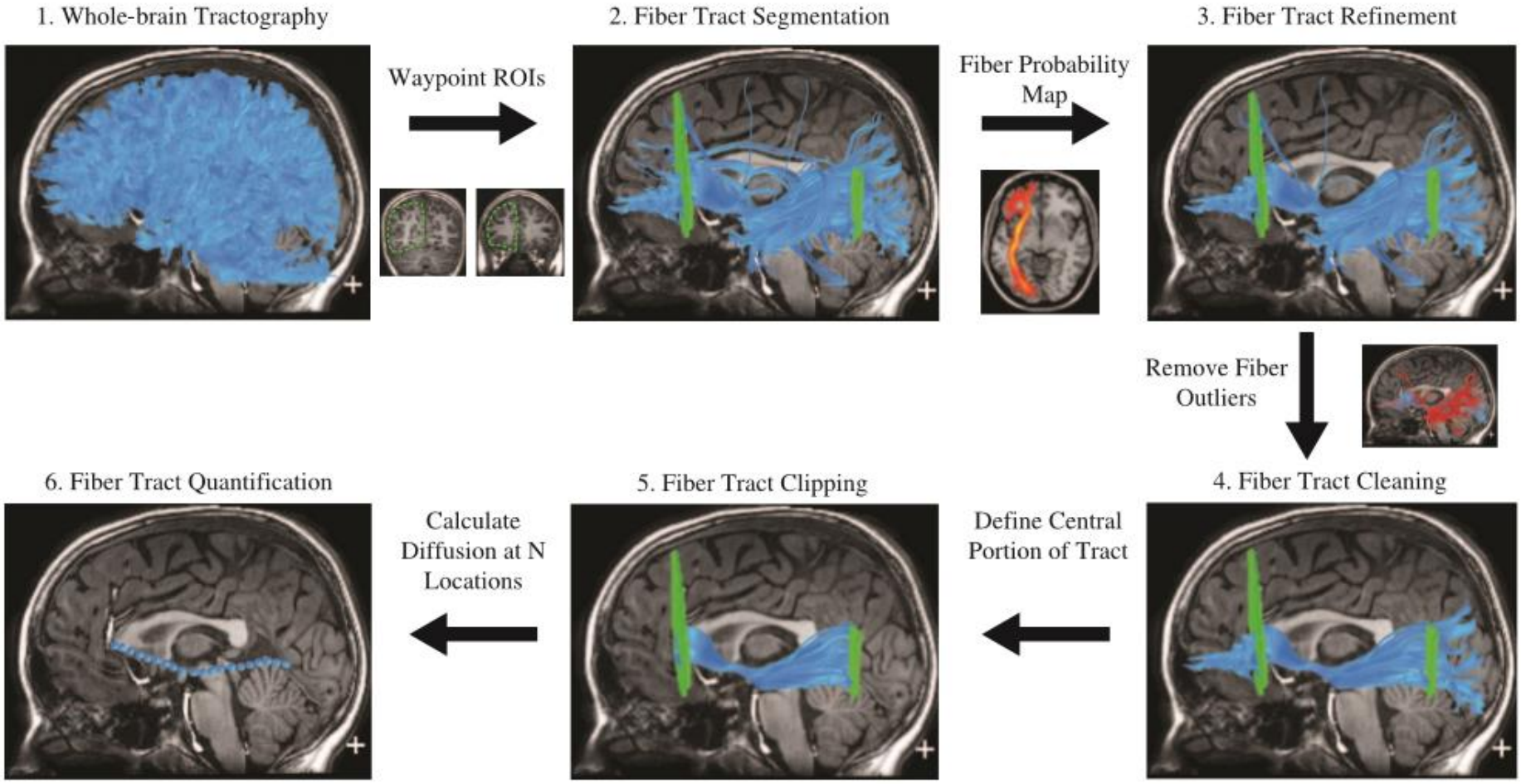

Figure 8. Automated Fiber Quantification (AFQ) procedure for the left hemisphere inferior fronto-occipital fasciculus. (1) Whole brain tractography is initiated from each white matter voxel with fractional anisotropy (FA) >0.3. (2) Fibers that pass through two waypoint regions of interest (ROIs) become candidates for the left IFOF fiber group. (3) Each candidate fiber is then scored based on its similarity to a standard fiber tract probability map. Fibers with high probability scores are retained. (4) Fibers tracts are represented as a 3-dimensional Gaussian distribution and outlier fibers that deviate substantially from the mean position of the tract are removed. (5) The fiber group is clipped to the central portion that spans between the two defining ROIs. (6) The fiber group core is calculated by resampling each fiber into 100 equidistant nodes and calculating the mean location of each node. Diffusion measurements are calculated at each node by taking a weighted average of the FA measurements of each individual fibers diffusion properties at that node. Weights are determined based on the Mahalanobis distance of each fiber node from the fiber core.
doi:10.1371/journal.pone.0049790.g008

Corticospinal Tract (CST)

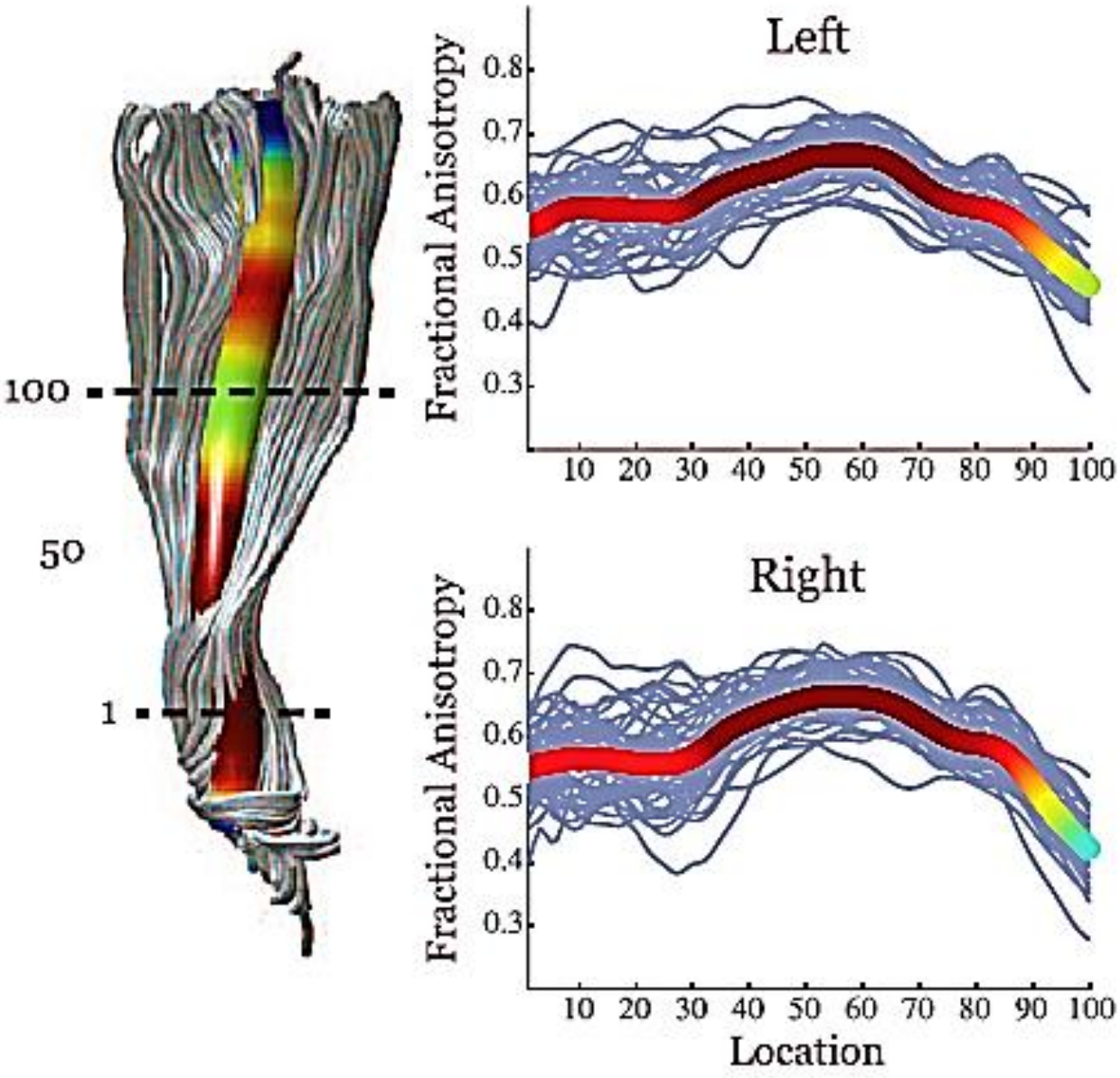

Corticospinal Tract (CST). The CST shows a dramatic reduction in FA at an equivalent location in all individuals and at that point FA falls to a similar level in each subject. The CST ascends from the brainstem, paralleling the ventricles to the cortex. FA for the CST starts off relatively low due to partial voluming in the brain stem. FA peaks roughly half way between the two defining ROIs, at the level of the internal capsule. At this location fibers are coherently oriented inferior-superior. FA then declines substantially at the level of the centrum-semiovale, a location where callosal fibers cross medial to lateral through the CST and superior longitudinal fasciculus (SLF) fibers cross posterior to anterior through the CST [38].

Corticospinal Tract (CST)

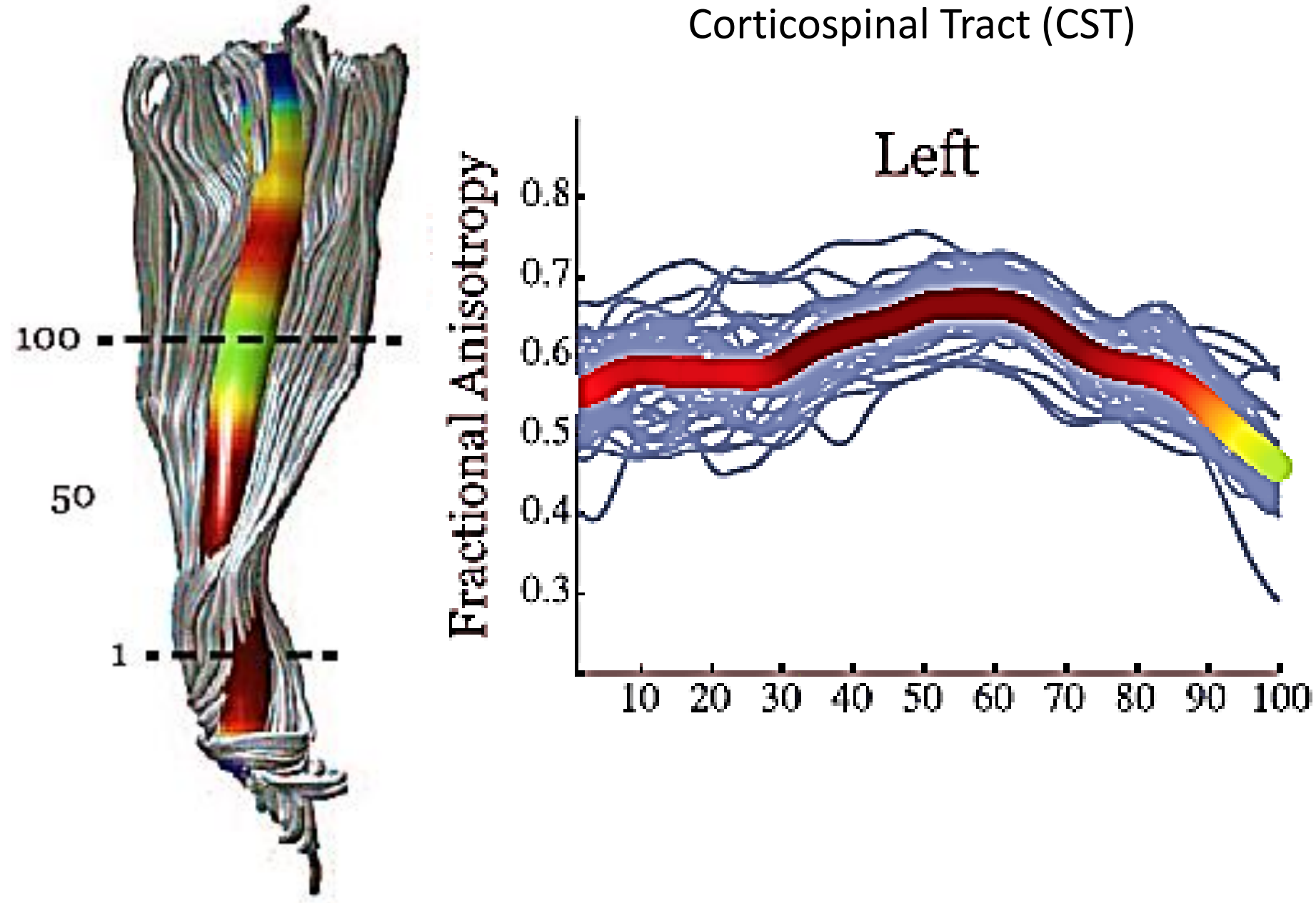

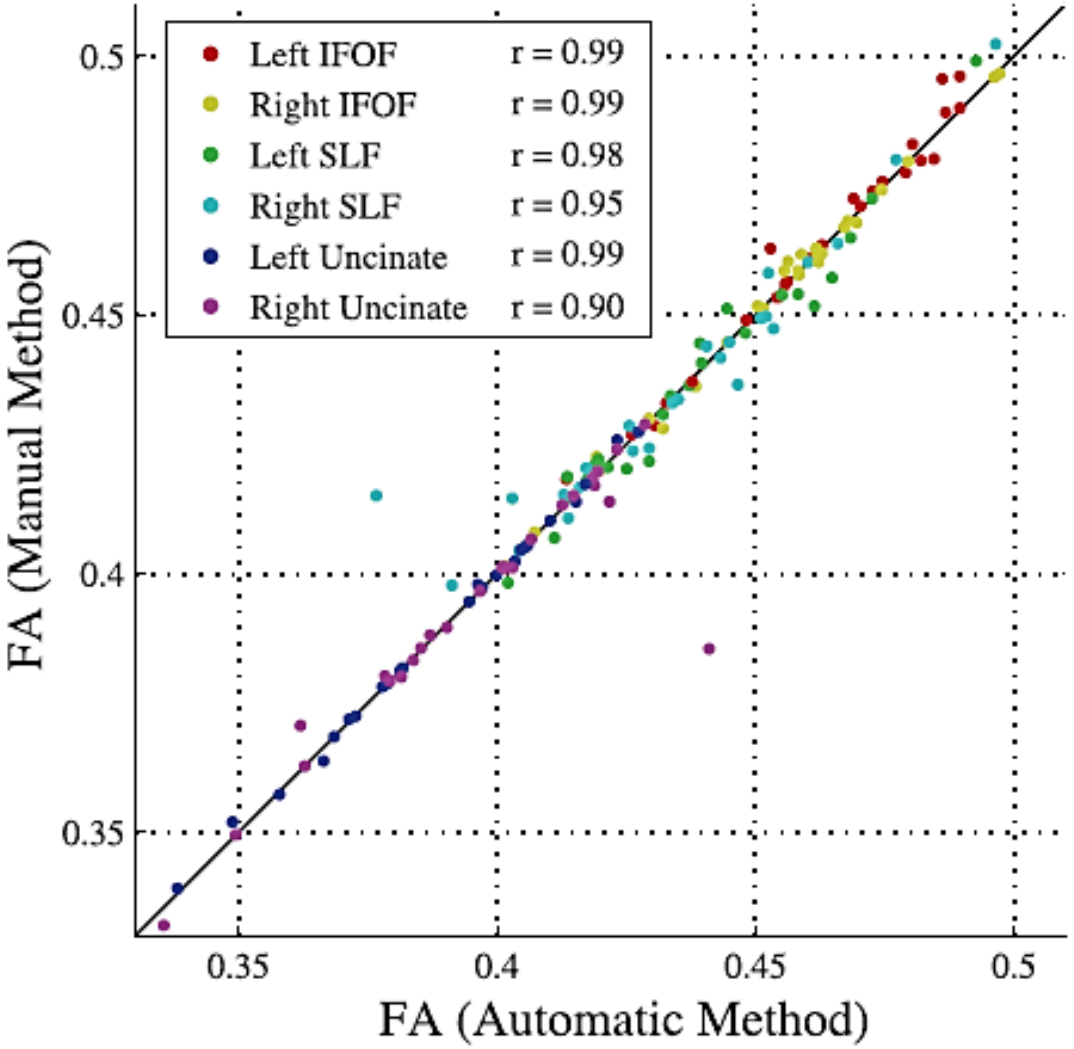

Figure 9. Automated fiber tract segmentation is consistent with manual segmentation. Each point represents the mean FA value for a subject's fiber tract obtained from the automated segmentation (x-axis) and the manual segmentation (y-axis). Mean FA measurements for fiber tracts identified by AFQ are highly correlated with FA measurements from the manual method. The correlation for each tract is in the legend.

AFQ will automatically identify 28 fascicles in an individual's brain and reliably quantify tissue properties along each fascicle.

Left Corticospinal Tract

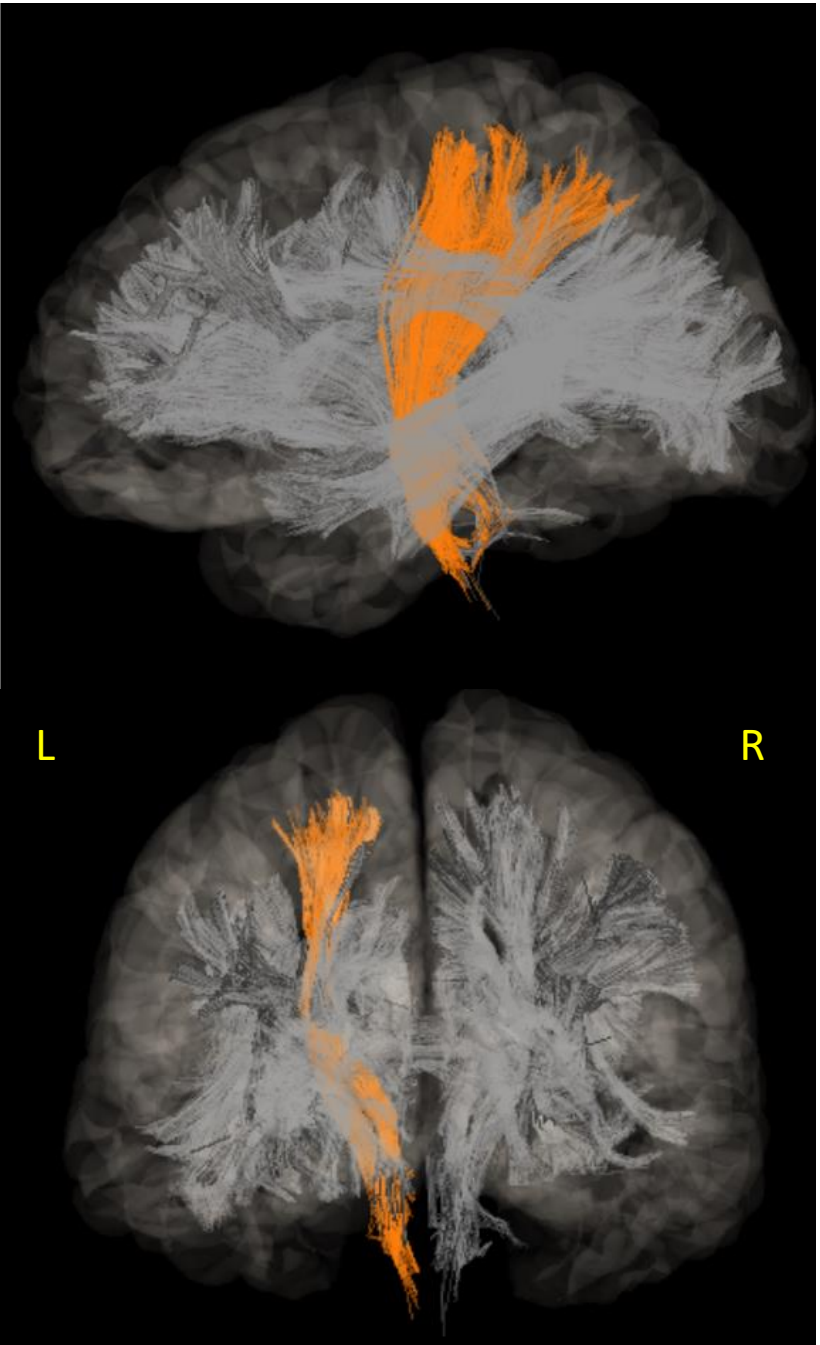

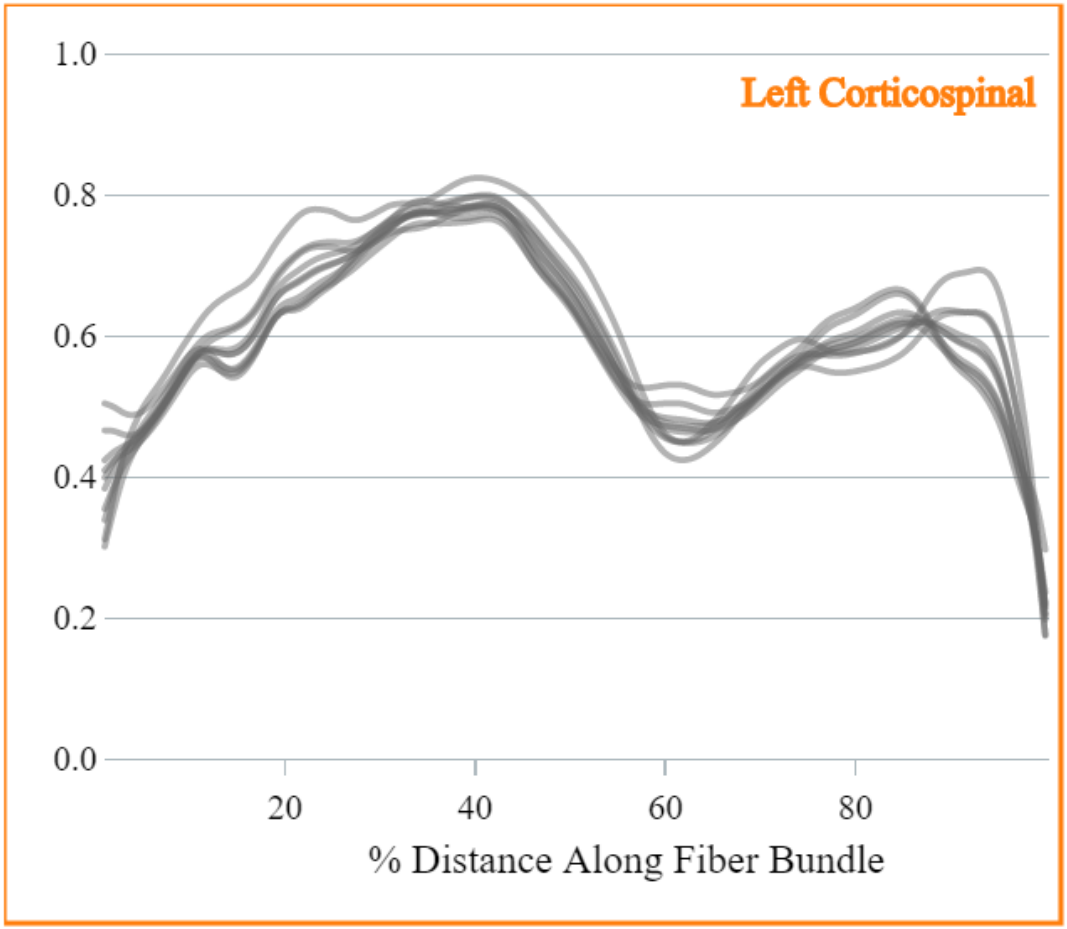

Callosum Forceps Major

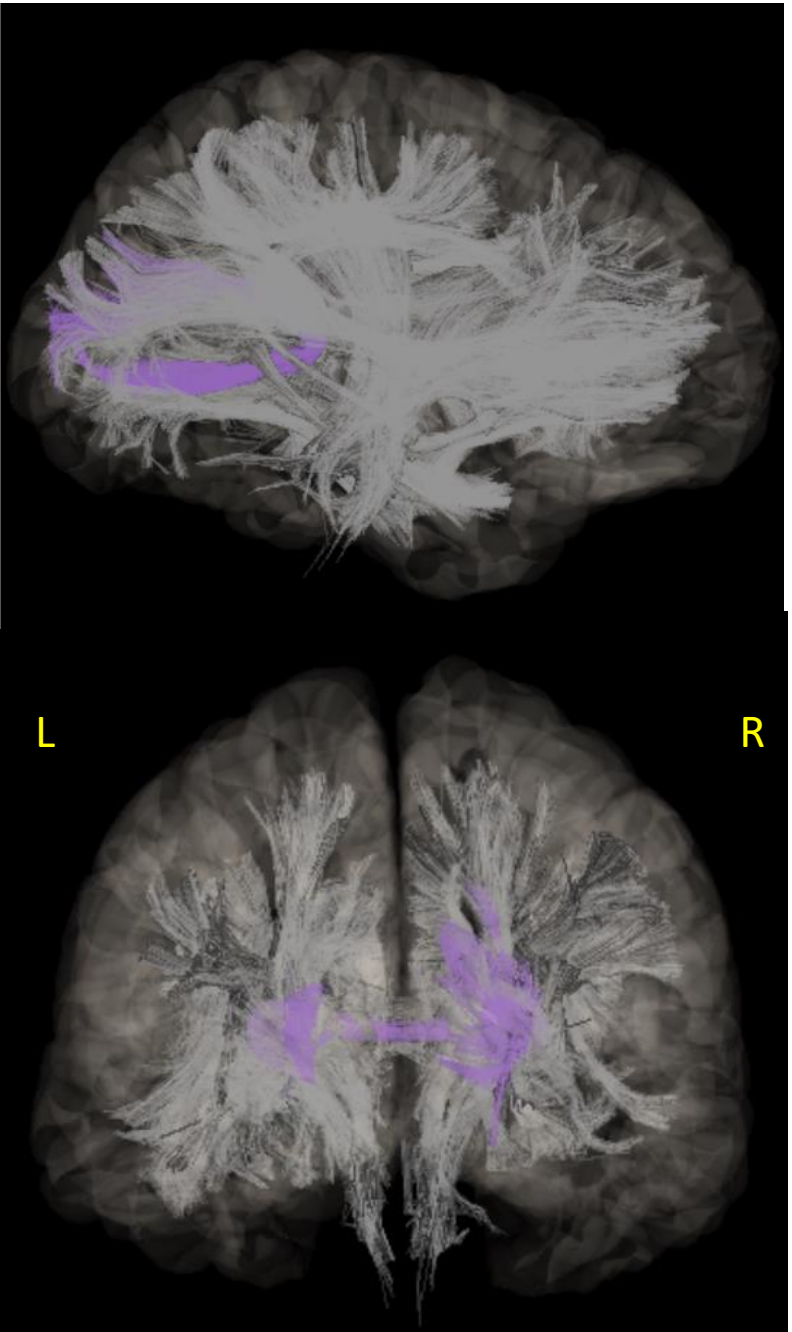

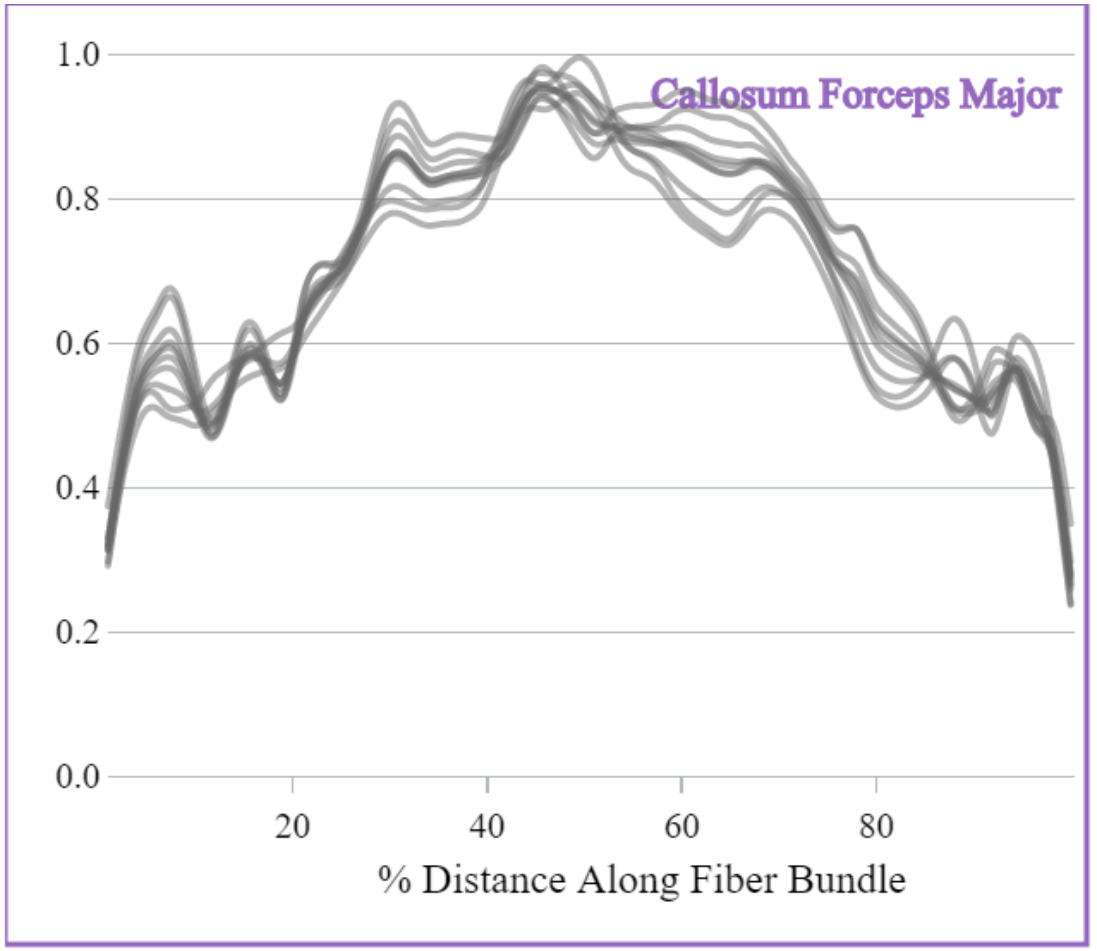

Left Arcuate Fasiculus

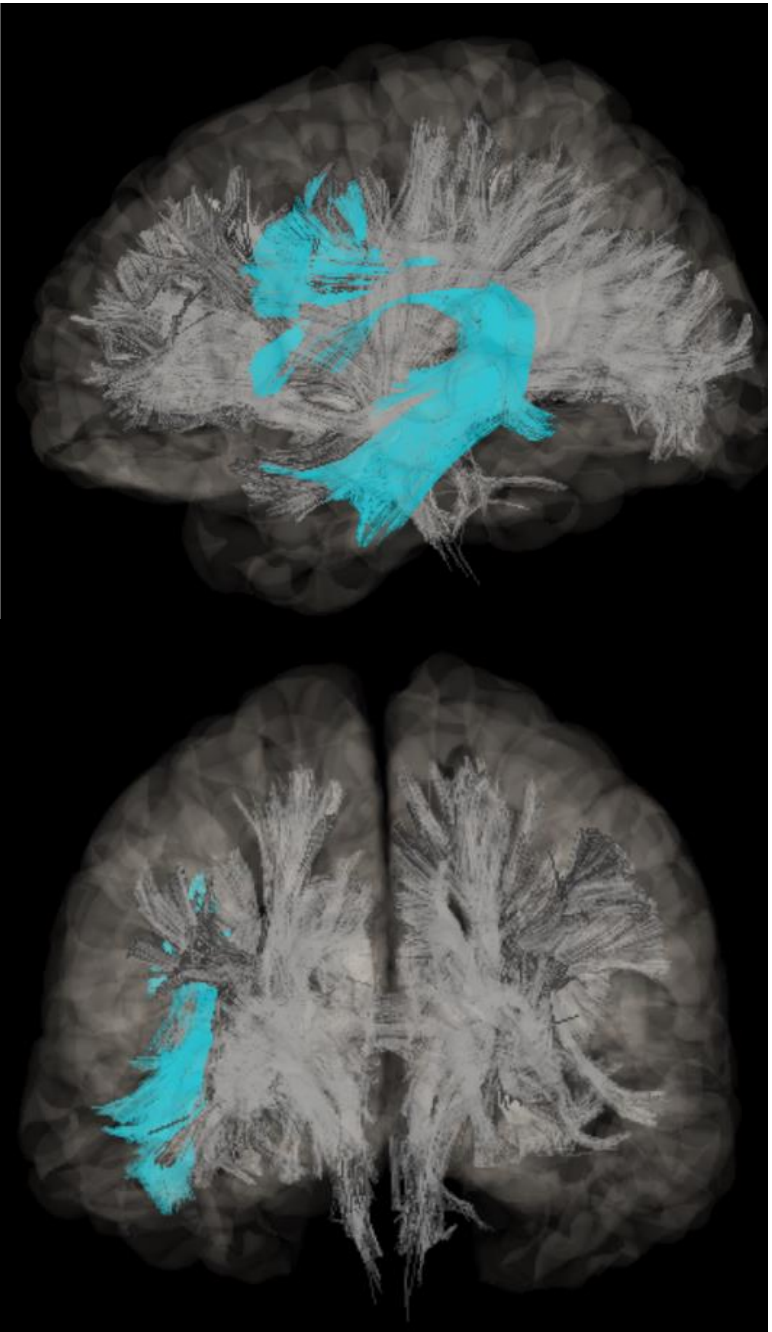

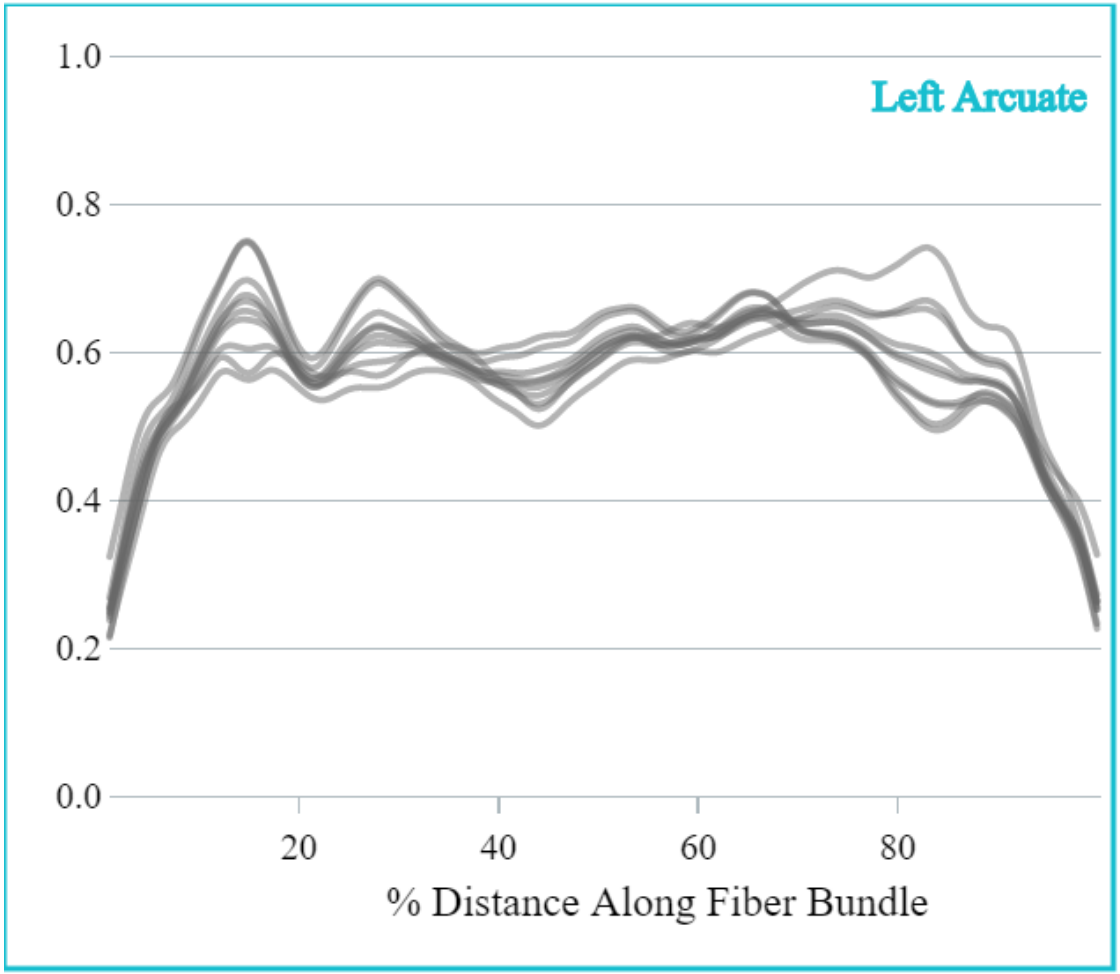

neurocritical care society Neurocrit Care (2016) 24:342–352
DOI 10.1007/s12028-015-0216-8

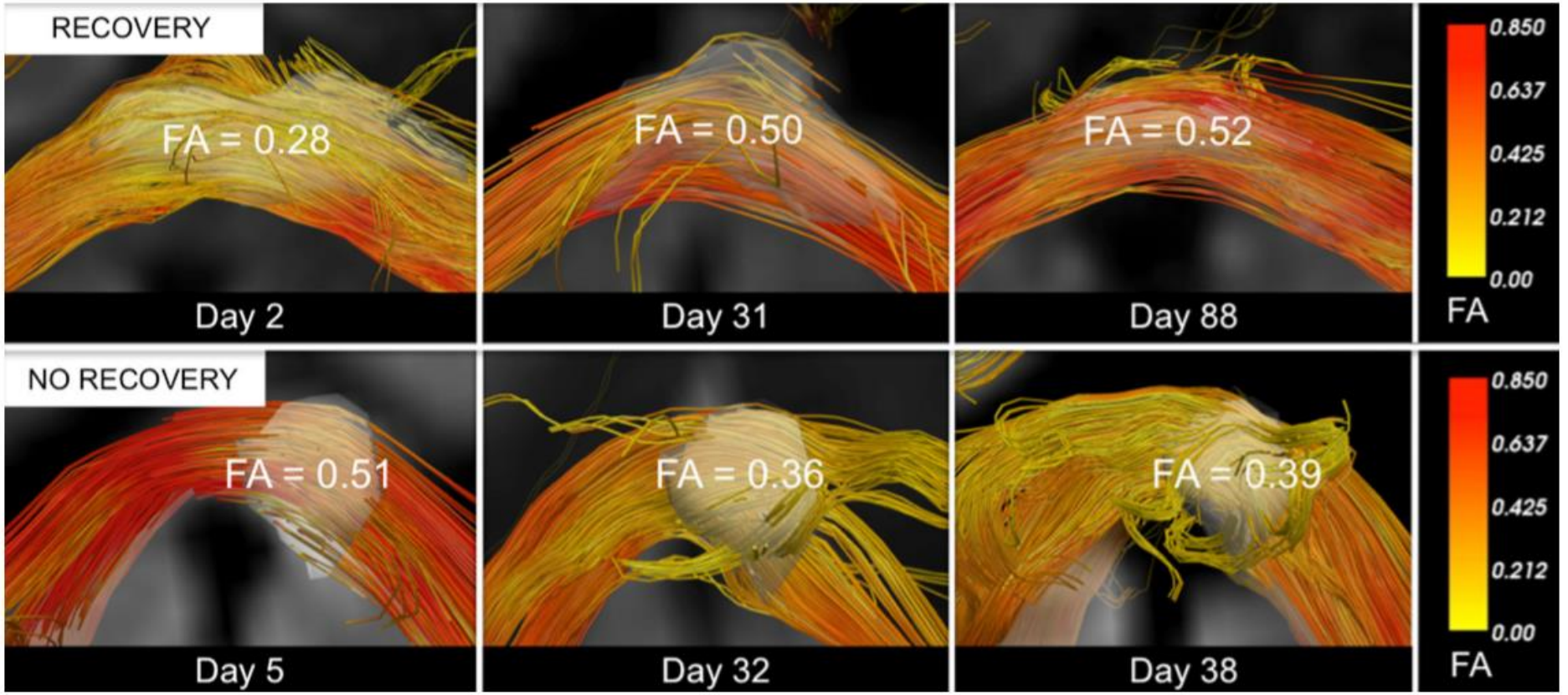

Fig. 2 Longitudinal fractional anisotropy changes within white matter tracts affected by traumatic axonal injury. A traumatic axonal injury (TAI) lesion in the splenium of the corpus callosum of patient 6 (*top row*) demonstrates FA recovery, as defined by a longitudinal increase in FA that exceeds the coefficient of variation for FA within the splenium of the corpus callosum in the two control datasets. A splenium TAI lesion for patient 7 undergoes a longitudinal decline in FA (*bottom row*). Each TAI lesion is rendered in 3-dimensions as a semi-transparent white region of interest so that tracts can be visualized passing through the lesions. Fiber tracts were generated using the lesions as seeds. Tracts are color-coded using mean tract FA as a scalar (*right panels*). All tracts were reconstructed using Diffusion Toolkit version 0.6.2 and TrackVis version 5.2 (Wang and Wedeen, Athinoula A. Martinos Center for Biomedical Imaging, www.trackvis.org)

Brain Segmentation

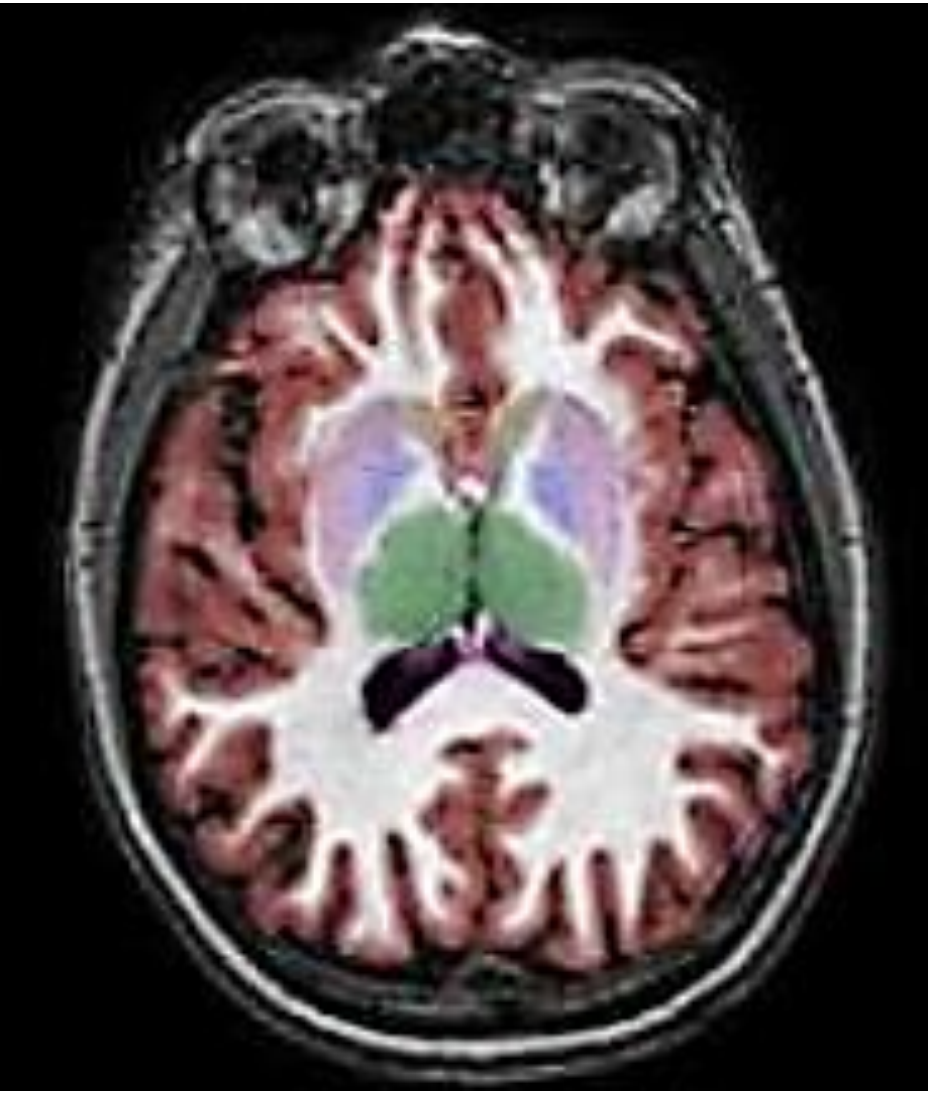

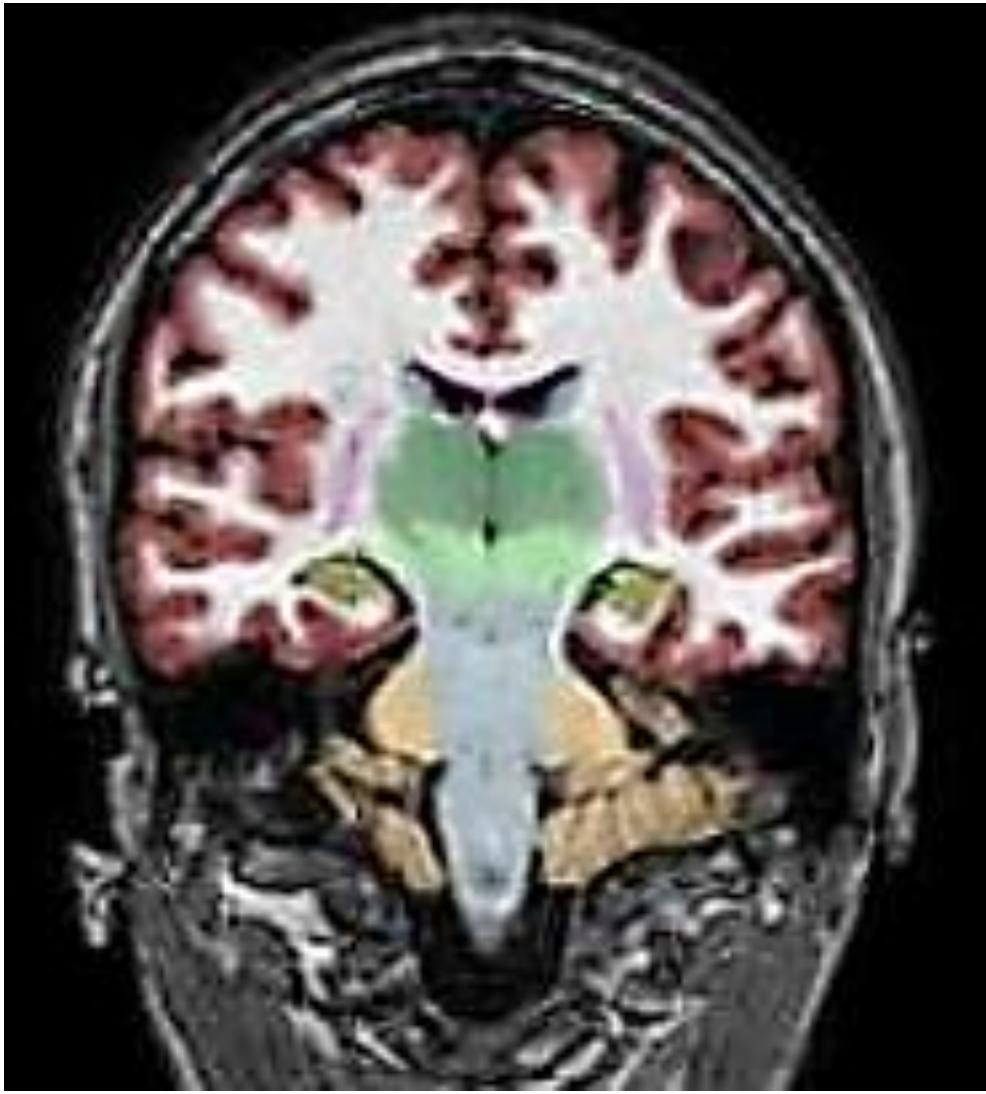

MORPHOMETRY RESULTS

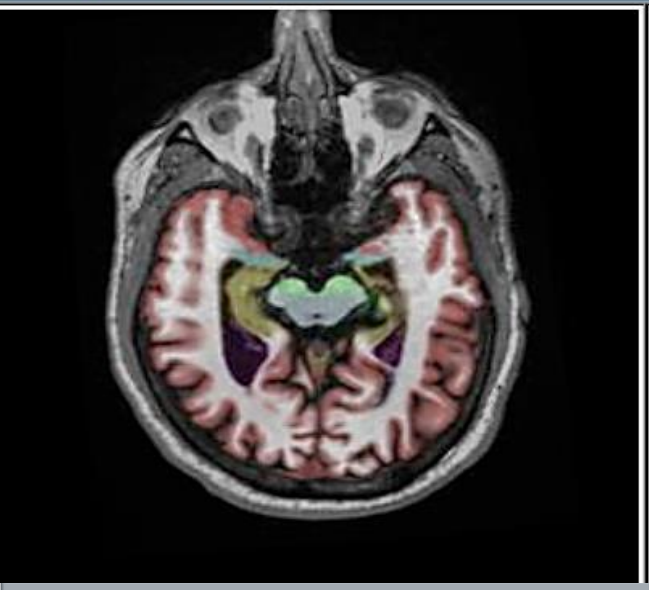
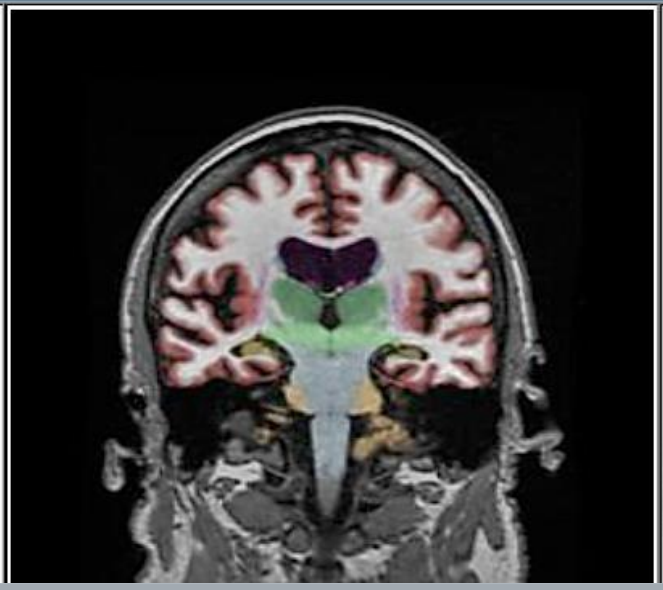
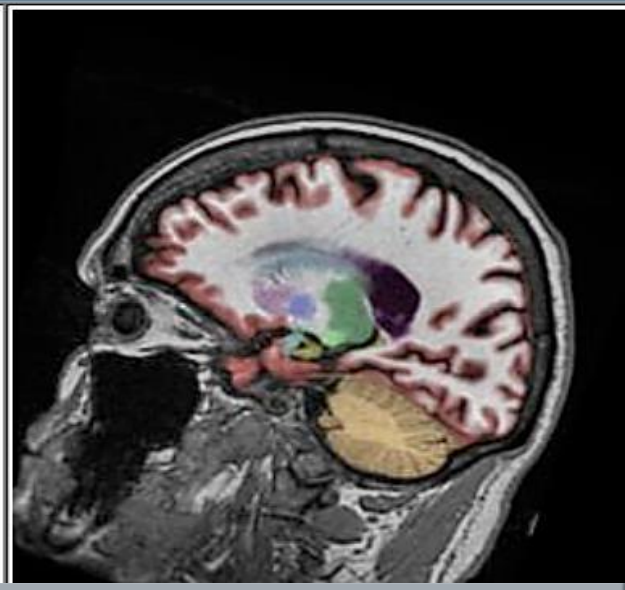

Brain Structure	LH Volume (cm^3)	LH Volume (% of ICV)	RH Volume (cm^3)	RH Volume (% of ICV)	Asymmetry Index (%)*
Forebrain Parenchyma	534.01	31.58	499.92	29.56	6.59
Cortical Gray Matter	234.89	13.89	214.77	12.70	8.95
Lateral Ventricle	24.87	1.47	31.27	1.85	-22.81
Inferior Lateral Ventricle	2.20	0.13	2.54	0.15	-13.96
Hippocampus	2.76	0.16	3.08	0.18	-11.00
Amygdala	0.96	0.06	1.20	0.07	-22.70
Caudate	4.40	0.26	4.76	0.28	-7.97
Putamen	4.19	0.25	3.78	0.22	10.16
Pallidum	0.75	0.04	0.79	0.05	-5.45
Thalamus	9.47	0.56	9.41	0.56	0.68
Cerebellum	62.95	3.72	62.90	3.72	0.07

*The Asymmetry Index is defined as the difference between left and right volumes divided by their mean (in percent)

3T 3D Volume Imaging
T1W 3D TFE with Sense

- TR 7
- TE 3.2
- 1.2mm sagittal slices, no gap
- 255 x 256 matrix
- Acquisition Time 9:13
- 180 slices (160 usable slices)

Pulse Sequence Chosen to Provide Thin Slices and Discrimination

G Los Gatos MRI

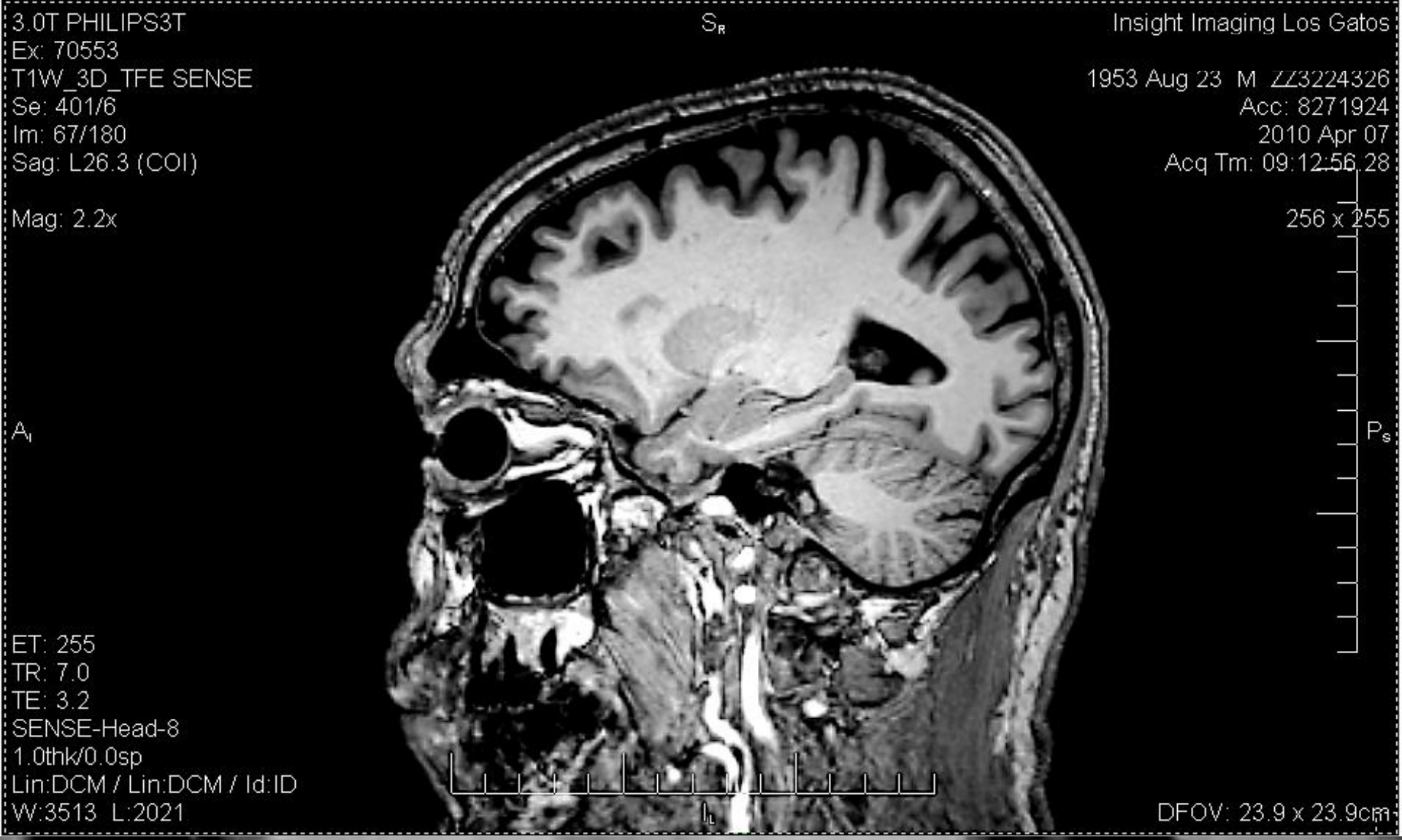
3.0T PHILIPS3T
Ex: 70553
T1W_3D_TFE SENSE
Se: 401/6
Im: 67/180
Sag: L26.3 (COI)
Mag: 2.2x
ET: 255
TR: 7.0
TE: 3.2
SENSE-Head-8
1.0thk/0.0sp
Lin:DCM / Lin:DCM / Id:ID
W:3513 L:2021
S
R
A
I
P
S
L
Insight Imaging Los Gatos
1953 Aug 23 M ZZ3224326
Acc: 8271924
2010 Apr 07
Acq Tm: 09:12:56.28
256 x 255
DFOV: 23.9 x 23.9cm

NeuroQuant Brain Volumetrics Reveals Significant Post-Traumatic Volume Loss of the Left Forebrain, Left Cortical Gray Matter, Left Hippocampus/Amygdala and Basal Ganglia on the Left Side.

Brain Structure	LH Volume (cm^3)	LH Volume (% of ICV)	RH Volume (cm^3)	RH Volume (% of ICV)	Asymmetry Index (%)*
Forebrain Parenchyma	458.83	29.62	538.23	34.75	-15.93
Cortical Gray Matter	245.68	15.86	284.53	18.37	-14.66
Lateral Ventricle	12.43	0.80	7.90	0.51	44.61
Inferior Lateral Ventricle	1.08	0.07	0.71	0.05	41.61
Hippocampus	2.44	0.16	5.19	0.34	-72.21
Amygdala	1.01	0.07	2.63	0.17	-88.72
Caudate	3.17	0.20	3.68	0.24	-15.07
Putamen	5.71	0.37	6.44	0.42	-12.01
Pallidum	0.39	0.02	1.34	0.09	-110.52
Thalamus	7.63	0.49	9.53	0.62	-22.10
Cerebellum	59.21	3.82	54.88	3.54	7.59

*The Asymmetry Index is defined as the difference between left and right volumes divided by their mean (in percent)

NeuroQuant™

Age-Related Atrophy Report

Insight Imaging Los Gatos MRI
800 Pollard Rd. #B-101
Los Gatos, CA 95032
Tel: 408-374-8897

MRI and CT in Traumatic Brain Injury

Arterial Spin Labeling

ASL

What is ASL?

What is ASL?

ASL is an MRI method that enables the measurement of tissue perfusion (CBF) without the use of exogenous contrast agents by magnetically tagging (nulling the signal of) water in inflowing blood. Recent advances in pulse sequence design and the availability of 3T scanners have resulted in increased clinical adoption of ASL.

Cerebral Blood Flow (CBF) can be defined as the steady state delivery of blood to the tissue capillary bed. It is measured in ml/min/100g

What is arterial spin labeling (ASL)?

- *normal blood signal (control image)*

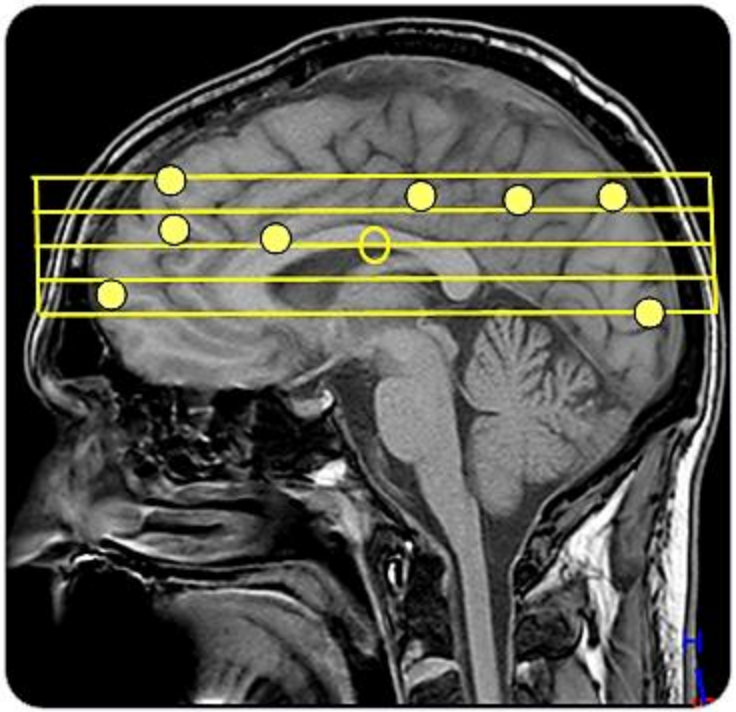

Control imaging

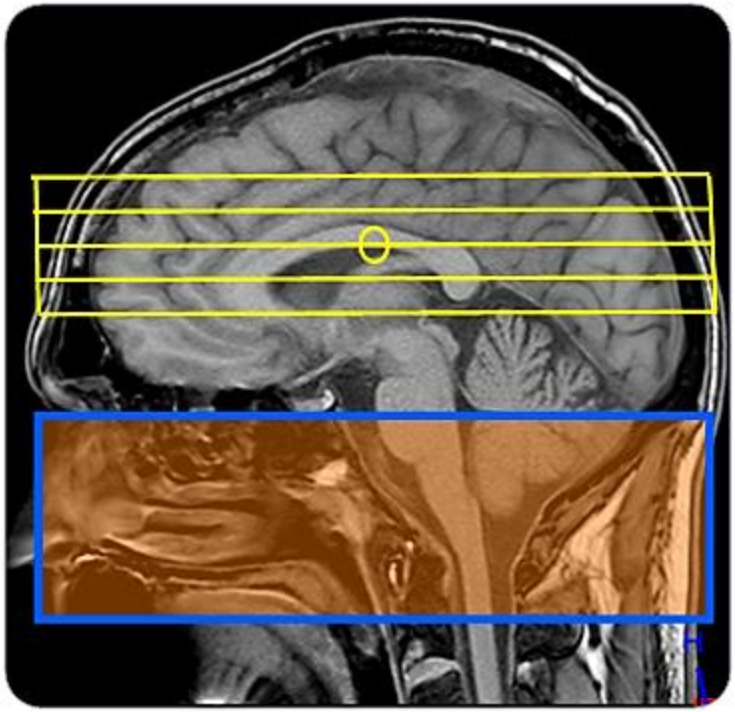

What is arterial spin labeling (ASL)?

- *normal blood signal (control image)*
- *inverted (labeled) blood signal (labeled image)*

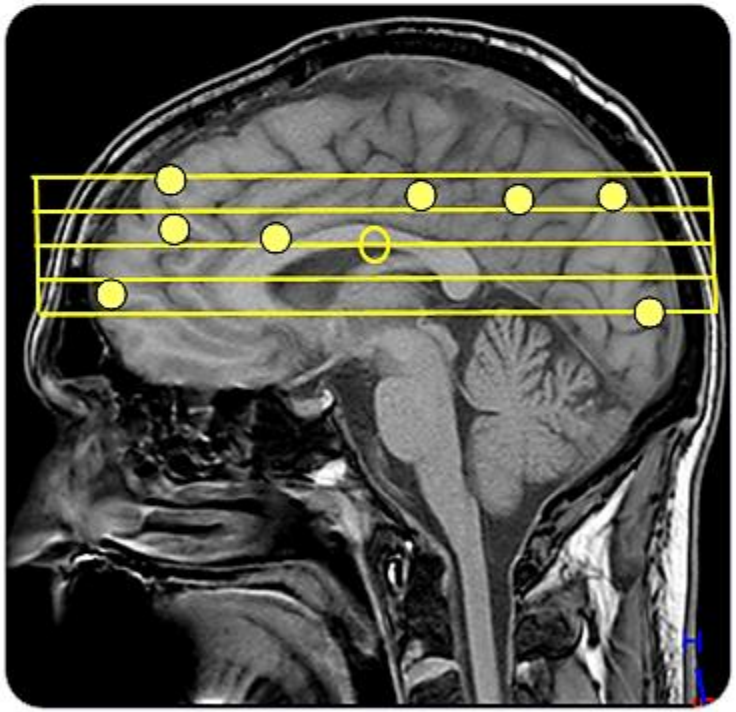

Control imaging

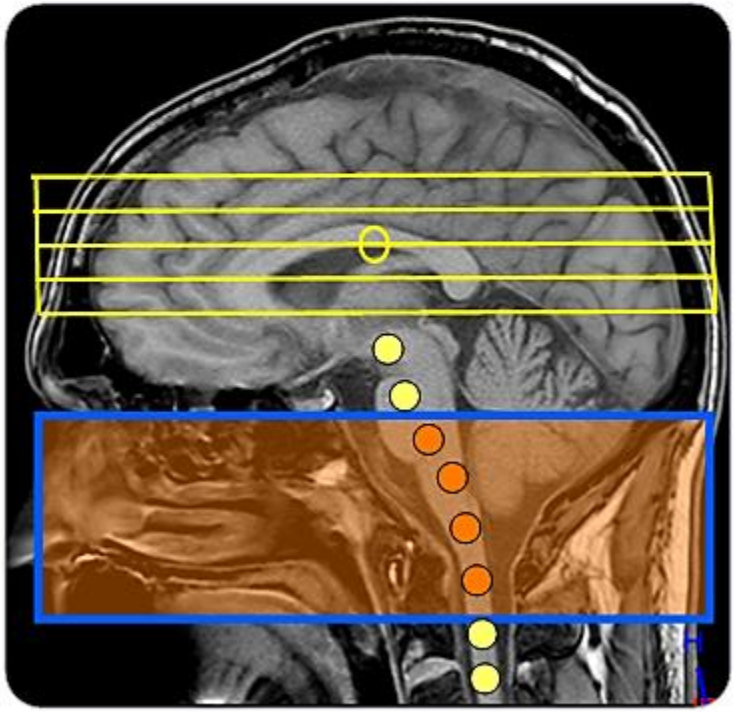

What is arterial spin labeling (ASL)?

- *normal blood signal (control image)*
- *inverted (labeled) blood signal (labeled image)*

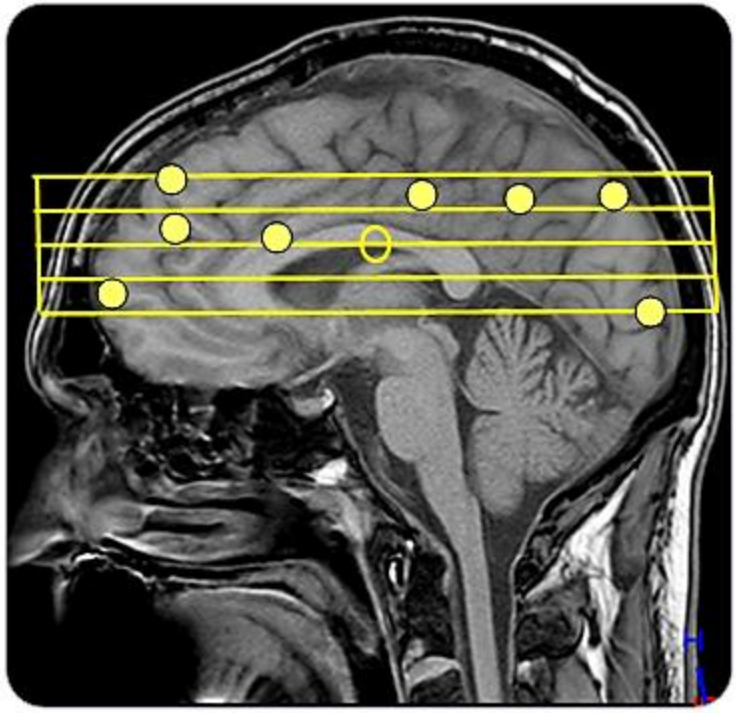

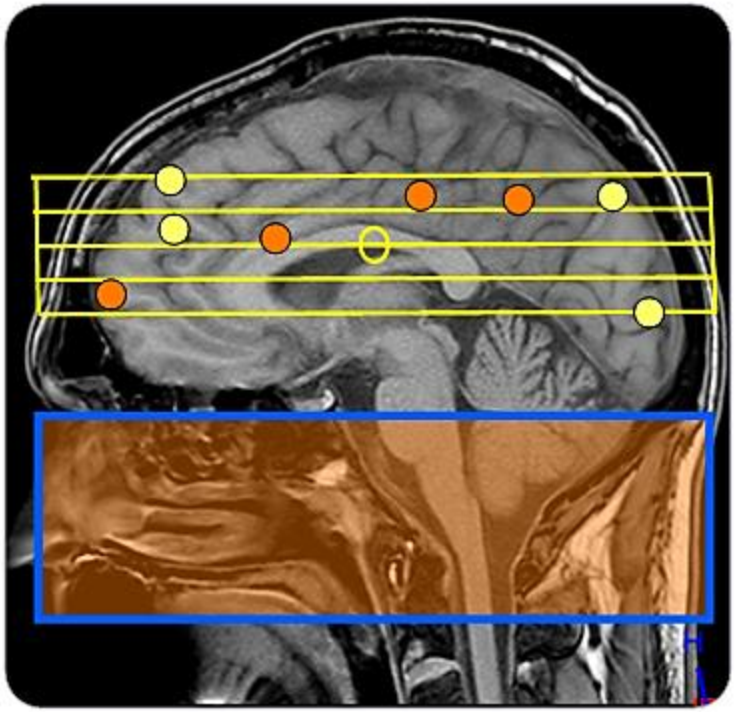

ASL Subtraction Experiment

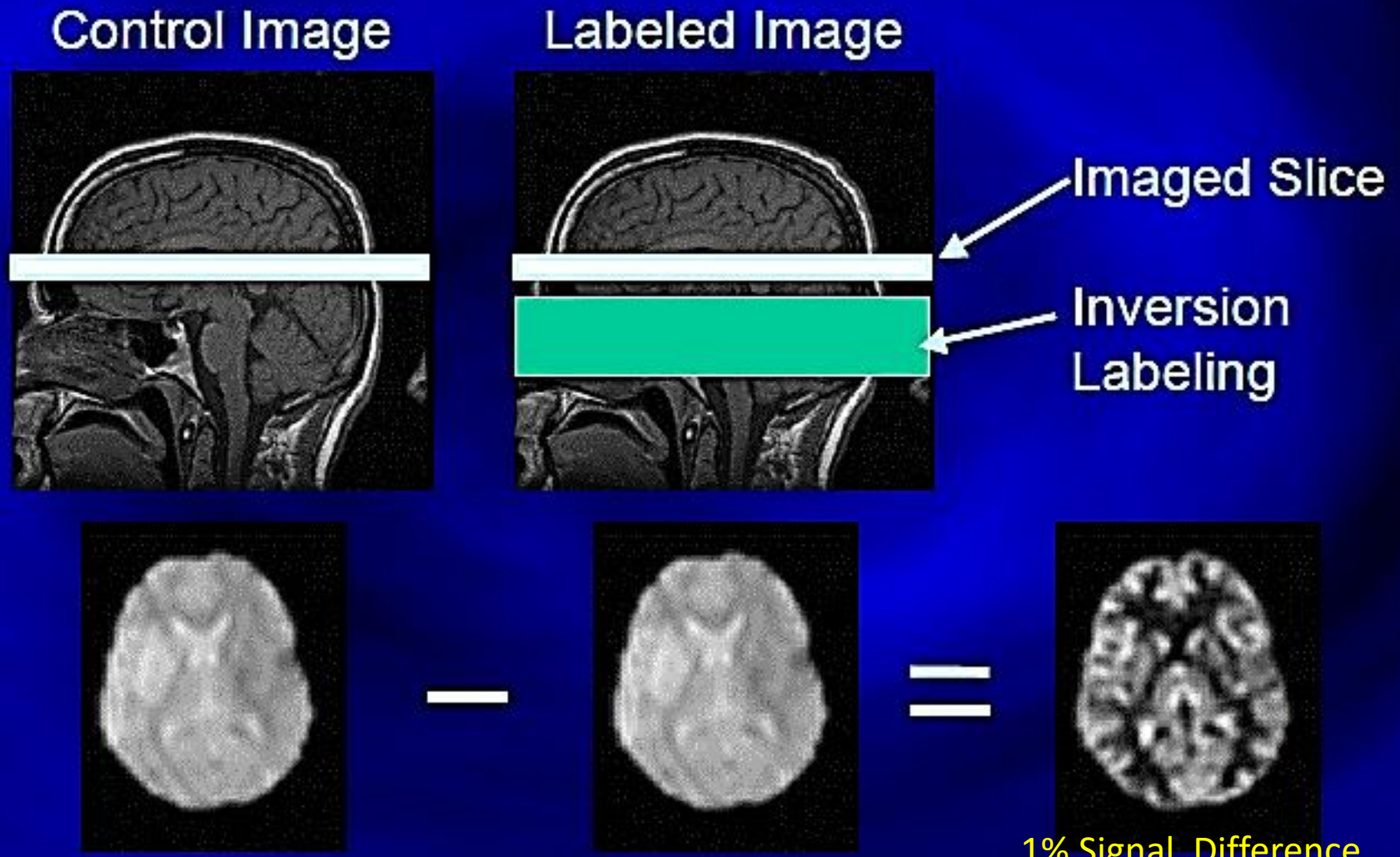

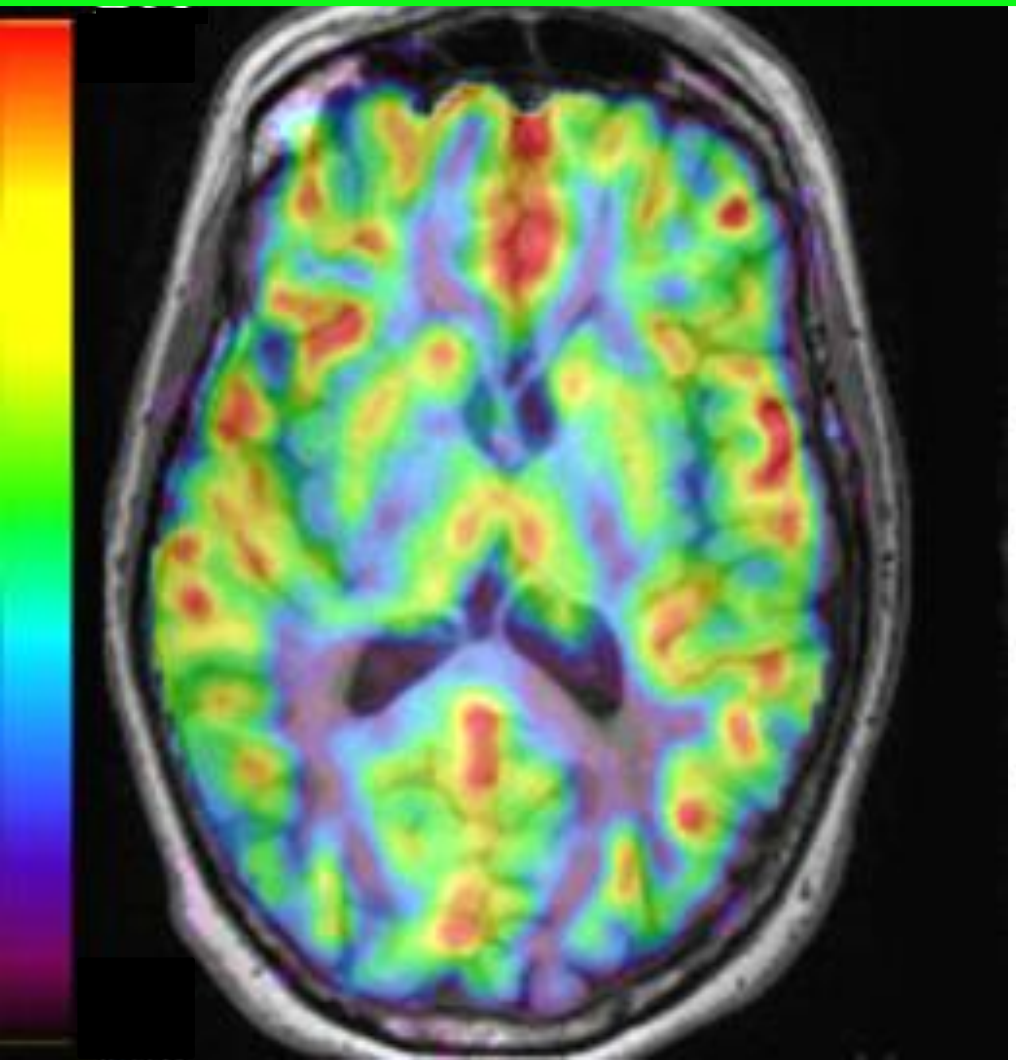

How Long Does It Take?

3T

- Acq time: 4:50 min
- 1.5mmx1.5mm

1.5T

- Acq time: 9 min

Displaying ASL Data

Black and White

Colorized and Quantitative

Colorized Superimposed on T1W Images

Los Gatos MRI

Black and White

Colorized/Quantitative

Superimposed on T1W

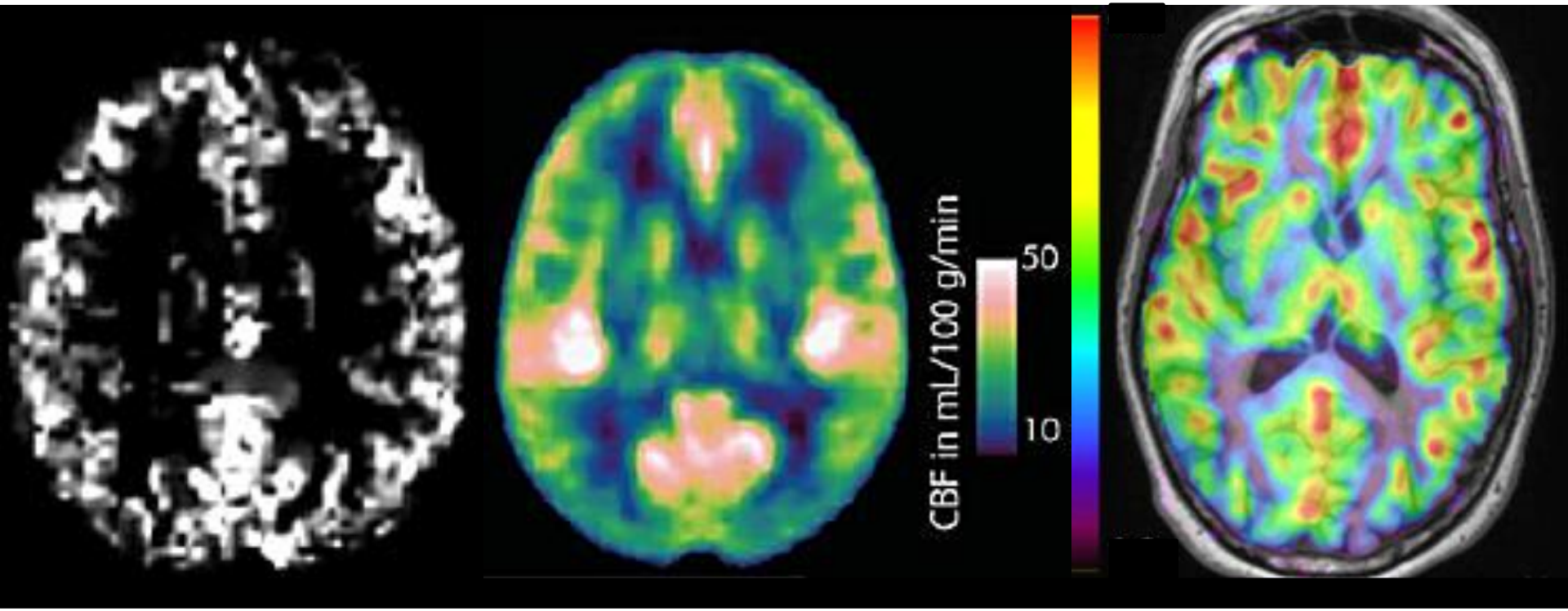

JOURNAL OF NEUROTRAUMA 34:996–1004 (March 1, 2017)

Cerebral Perfusion Changes in Post-Concussion Syndrome: A Prospective Controlled Cohort Study

Karen M. Barlow,[1–3] Lorenzo D. Marcil,[4] Deborah Dewey,[1,3,5] Helen L. Carlson,[3,6] Frank P. MacMaster,[1,3,7–9] Brian L. Brooks,[1–3,6,13] and R. Marc Lebel[3,10–12]

[1]Department of Pediatrics, [2]Department of Clinical Neurosciences, [4]Health Sciences, [5]Department of Community Health Sciences, [9]Department of Psychiatry, [10]Department of Radiology, [11]Biomedical Engineering, [13]Department of Psychology, University of Calgary, Calgary, Alberta, Canada.
[3]Alberta Children's Hospital Research Institute, Calgary, Alberta, Canada.
[6]Alberta Children's Hospital, Calgary, Alberta, Canada.

Abstract

The biology of post-concussive symptoms is unclear. Symptoms are often increased during activities, and have been linked to decreased cerebrovascular reactivity and perfusion. The aim of this study was to examine cerebral blood flow (CBF) in children with different clinical recovery patterns following mild traumatic brain injury (mTBI). This was a prospective controlled cohort study of children with mTBI (ages 8 to 18 years) who were symptomatic with post-concussive symptoms at one month post-injury (symptomatic, $n=27$) and children who had recovered quickly (asymptomatic, $n=24$). Pseudo continuous arterial spin labeling magnetic resonance imaging (MRI) was used to quantify CBF. The mTBI groups were imaged at 40 days post-injury. Global and regional CBF were compared with healthy controls of similar age and sex but without a history of mTBI ($n=21$). Seventy-two participants (mean age: 14.1 years) underwent neuroimaging. Significant differences in CBF were found: global CBF was higher in the symptomatic group and lower in the asymptomatic group compared with controls, (F(2,69) 9.734; $p<0.001$). Post-injury symptom score could be predicted by pre-injury symptoms and CBF in presence of mTBI (adjusted $R^2=0.424$; $p<0.001$). Altered patterns of cerebral perfusion are seen following mTBI and are associated with the recovery trajectory. Symptomatic children have higher CBF. Children who ''recovered'' quickly, have decreased CBF suggesting that clinical recovery precedes the cerebral recovery. Further longitudinal studies are required to determine if these perfusion patterns continue to change over time.

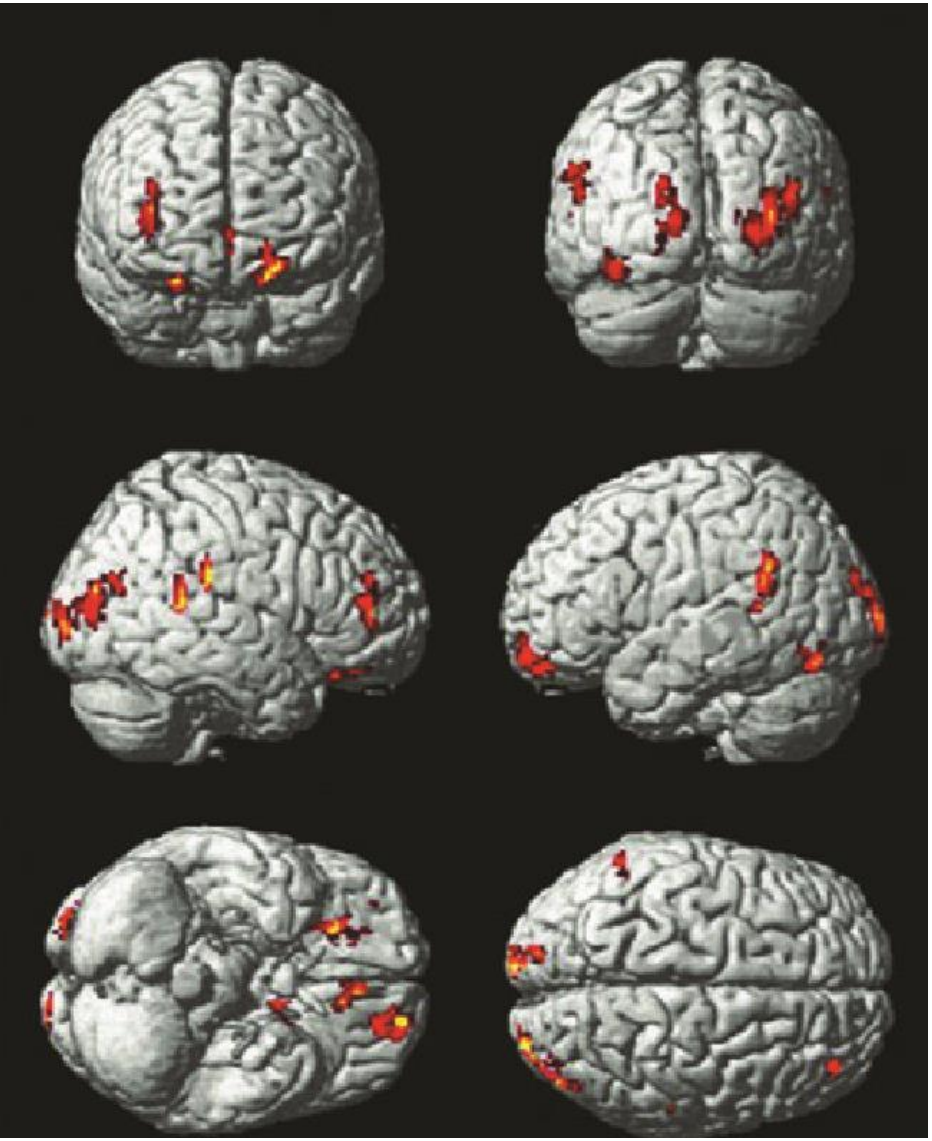

MNI Coordinates (Anatomical area)	Cluster Size (Voxels)	p-value
54 -30 24 (R supramarginal)	103	0.028
-52 -50 22 (L middle temporal)	144	0.011
36 42 12 (R middle frontal)	108	0.025
56 -42 12 (R middle temporal)	117	0.020
34 -82 10 (R middle occipital)	299	0.001
26 28 -22 (R inferior frontal, orbital)	105	0.027
-8 -102 8 (L superior occipital)	141	0.012
-18 50 -18 (L supraorbital frontal)	151	0.010
-8 32 -14 (L rectus, inferior frontal)	141	0.012
-34 -74 -14 (L fusiform)	132	0.015

FIG. 3. The regions where cerebral perfusion is significantly greater in children who remained symptomatic at 40 days following an mTBI when compared with healthy controls are shown. The cluster size and coordinates of these areas are reported in the table. MNI, Montreal Neurological Institute; mTBI, mild traumatic brain injury.

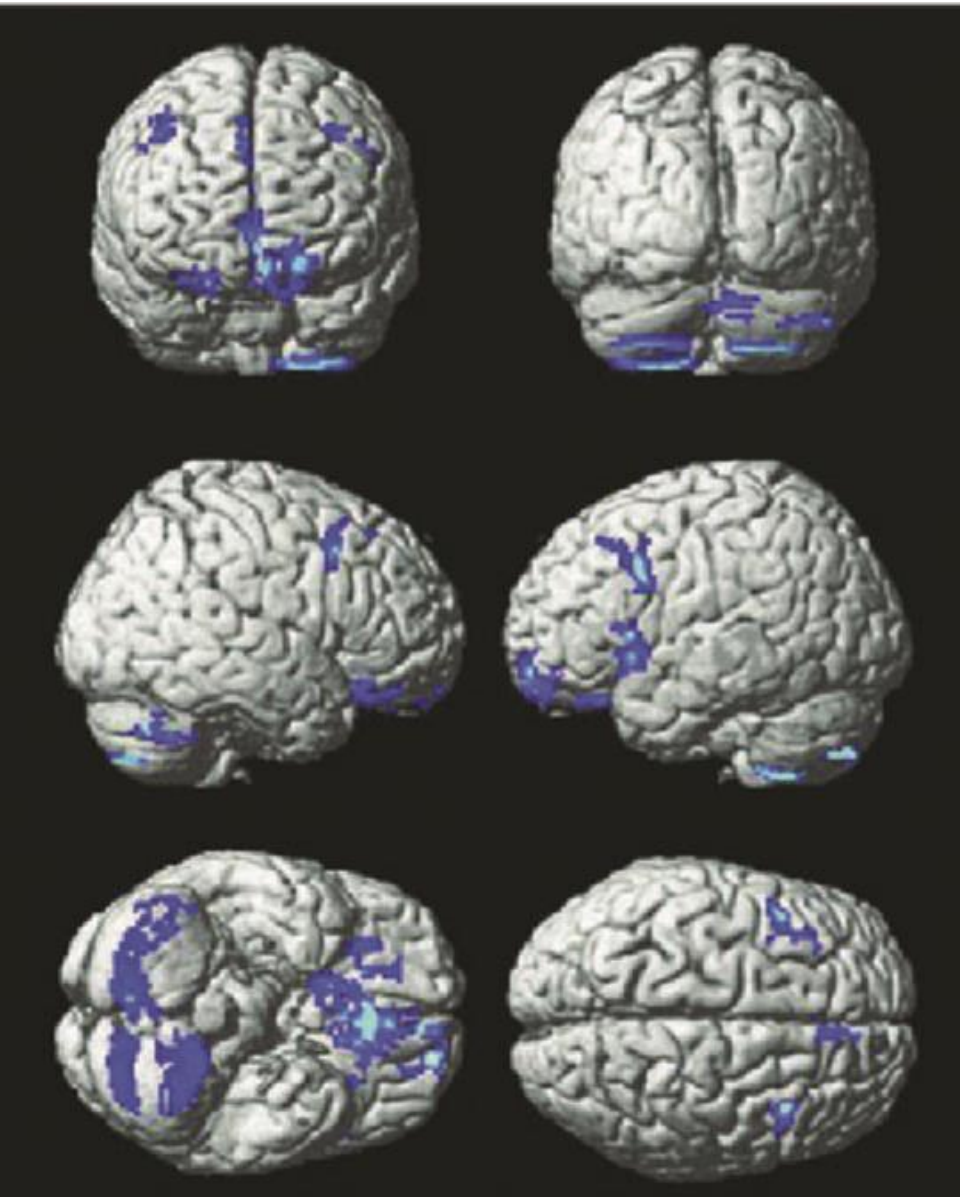

MNI Coordinates (mm)	Cluster Size (Voxels)	p-value
-18 58 -12 (L supraorbital, frontal)	126	0.011
-2 16 -20 (L rectus, frontal)	1483	0.000
-30 16 -12 (L insula)	295	0.000
36 14 38 (R middle frontal)	130	0.010
-44 14 32 (L pre-central)	209	0.002
32 28 -16 (R inferior frontal, orbital)	108	0.017
-20 -40 -54 (L cerebellum)	209	0.002
10 -72 -48 (R cerebellum)	129	0.010
40 -62 -30 (R crus cerebellum)	126	0.011

FIG. 5. The regions where cerebral perfusion is significantly decreased in children who were asymptomatic at 40 days following an mTBI when compared with healthy controls are shown. The cluster size and coordinates of the areas are reported in the table (overall pcrit <0.05, voxel cluster-level >100). MNI, Montreal Neurological Institute; mTBI, mild traumatic brain injury.

Mr. XX Accident History

- Mr. XX is a 41YM, with a history of three prior concussions from which he completely recovered, who was involved in a motor vehicle accident suffering head trauma on 5/3/2017.

- Since the accident, Mr. XX has been experiencing memory difficulties including trouble with name recall, difficulty concentrating, and attention and focus impairment.

- Mr. XX's symptoms are interfering with completing tasks and performance. He has been diagnosed with post concussive syndrome.

Mr. XX MRI of the Brain 3/7/19

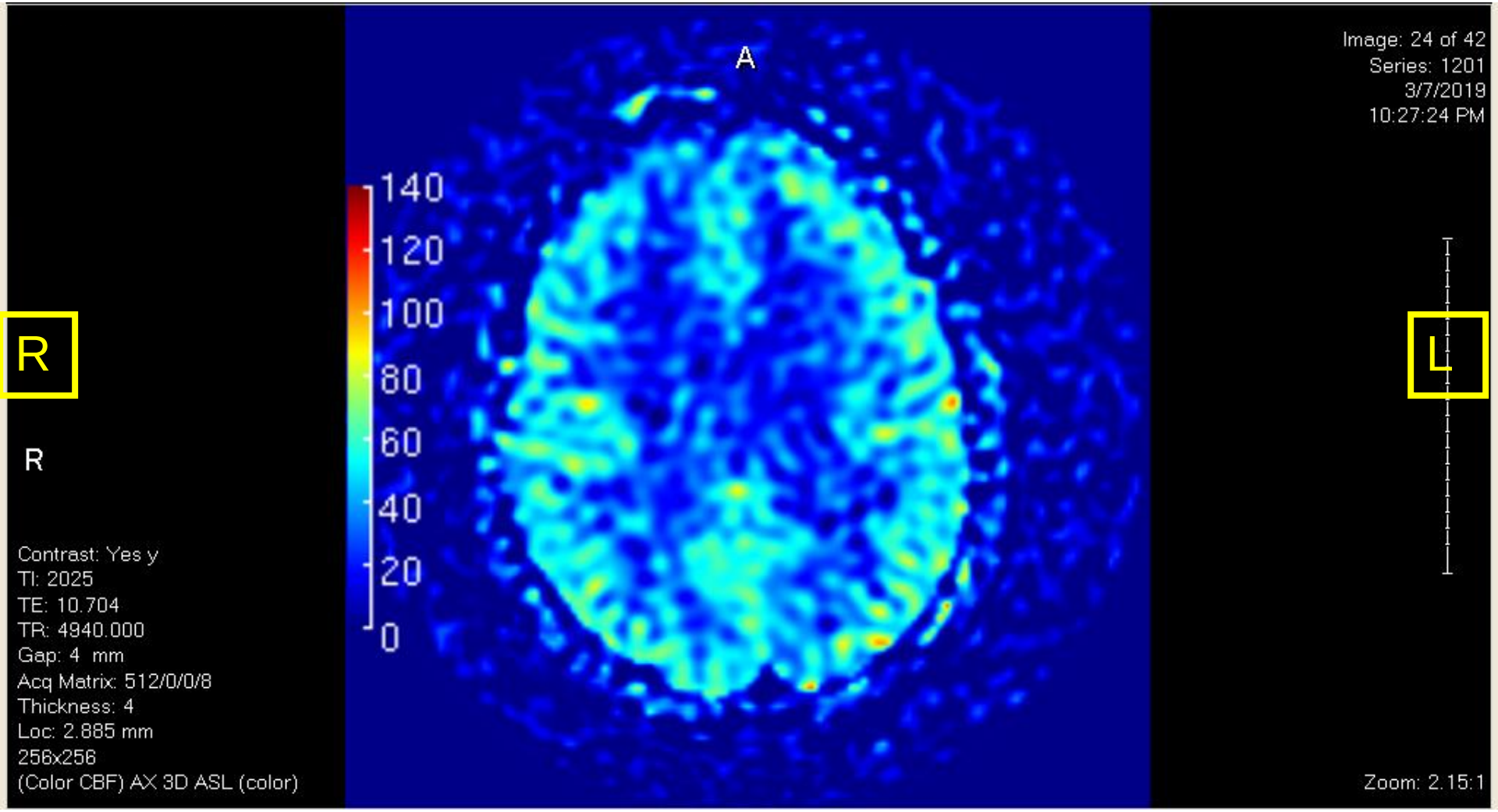

Mr. XX MRI of the Brain 3/7/19

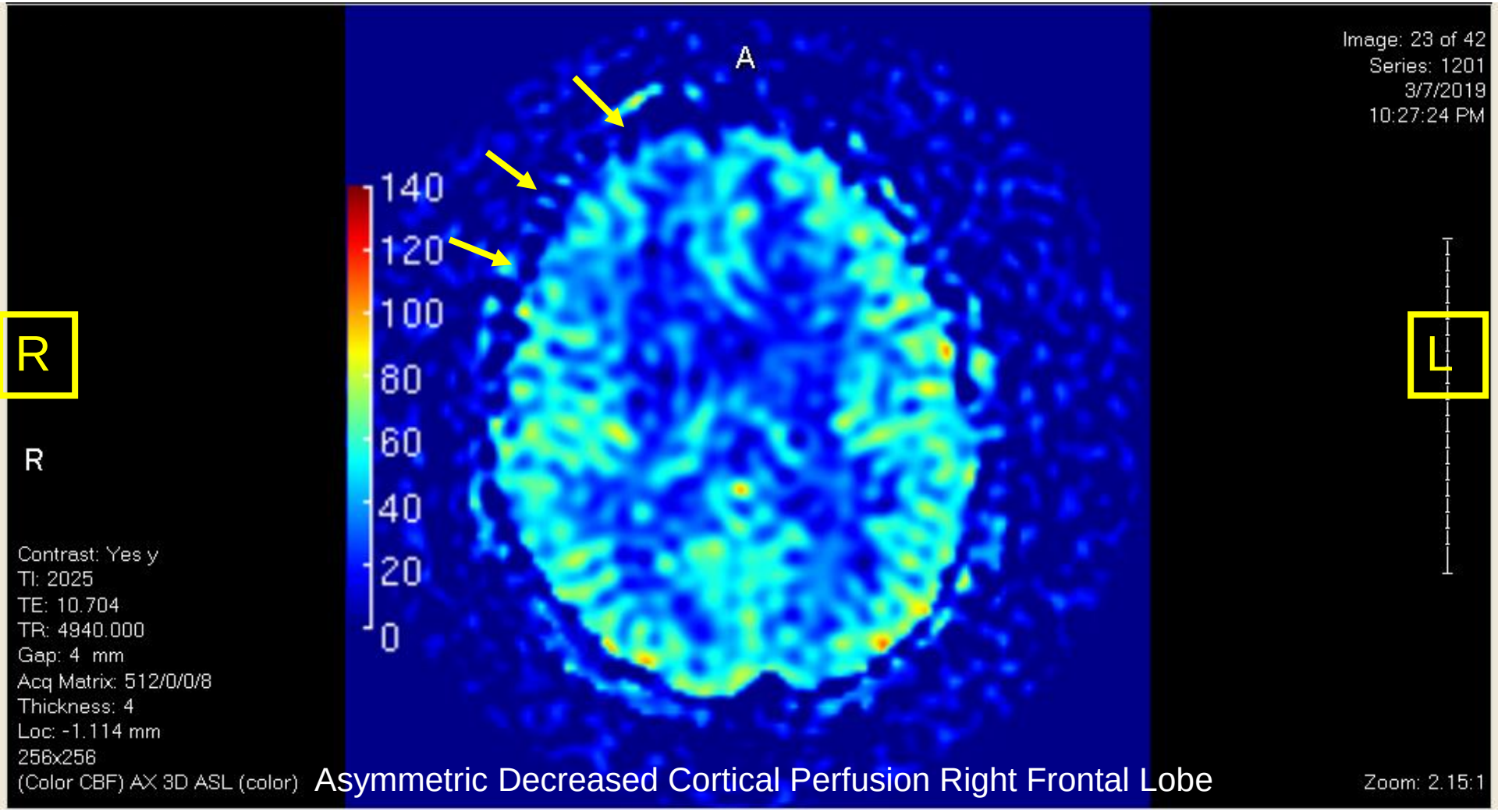

Mr. XX MRI of the Brain 3/7/19

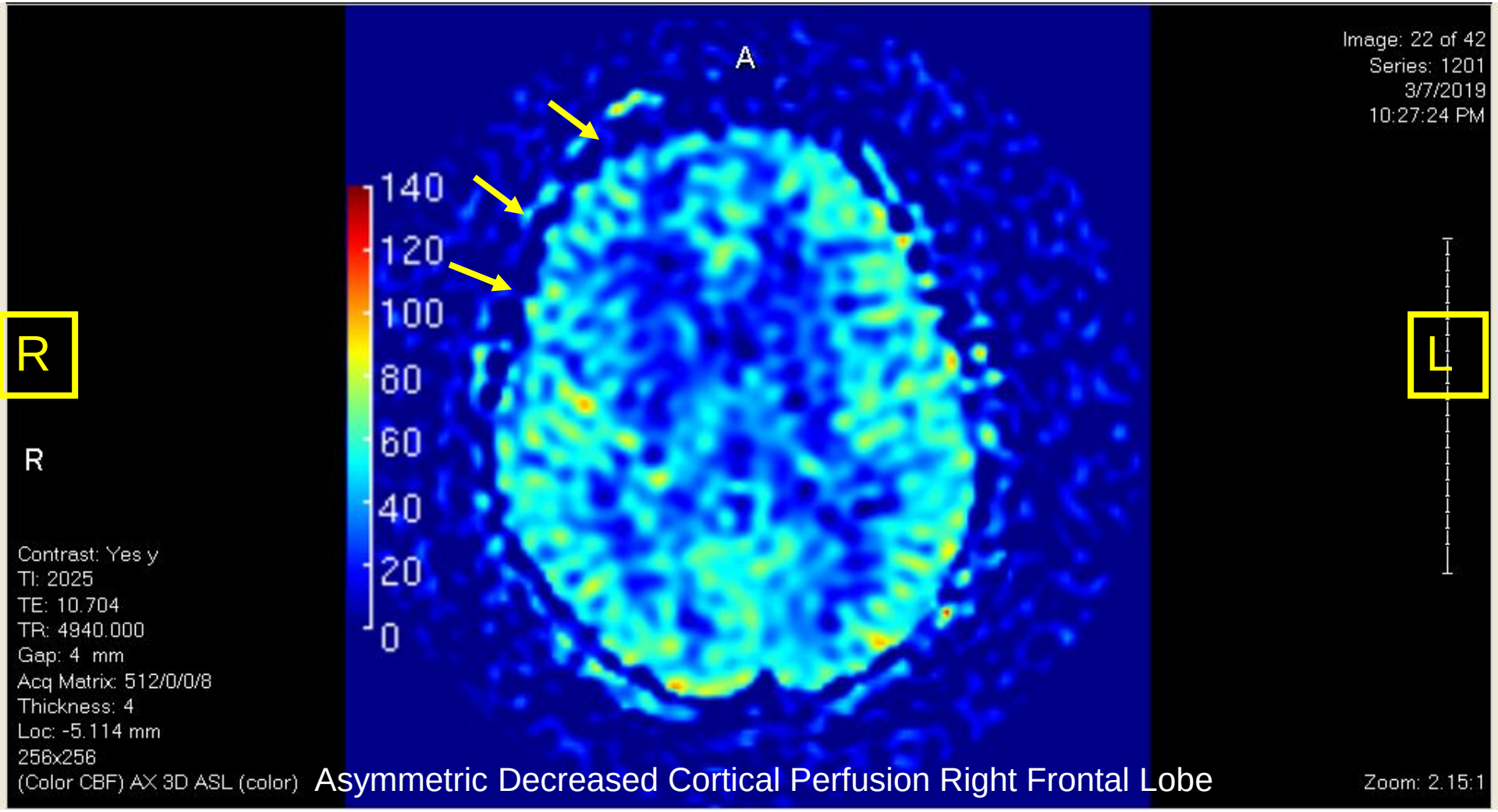

Robert Thompson MRI of the Brain 3/7/19

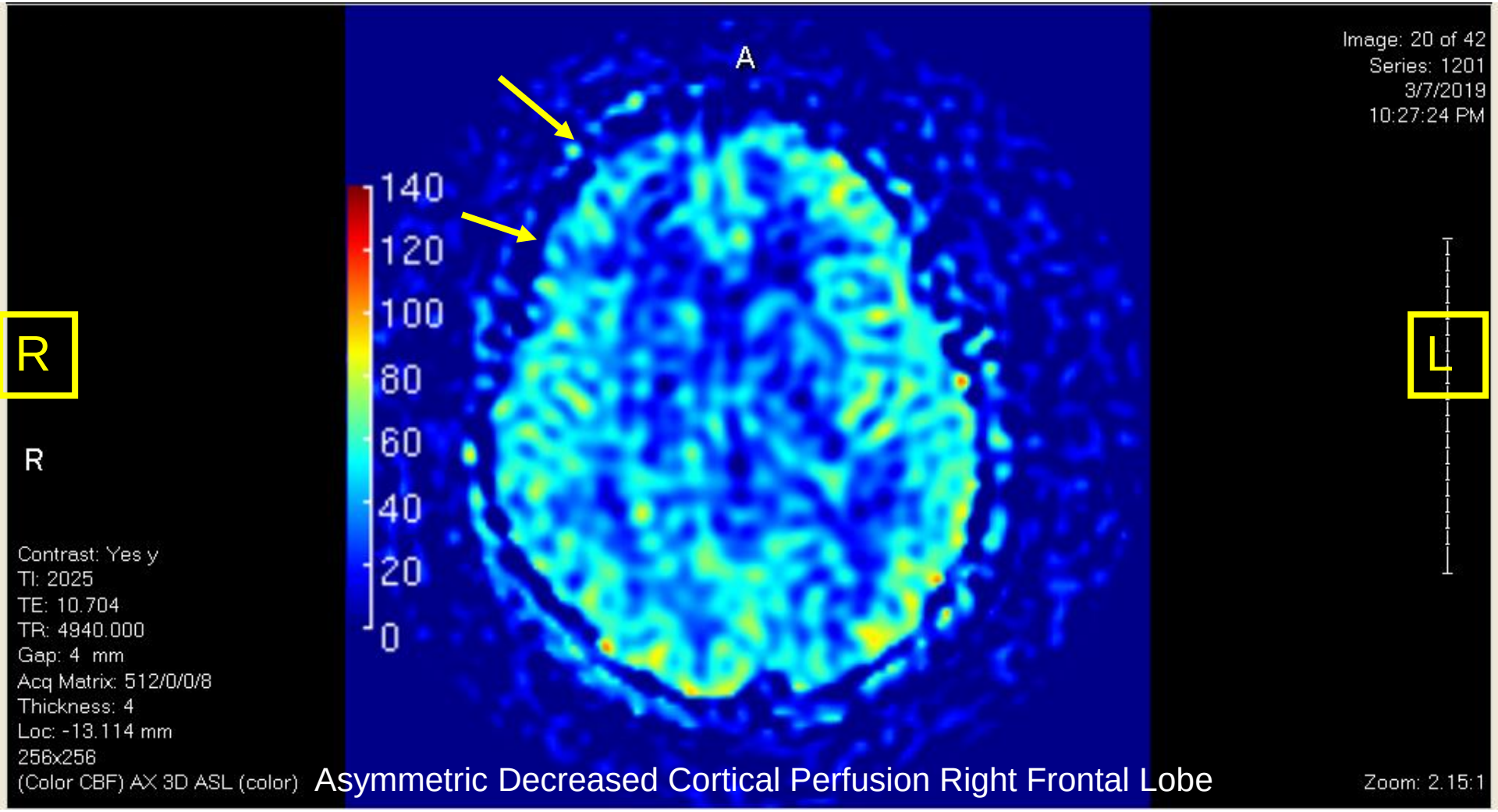

MRI and CT in Traumatic Brain Injury

Quiz

AuntMinnie's PopQuiz

History: A 26-year-old man with loss of consciousness after being struck by an automobile as he was walking.

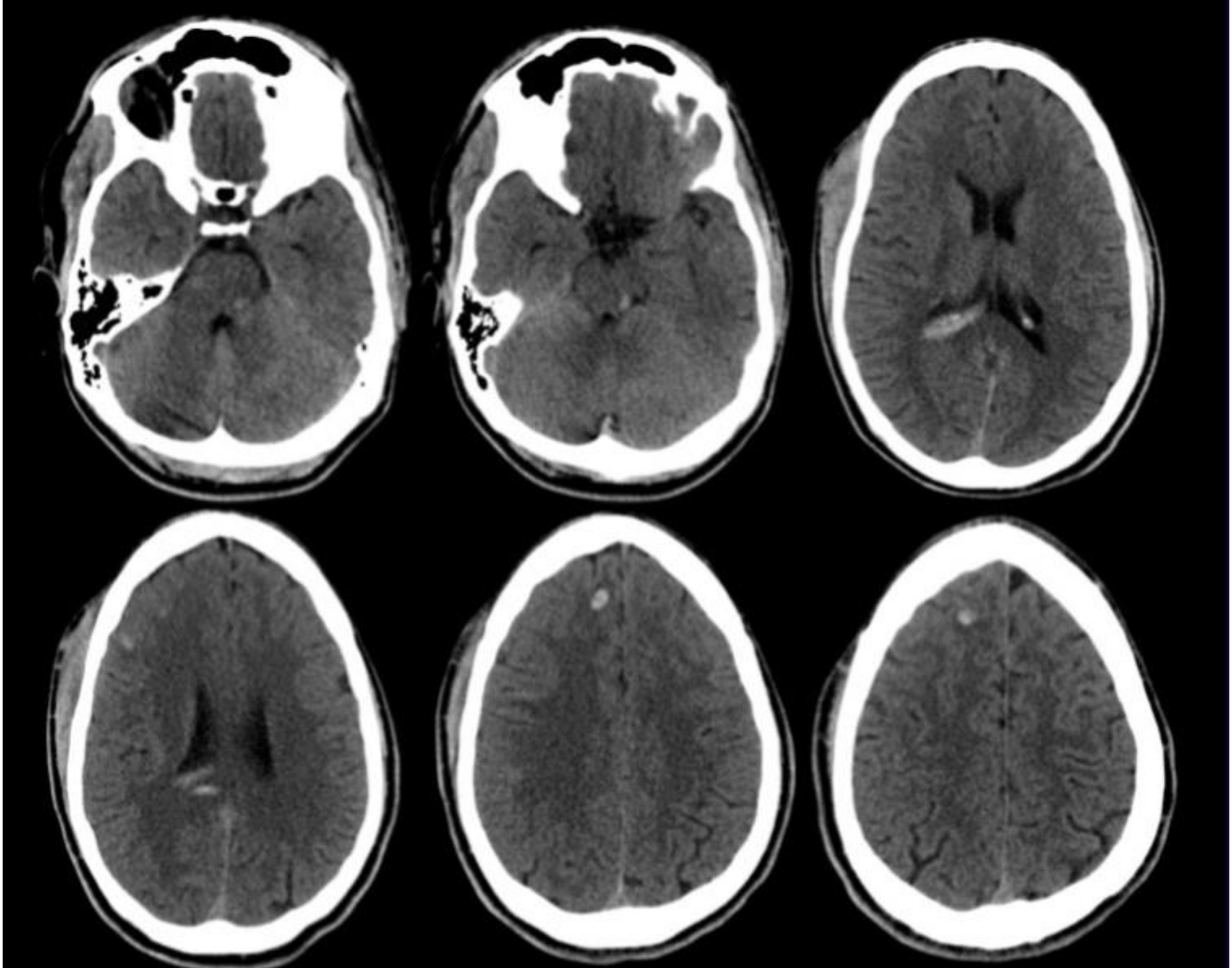

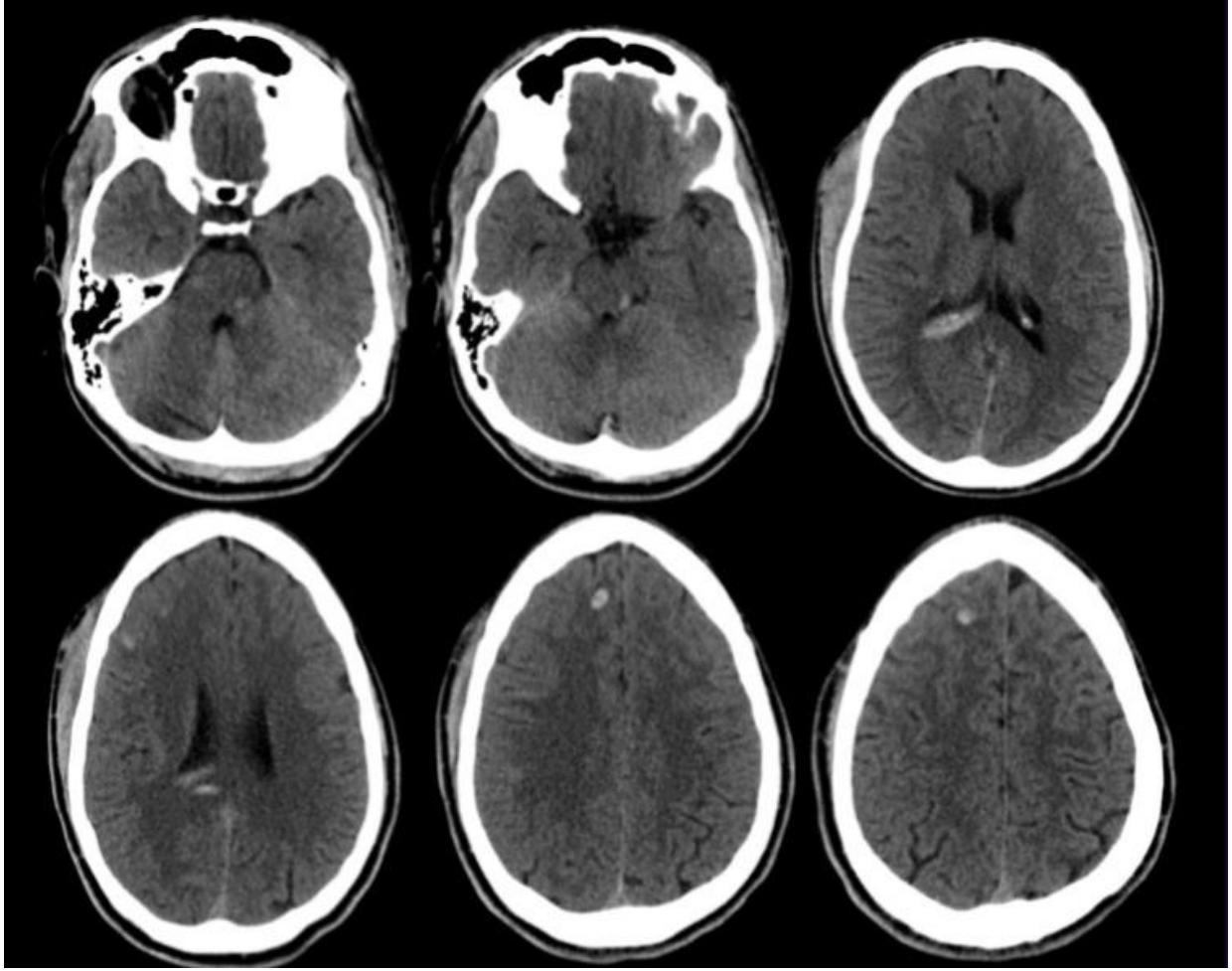

What is the predominant location of the lesions?

- ○ Gray matter
- ○ White matter
- ○ Gray-white matter junction
- ○ Extra-axial

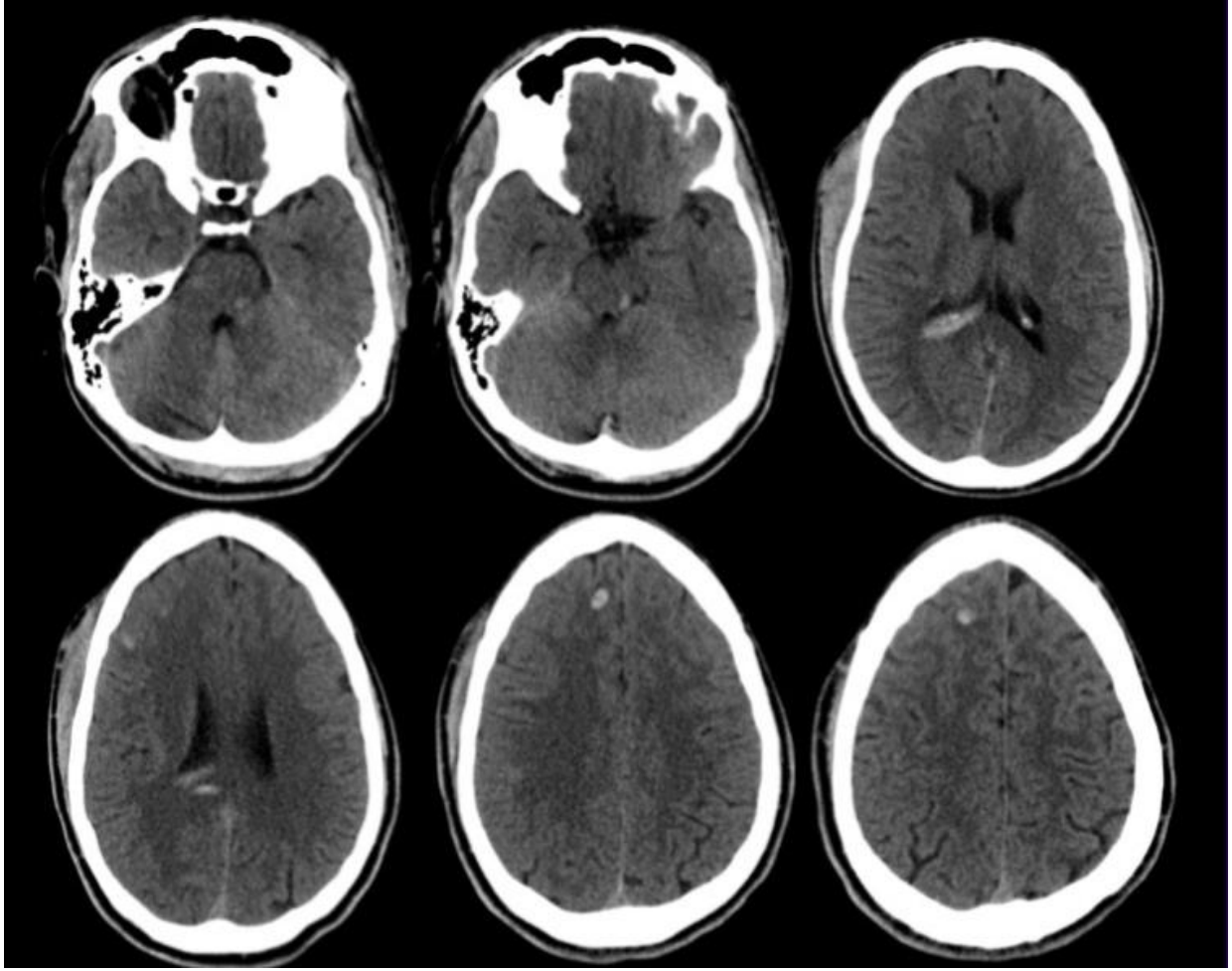

What is the predominant location of the lesions?

- ○ Gray matter
- ○ White matter
- ○ Gray-white matter junction (correct!)
- ○ Extra-axial

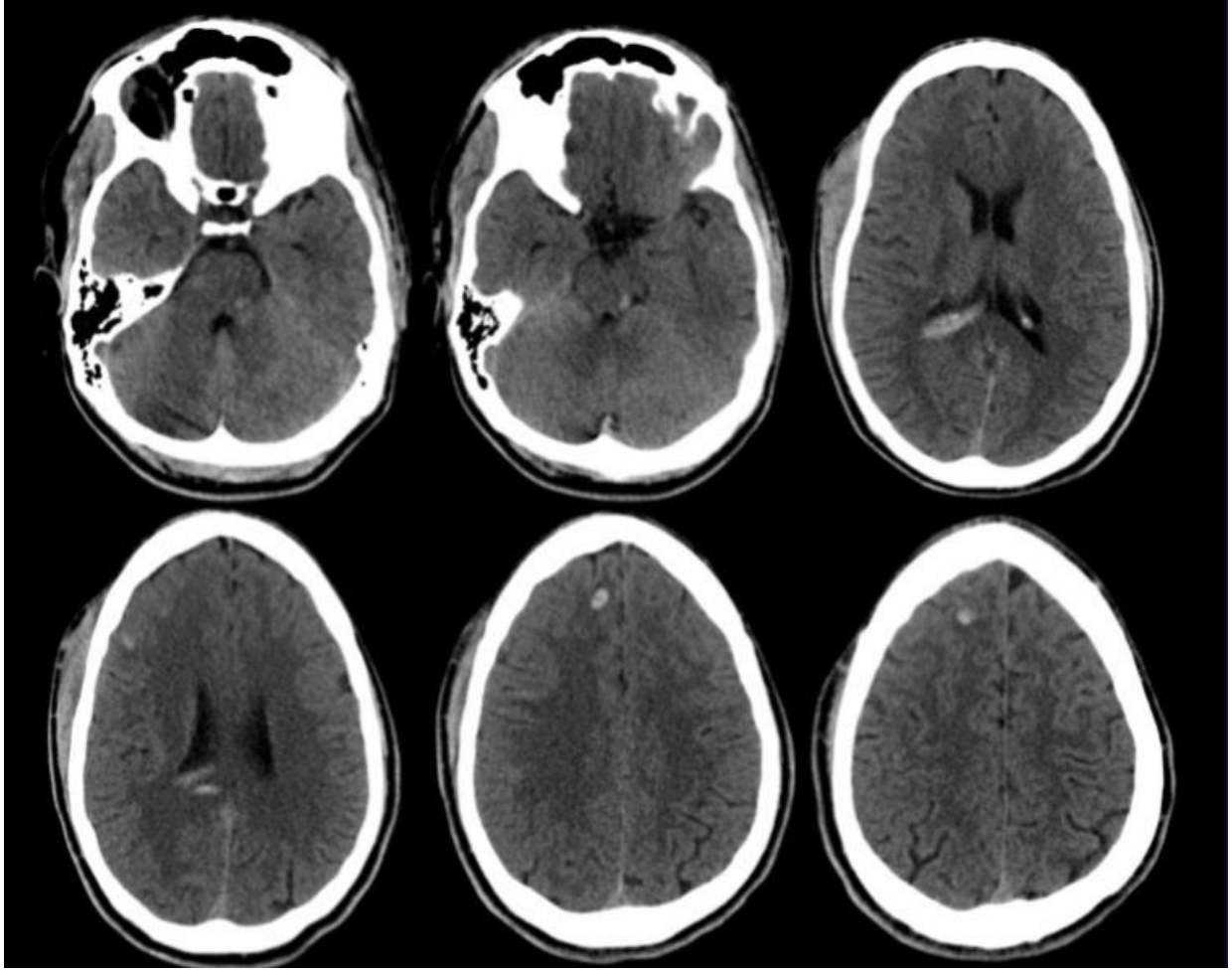

There is intraventricular blood.

- ○ True
- ○ False

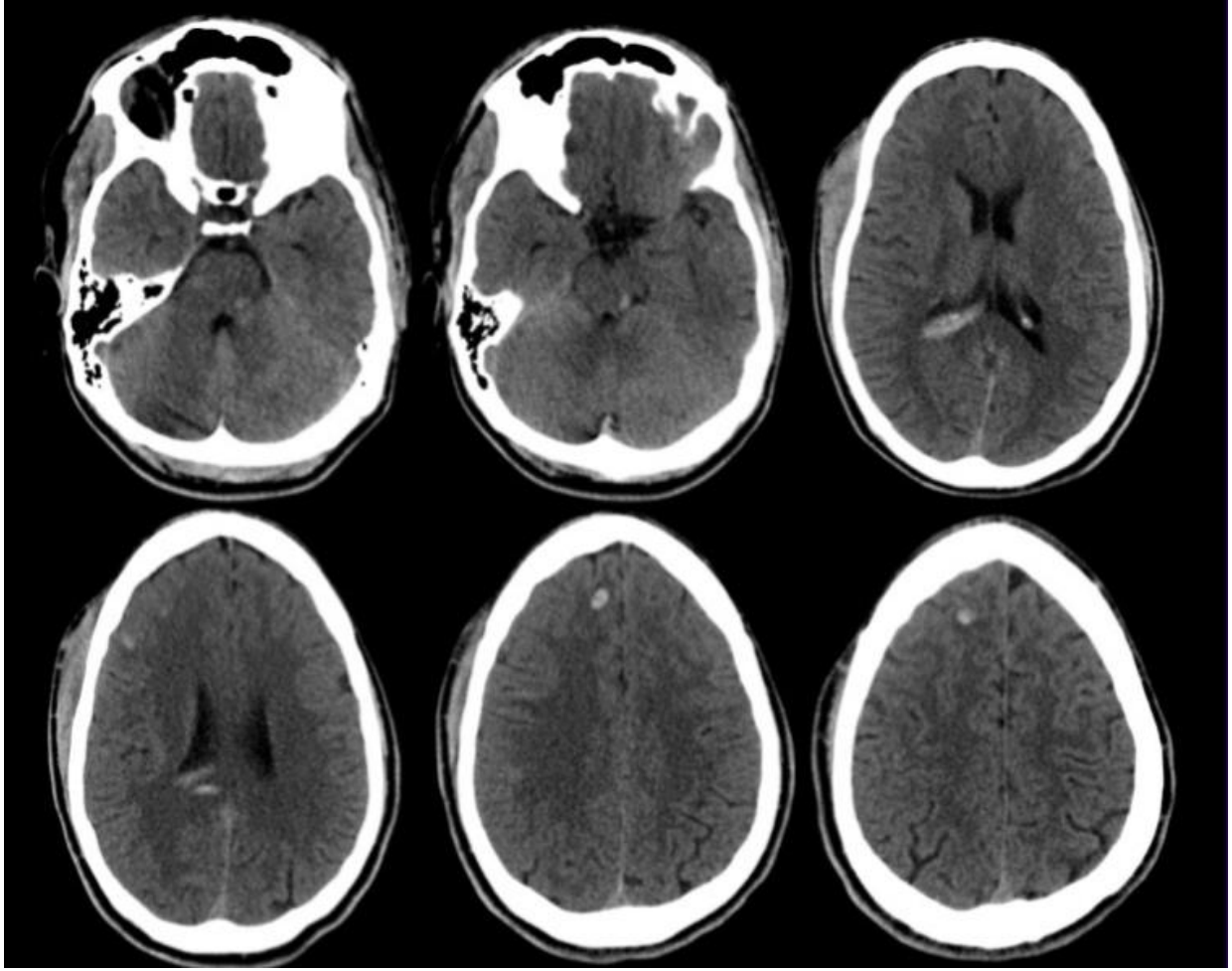

- ○ True (correct!)
- ○ False

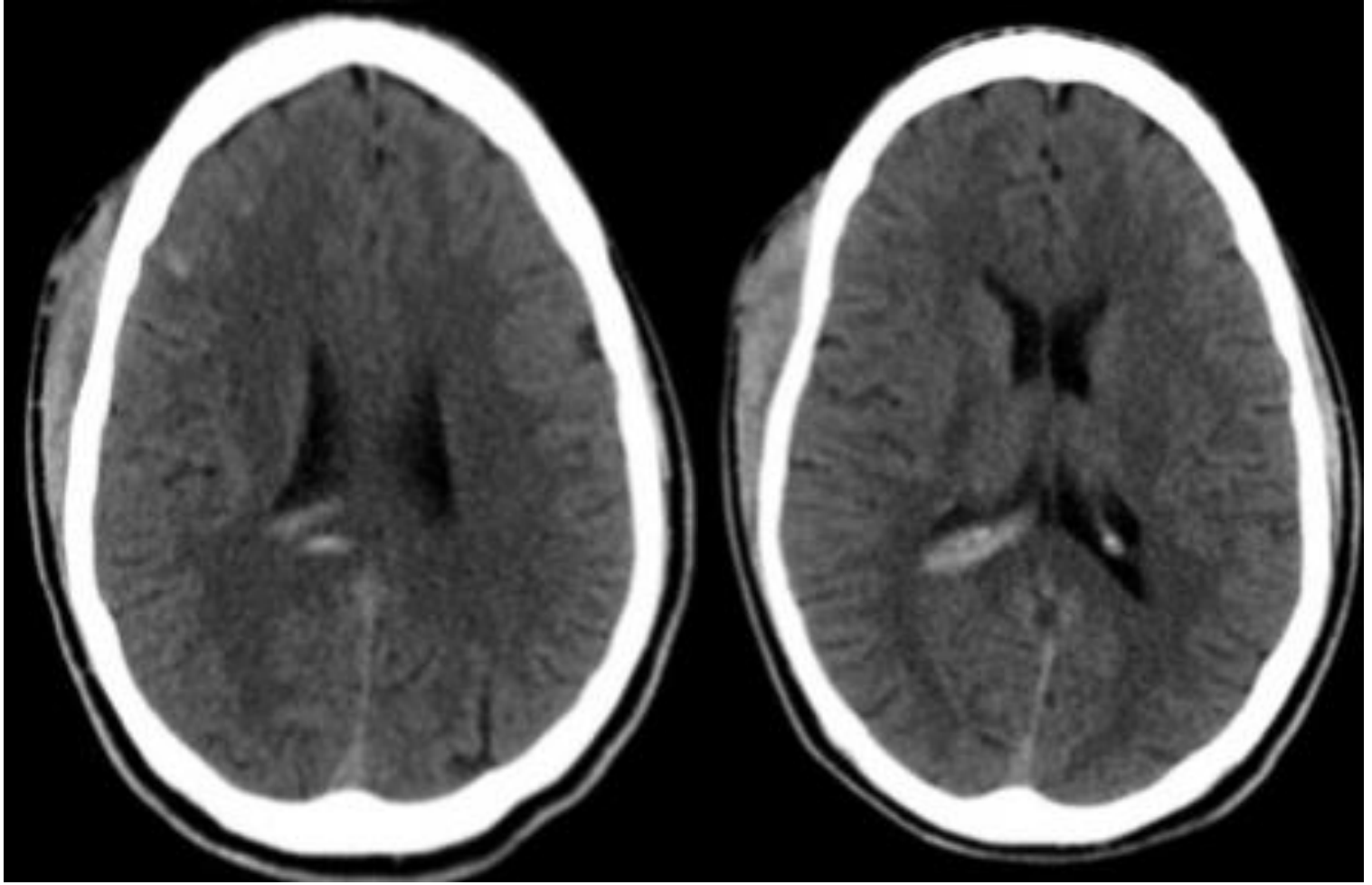

- ○ True (correct!)
- ○ False

What is the next most appropriate imaging step?

- ○ CT angiography of the head
- ○ Brain MRI
- ○ MR angiography of the head
- ○ Cerebral angiogram

What is the next most appropriate imaging step?

- ○ CT angiography of the head
- ● Brain MRI (correct!)
- ○ MR angiography of the head
- ○ Cerebral angiogram

After a right, frontal approach ventricular drain was placed and the patient was stabilized, brain MRI was performed.

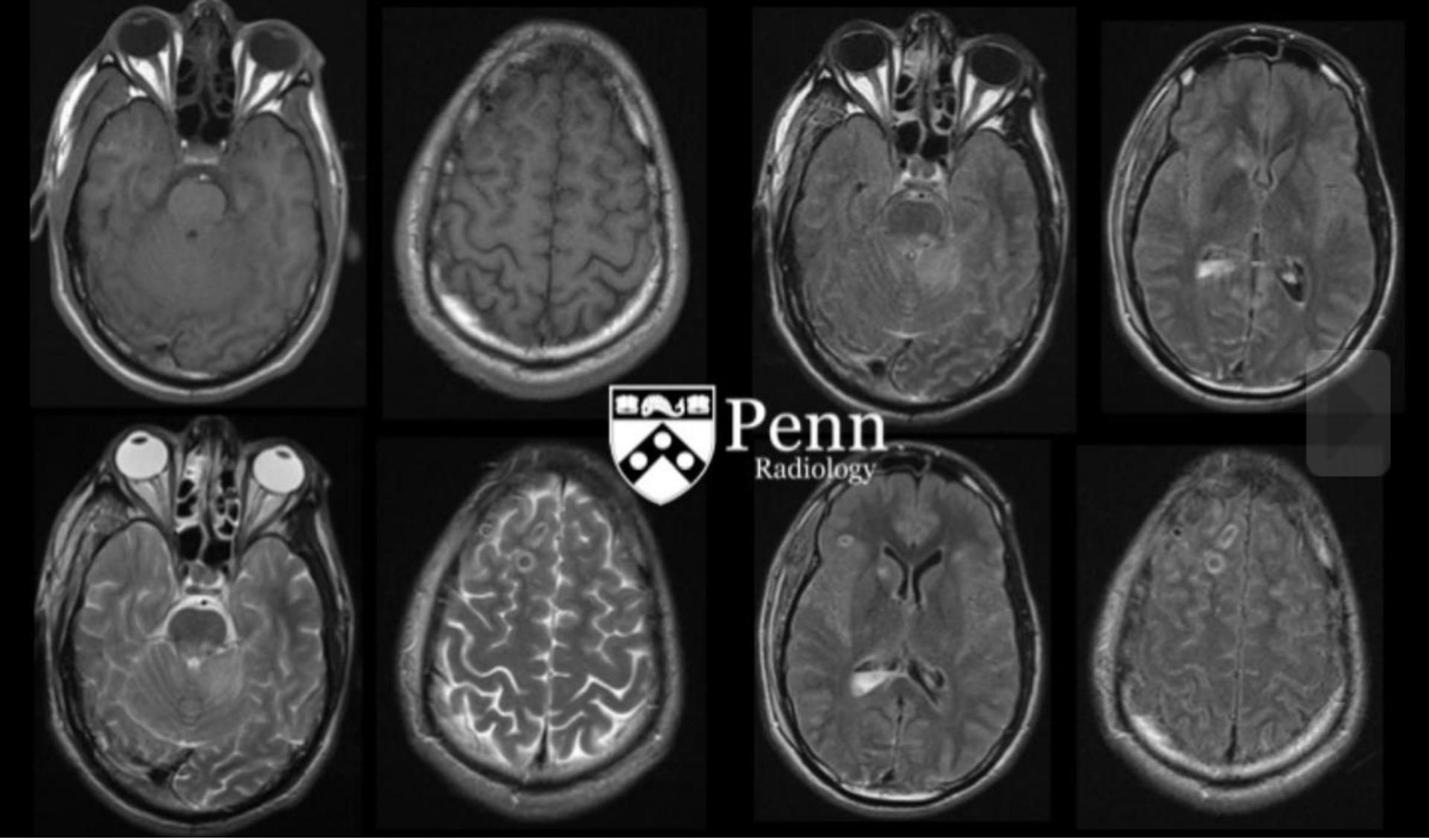

Axial T1-, T2-, and T2-weighted fluid-attenuated inversion-recovery (FLAIR), diffusion-weighted (DWI), apparent diffusion coefficient (ADC), and gradient-recalled echo (GRE) MR images of the head are shown below.

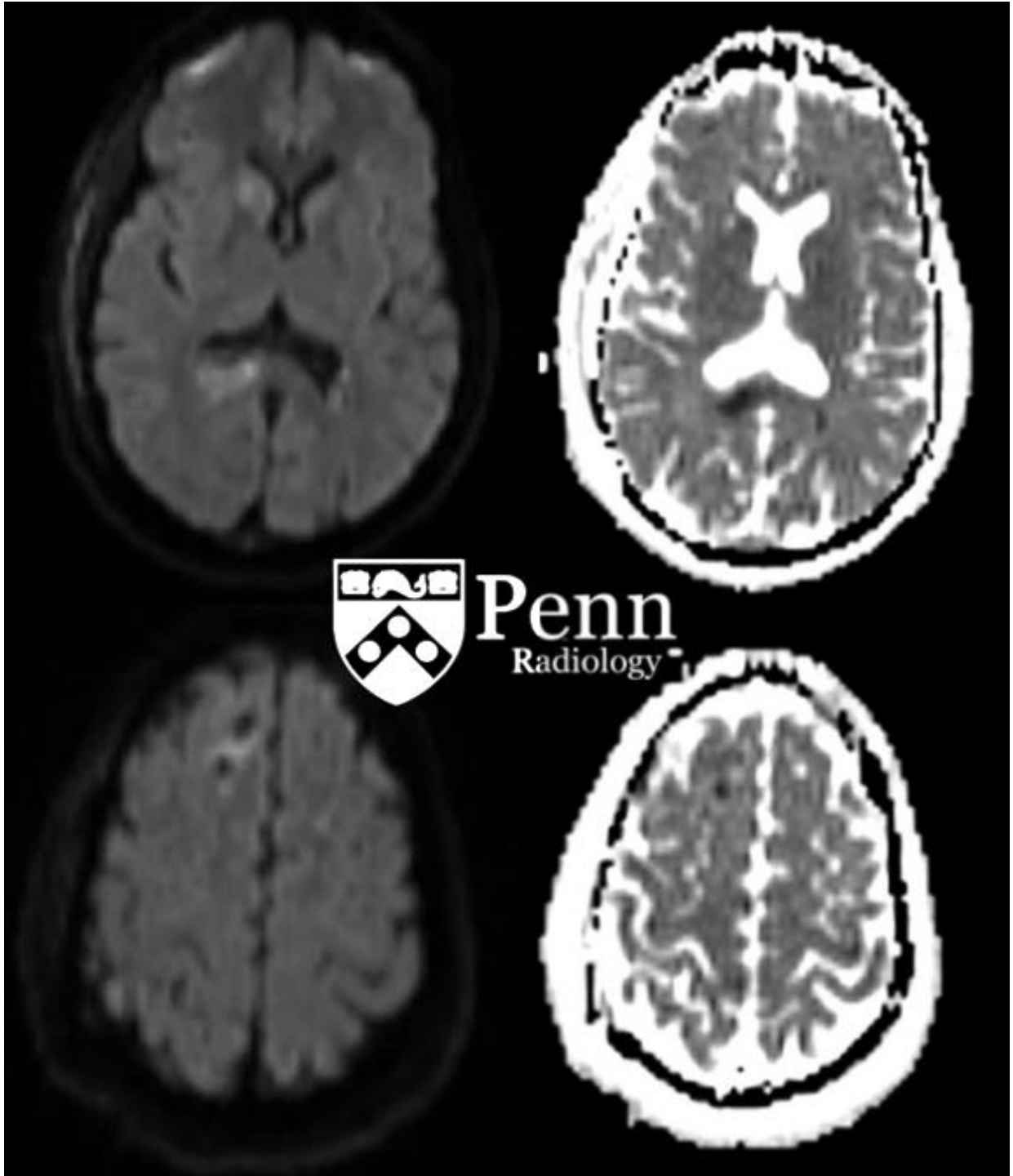
Penn
Radiology

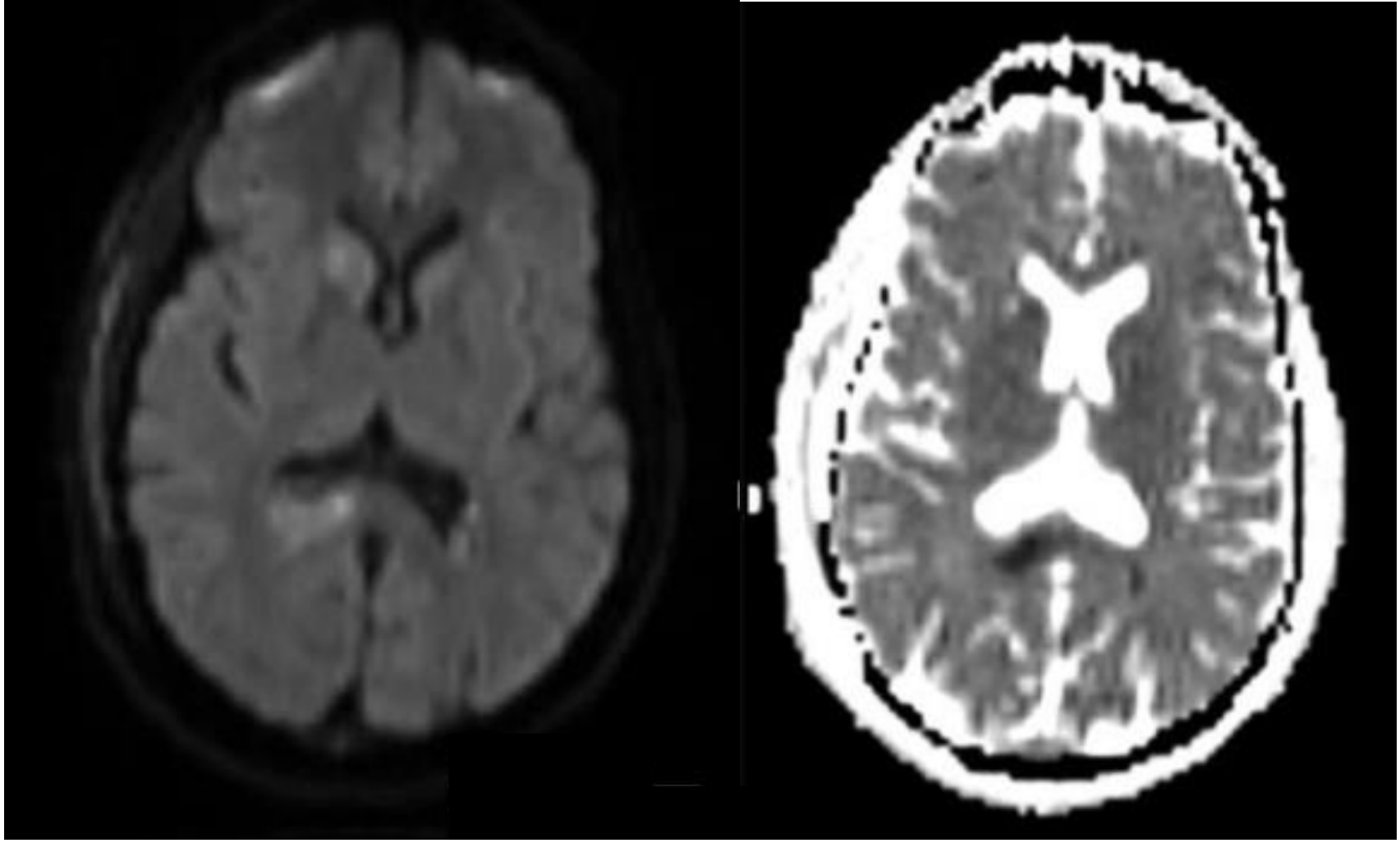

Some of the lesions have restricted diffusion.

- ○ True
- ○ False

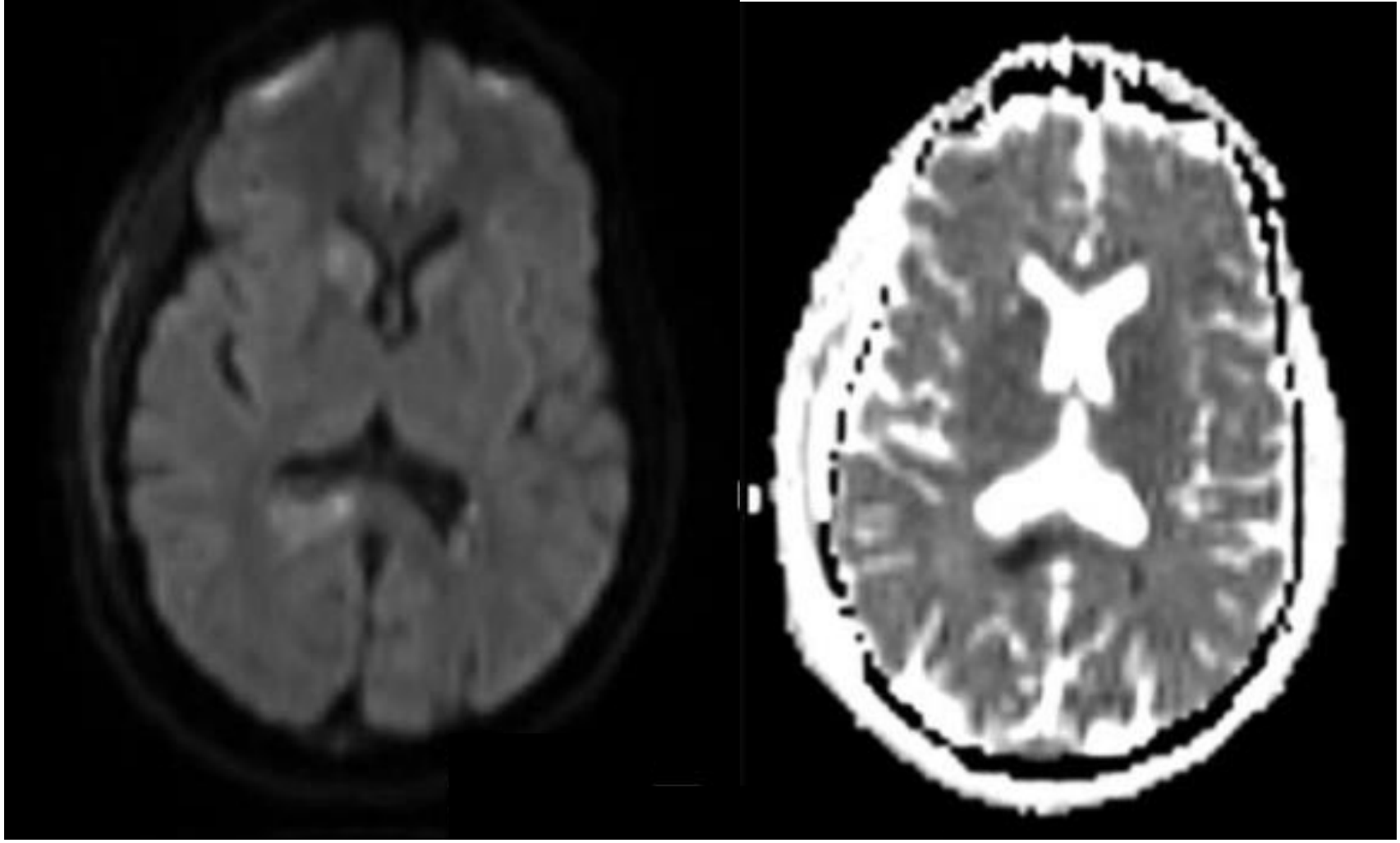

Some of the lesions have restricted diffusion.

- ○ True (correct!)
- ○ False

What is the most likely diagnosis?

- ○ Intraparenchymal contusions
- ○ Diffuse axonal injury
- ○ Multiple cerebral cavernous venous malformations
- ○ Hemorrhagic metastases

What is the most likely diagnosis?

- ○ Intraparenchymal contusions
- ● Diffuse axonal injury (correct!)
- ○ Multiple cerebral cavernous venous malformations
- ○ Hemorrhagic metastases

Diffuse axonal injury is characterized by multiple focal lesions, usually seen at the gray-white matter junction, corpus callosum, and brainstem. Cortical lesions are more common in the frontal and temporal lobes. The splenium of the corpus callosum is most common, because this portion of the callosum is relatively mobile.

MRI is much more sensitive than CT for imaging of diffuse axonal injuries. Delayed imaging may also be abnormal when initial imaging is normal.

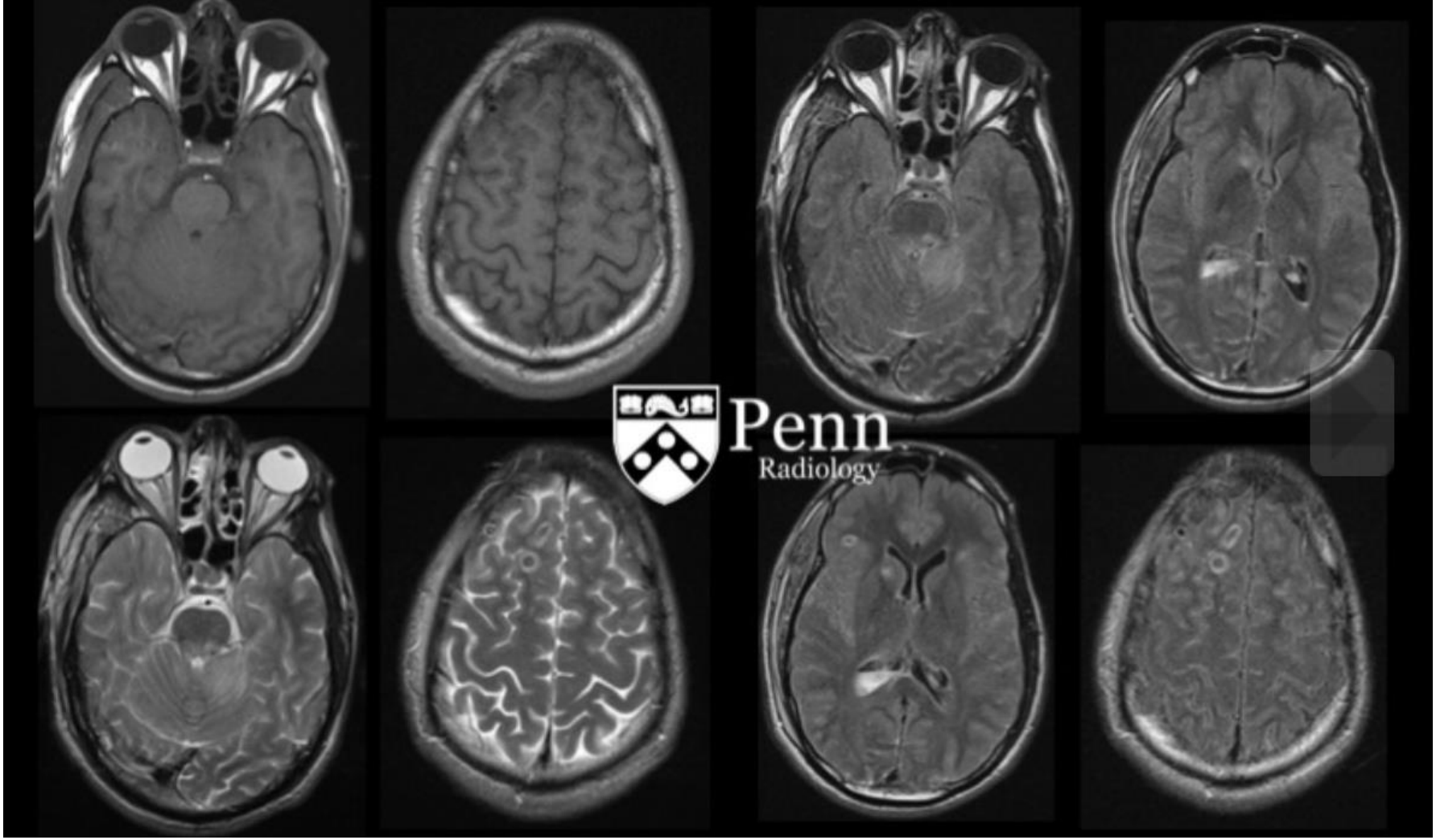

What is the grade of this injury?

- ○ Grade I
- ○ Grade II
- ○ Grade III

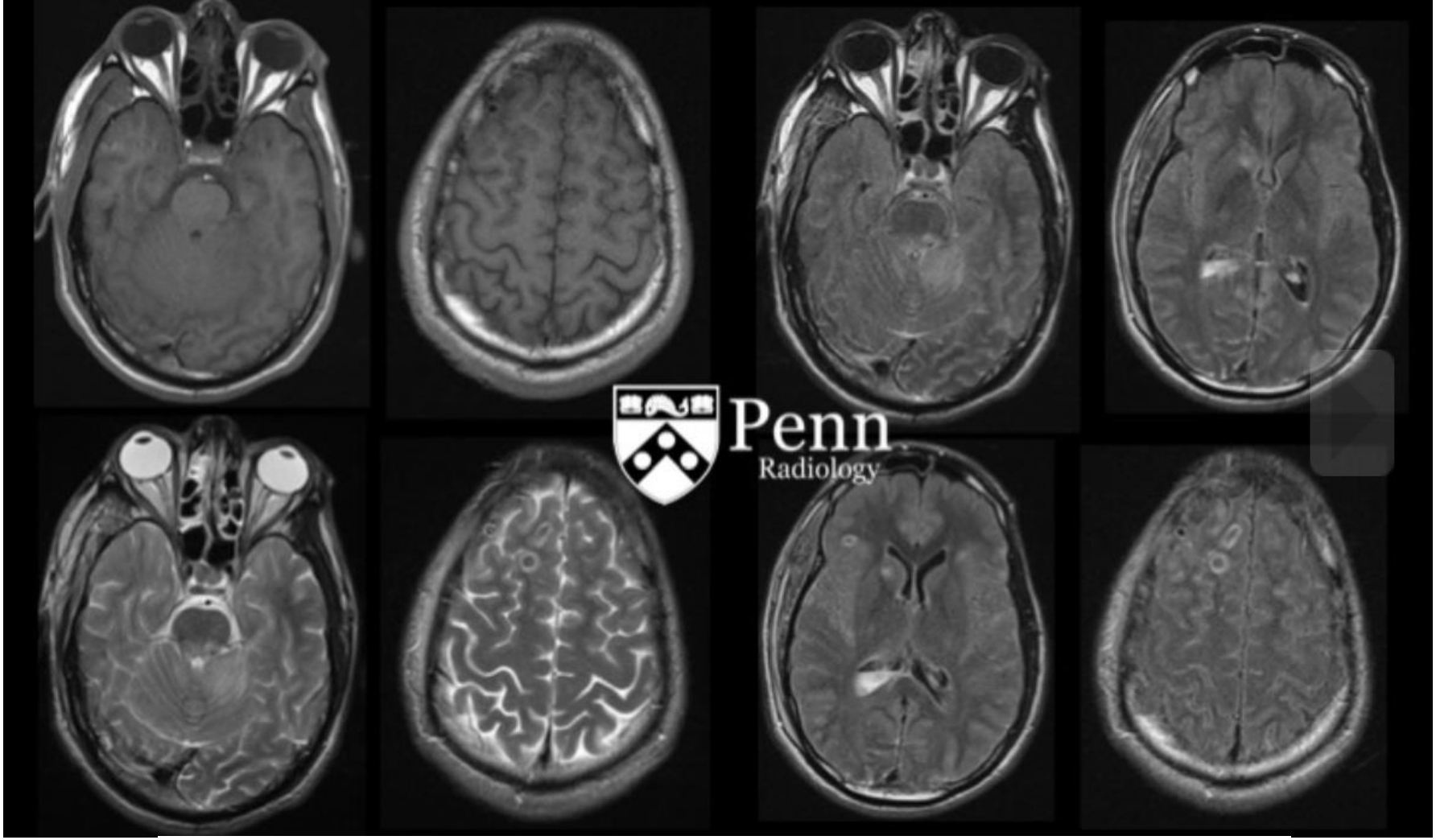

What is the grade of this injury?

- ○ Grade I
- ○ Grade II
- ○ Grade III (correct!)

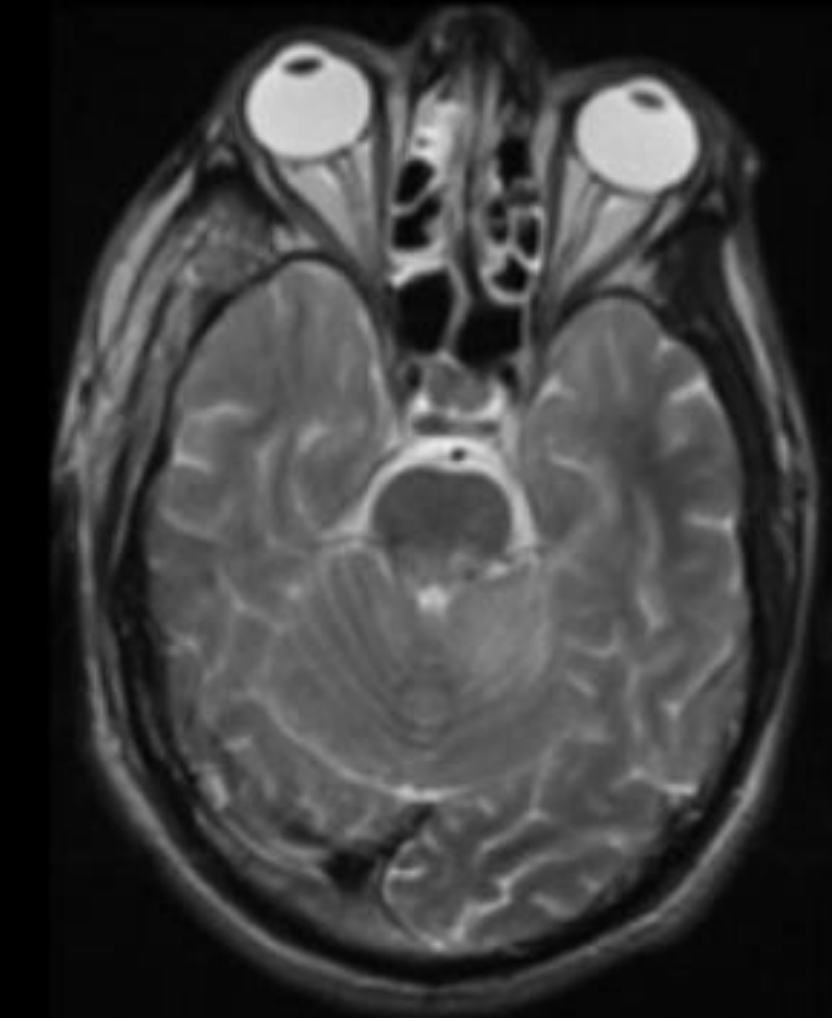

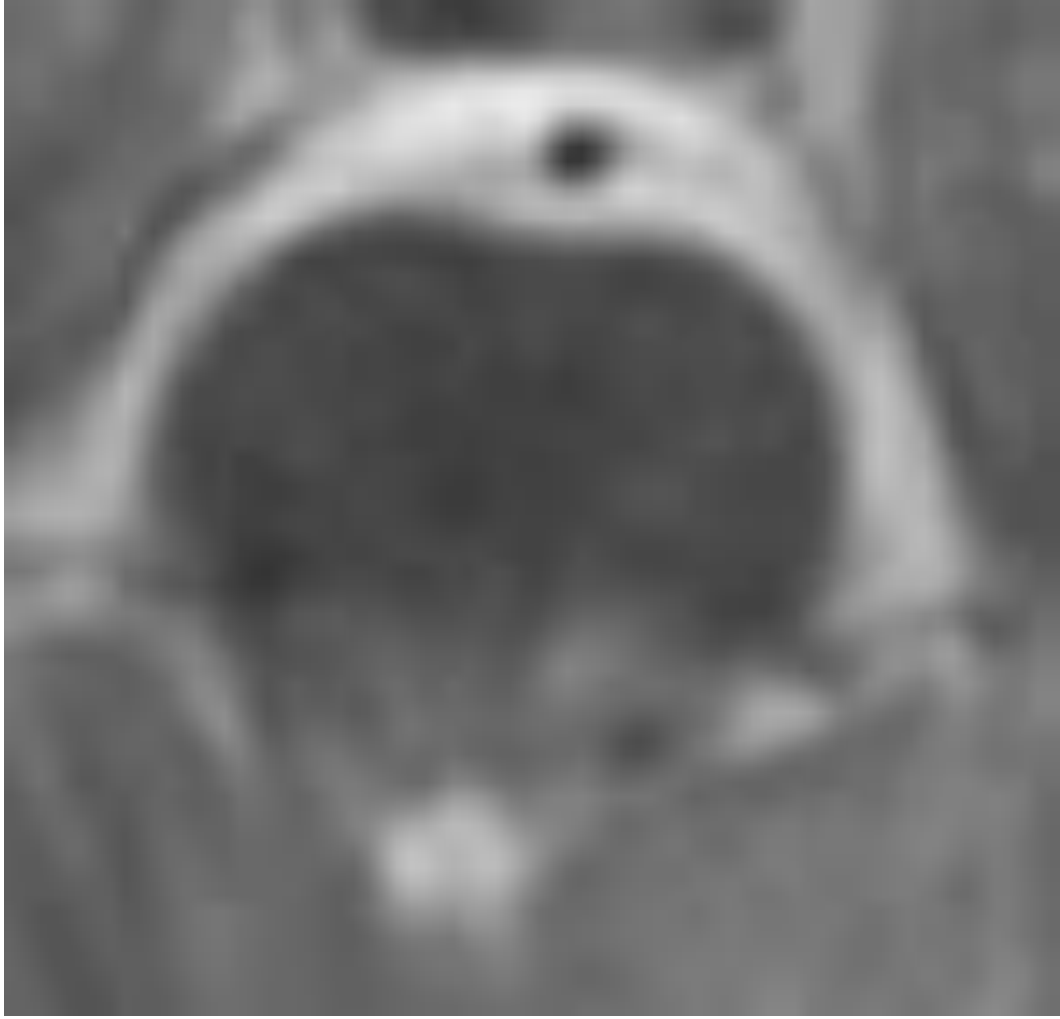

What is the grade of this injury?

- ○ Grade I
- ○ Grade II
- ● Grade III (correct!)

Diffuse axonal injury grading system (Adams et al, 1999)

- Grade I: Lesion involves gray-white interfaces; most often in parasagittal frontal lobes and periventricular temporal lobe.
- Grade II: Involves the corpus callosum in addition to grade 1 location.
- Grade III: Involves brainstem in addition to grade 1 and 2 locations.

Treatment and prognosis

The prognosis of diffuse axonal injury is generally poor for higher grades, with high morbidity and mortality, often with death or persistent vegetative states. The amount of axonal injury is highly predictive of long-term vegetative state. However, in mild cases, patients may be minimally affected. Diffuse axonal injury lesions in the cerebral cortex can also result in focal neurologic and/or neuropsychiatric deficits. Aside from limiting further damage caused by cerebral edema with steroids and other supportive treatments, as well as long-term rehabilitation, there are no treatments for diffuse axonal injuries.

There is a high association with callosal diffuse axonal injury and intraventricular hemorrhage.

CT findings:

- Lesions are usually seen on CT if hemorrhagic, and they will appear as hyperdense oval or elliptical lesions that range in size from a few millimeters to a few centimeters.
- CT is relatively insensitive for diffuse axonal injuries, especially in milder cases and if lesions are nonhemorrhagic.
- If lesions are large enough, they may be surrounded by areas of hypoattenuation (representing edema) and may cause mild, local mass effect.
- There is a high association with callosal diffuse axonal injury and intraventricular hemorrhage.

What is the most sensitive sequence for detecting postraumatic “microbleeds”?

- ○ FLAIR
- ○ Diffusion
- ○ GRE/susceptibility-weighted (SWI)
- ○ Postcontrast T1-weighted

What is the most sensitive sequence for detecting postraumatic “microbleeds”?

- ○ FLAIR
- ○ Diffusion
- ● GRE/susceptibility-weighted (SWI) (correct!)
- ○ Postcontrast T1-weighted

MRI findings:

- SWI/GRE sequences are the most sensitive for even tiny hemorrhagic lesions as they will show susceptibility artifact in regions with blood/hemosiderin.
- Nonhemorrhagic lesions will show high FLAIR signal, representing edema.
- Even without a positive MRI, diffuse axonal injury is not entirely excluded as the actual diagnosis is based on the pathologic finding of axonal bulbs (irregular swelling) microscopically.

Los Gatos MRI